AD-A040 627 CALIFORNIA UNIV LIVERMORE LAWRENCE LIVERMORE LAB F/G 4/1
LAWRENCE LIVERMORE LABORATORY FIRST ANNUAL REPORT TO THE HIGH A--ETC(U)
JUN 76 F M LUTHER DOT-TSC-76-1

UNCLASSIFIED UCRL-50042-76 FAA-EQ-77-6 NL

1 OF 1
ADA
040627

END
DATE
FILMED
7-77

FAA-EQ-77-6

LAWRENCE LIVERMORE LABORATORY FIRST ANNUAL REPORT TO THE HIGH ALTITUDE POLLUTION PROGRAM

FREDERICK M. LUTHER,
PRINCIPAL INVESTIGATOR

JUNE 1976

Prepared for
High Altitude Pollution Program

U.S. Department of Transportation
Office of Environmental Quality
Washington, D.C. 20591

Technical Report Documentation Page

1. Report No.	2. Government Accession No.	3. Recipient's Catalog No.
FAA-EQ-77-6		
4. Title and Subtitle		**5. Report Date**
Lawrence Livermore Laboratory First Annual Report to the High Altitude Pollution Program		Jun[illegible]976
		6. Performing Organization Code
7. Author(s)		**8. Performing Organization Report No.**
Frederick M. Luther, Principal Investigator		UCRL-50042-76
9. Performing Organization Name and Address		**10. Work Unit No. (TRAIS)**
Lawrence Livermore Laboratory P. O. Box 808 Livermore, California 94550		52 P.
		11. Contract or Grant No.
		DOT-TSC-76-1
12. Sponsoring Agency Name and Address		**13. Type of Report and Period Covered**
U.S. Department of Transportation Federal Aviation Administration Office of Environmental Quality Washington, D.C. 20591		Annual Report,
		14. Sponsoring Agency Code

15. Supplementary Notes

16. Abstract

This report presents major accomplishments and significant findings of research conducted during the first year of contract to the FAA High Altitude Pollution Program, ending June 30, 1976. The overall research effort is concerned with numerical modeling of the atmospheric response to aerospace utilization of the stratosphere. It encompasses four areas of study: photochemical kinetics; coupled kinetics and transport; radiative transfer; and meteorological analysis. Additional limited studies have been conducted using the Laboratory's two-dimensional climate model (ZAM2).

17. Key Words	18. Distribution Statement
Numerical modeling Stratosphere Photochemical reactions Atmospheric transport Radiative transfer	DISTRIBUTION STATEMENT A Approved for public release; Distribution Unlimited

19. Security Classif. (of this report)	20. Security Classif. (of this page)	21. No. of Pages	22. Price
		48	

Form DOT F 1700.7 (8-72) Reproduction of completed page authorized

390 999

PREFACE

During the fiscal year ending June 30, 1976, Lawrence Livermore Laboratory (LLL) participated in the High Altitude Pollution Program, which was instituted by the U.S. Department of Transportation's Federal Aviation Administration, under Reimbursable Agreement DOT-TSC-76-1 with the Transportation Systems Center in Cambridge, Massachusetts. This report describes the major accomplishments and significant findings of the LLL work performed to date. The overall research effort at LLL, which is primarily concerned with numerical modeling, has been divided into a number of subtasks according to research area. The successful accomplishment of these subtasks has required contributions and cooperation from many participants. The work reported here should be considered the collective effort of all those listed below.

Scientific Administration

Joseph B. Knox, Division Leader
Frederick M. Luther, Principal Investigator

Participants

Julius S. Chang
William H. Duewer
Arthur L. Edwards
Hugh W. Ellsaesser
Gerald L. Potter
Raymond L. Tarp
Donald J. Wuebbles

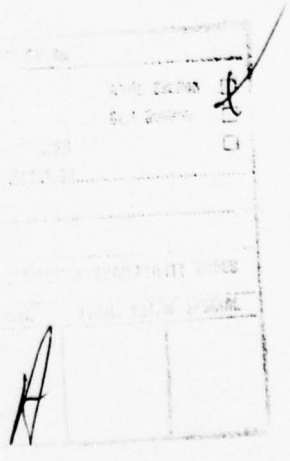

CONTENTS

1. INTRODUCTION

The High Altitude Pollution Program (HAPP) was initiated by the Federal Aviation Administration for the purpose of ensuring that stratospheric aircraft engine emissions will not result in unacceptable effects on the biosphere. The objective of HAPP is to quantitatively determine the requirements for reduced cruise-altitude exhaust emissions and, through international and interagency cooperation, to ensure that, if necessary, appropriate regulatory action is taken. HAPP incorporates many related activities, including modeling, field measurements, laboratory measurements, engines and fuels assessment, regulation, and monitoring.

As an active participant in HAPP during the fiscal year ending June 30, 1976, Lawrence Livermore Laboratory (LLL) has undertaken an extensive effort in numerical modeling of the atmospheric response to aerospace utilization of the stratosphere. A modeling effort is important to HAPP for two primary reasons. First, modeling constitutes a means of relating engine emissions to changes in atmospheric composition. Because of the complex physical processes and feedback mechanisms involved, it is essentially impossible to assess the effects of emissions without incorporating these processes into a model and allowing them to interact. Second, modeling contributes to the interpretation and analysis of experimental results and helps determine the relative priorities for carrying out this work. The modeling effort at LLL covers four major areas of research: photochemical kinetics, coupled kinetics and transport, radiative transfer, and meteorological analysis.

Photochemical kinetics modeling must span gas-phase reaction processes and heterogeneous (i.e., gas-particle) reaction processes, constant and diurnally (and seasonally) varying photochemical reaction rates, a wide range of ambient temperatures and pressures, neutral and ionized species, processes with both accurately and poorly known rates of reaction, and species of both acknowledged and questionable importance in the stratosphere. Considerable attention has been directed toward evaluation of the sensitivity of reaction mechanisms to deficiencies in our knowledge of reaction rates, quantum yields, and reaction mechanisms.

The transport-kinetics models are intended for time-dependent calculations of the response of the stratosphere to injections of trace species by aerospace vehicles. These one- and two-dimensional models incorporate interactive radiative and chemical processes coupled with transport, which is described by prescribed mean winds and eddy diffusion coefficients as appropriate. These models are designed to facilitate perturbation and sensitivity studies.

Radiative transfer modeling includes (1) application of highly detailed models to assessment of the effect on the radiation budget of perturbations to the stratospheric composition, and (2) development of simplified radiative transfer models for inclusion in the transport-kinetics models. Considerable attention has been directed toward including interactive radiative processes in the transport-kinetics models in order to assess possible feedback mechanisms.

Meteorological analysis provides guidance and support for the modeling efforts through in-depth studies of atmospheric processes and phenomena. A primary responsibility of this research is to develop test situations to validate various aspects of the numerical models.

In addition to these major research areas, special limited studies have been conducted using LLL's two-dimensional climate model (ZAM2). Climate model development at LLL is presently being supported by a related project involving assessment of the climatic effects of atmospheric nuclear explosions. This project, which is funded by the Division of Military Application of the Energy Research and Development Administration, and HAPP both take advantage of numerical modeling capabilities and scientific expertise developed at LLL during the Climatic Impact Assessment Program (CIAP) of the Department of Transportation. Although the same numerical models are used for both studies, the applications of the models are quite different. For example, the study of the climatic effect of nuclear explosions is primarily concerned with the time-dependent response of the atmosphere to pulse injections of NO_x, whereas the HAPP study is concerned with steady-state injections of NO_x. Tasks relating to model development or refinement benefit both projects, and consequently such tasks have been divided between the two projects. In this way each project's sponsor benefits from the participation of the other sponsor.

These two projects together constitute LLL's stratospheric research program. The various research activities included in the program and their interrelationships are diagrammed in Fig. 1. Except for the two-dimensional transport-kinetics model, we are beyond the model development stage. Because of rapidly changing chemistry and rate data, most of the effort in the transport-kinetics area during the past year has been devoted to model improvement and sensitivity studies. Research in the radiation transfer

area has concentrated on the development of subroutines for inclusion in the transport-kinetics and climate models. Several sensitivity and validation studies were conducted using the two-dimensional climate model (not sponsored by HAPP), and the results from these studies agreed well with other models. Meteorological analysis has consisted primarily of comparing model results with observations when possible and developing validation tests for the models.

A long-range objective of the research program is the development of a capability for assessing the possible climatic effects of various atmospheric perturbations. Currently, our assessments of perturbed species concentrations consider a large number of photochemical reactions and are capable of treating radiative and diurnal processes in detail, and they assume that the effects of transport on atmospheric composition can be represented parametrically. Our climatic assessments treat many interrelated thermodynamic and hydrologic processes, and the perturbed chemical composition is treated as a given quantity. Ultimately, our assessments will include interaction between the chemistry and the dynamics.

The sensitivity studies conducted during the past year were intended to increase our understanding of the characteristics of the numerical models and the uncertainties associated with their results. The perturbations (e.g., NO_x injections) used in these studies were chosen so as to cause a significant model response rather than on the basis of an expected SST fleet size. The reader is cautioned, therefore, not to interpret the results as predictions of the effects of aerospace operations, but rather as indications of the model sensitivity. Predictions of the effects of aerospace operations on atmospheric composition must include the simultaneous injection of several species (e.g., NO_x, H_2O, and SO_2). During the next year simultaneous injections will be considered.

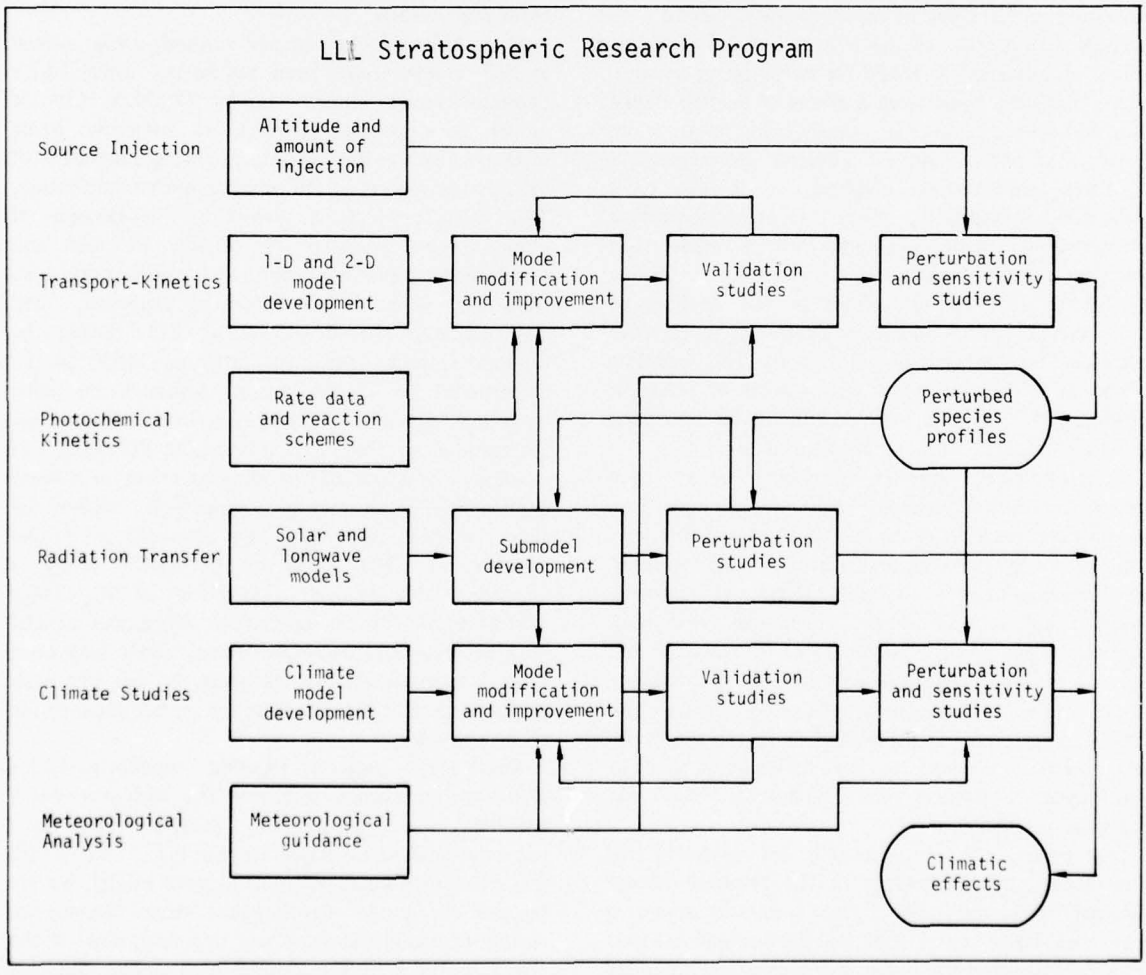

Fig. 1. Flow chart showing the approach LLL has taken in its stratospheric research program.

2. RESEARCH ACTIVITIES

Because of the complex nature of the work, most of the research tasks represent the combined effort of several scientists rather than individual contributions. It is not possible to separate the tasks by research area because of the team approach. Major tasks that have been completed are reported here in considerable detail. Work still in progress and several shorter tasks that have been finished are summarized at the end of this section. Those contributions which we feel are particularly significant have been, or are in the process of being, submitted for publication in technical journals.

2.1 NO_x CATALYTIC OZONE DESTRUCTION: SENSITIVITY TO RATE COEFFICIENTS

In recent years it has been suggested that several of man's activities could result in a reduction of stratospheric ozone. This would increase the UV-B* flux at the earth's surface, and presumably result in an increase in the incidence of skin cancer. It has also been suggested that changes in stratospheric ozone might alter the climate (Grobecker et al. 1974). Among others, NO_x from stratospheric aircraft flights (Johnston 1971, Crutzen 1972), NO_x from nuclear tests (Foley and Ruderman 1973), and nuclear warfare (MacCracken and Chang 1975, National Academy of Sciences 1975a) have been proposed as capable of reducing stratospheric ozone. In order to estimate the magnitudes of these hypothesized effects, considerable effort has been devoted to the construction of numerical models of the stratosphere (Grobecker et al. 1974, National Academy of Sciences 1975b, Interdepartmental Committee for Atmospheric Sciences 1975) and acquisition of data to be used for model input and to verify model results. The major reasons for current credence in the models have been that they have used measured inputs (so that the components of the model are presumed to be separately tested) and that the models generate concentrations of stratospheric species that fall within the sometimes rather wide range of measured values.

While the above considerations are necessary for model credibility, they are not conclusive for several reasons. First, the models are known to be incomplete in various ways. All use more or less severe approximations in treating photon flux densities. All 1-D and 2-D (one dimensional and two-dimensional) models use parameterized transport. All the models use an incomplete representation of the chemistry (for example, ionic processes and heterogeneous processes are omitted or very crudely represented in existing models). Second, comparison of computed and observed concentrations is subjective since most parameters reveal a substantial range of measured values and hence some selection must be made of the actual data to be compared. Finally, each of the input parameters has some uncertainty associated with it (e.g., in the case of the chemical rate data the uncertainties that have been estimated for many of the processes range from a few percent up to a factor of 10 (Hampson and Garvin 1975)).

The first two problems mentioned are in a sense philosophical and may not be addressable in the framework of existing "mean state" models with admittedly restricted degrees of freedom. The estimated effects of processes known to be omitted are a few percent or less. Although ionic processes have recently been suggested to be important (Ruderman et al. 1976), this argument is speculative. However, the third source of uncertainty can be examined:

In principle there are several techniques available to study quantitatively the propagation of error in a complex model (Dickinson and Gelinas 1975, Cukier et al. 1973, Schaibly and Schuler 1973, and Atherton et al. 1975). Unfortunately, at present these techniques are prohibitively expensive and are difficult to apply. Nonetheless, it is feasible to perform experiments which examine model sensitivity to perturbations in individual rate coefficients or ensembles of rate coefficients chosen with the intent of maximizing or minimizing the model response to an incremental change in some other parameter. This would then provide approximate bounds for the model's sensitivity to rate coefficient uncertainties. In this study we adjust the rate constants involved in a model of the HO_x, NO_x, and O_x reactions in the stratosphere and then examine the effects on the response of the model to an NO_x injection. This technique is useful in determining extreme ranges of possible effects, and in identifying highly sensitive parameters or groups of parameters. It is recognized that this is not very useful in estimating the probability of errors of any given magnitude. But it could give qualitative lower-limit estimates of the expectation of an effect. For even this to be done, it is necessary to estimate the

*Ultraviolet flux in the biologically active wavelength region, 280-320 nm.

distribution of expected error in the individual rate coefficients and the sensitivity of the model to subsets of the rate coefficients.

The quantitative meaning of the uncertainties quoted by Hampson and Garvin (1975) and used in this study is not easily specified. The quoted uncertainties were intended to define a range that would be expected by a panel of experienced chemical kineticists to contain the correct value (Hampson 1976). We have examined data published after the evaluations given by Hampson and Garvin for six reactions of particular importance to our model and some $O(^1D)$ reactions.* We find that for lower stratospheric conditions the mean divergence between new data and the value cited by Hampson and Garvin was about 1.2 times the cited uncertainty, but that the error distribution was very different from a normal distribution.

If, in spite of the above finding, one treats the quoted uncertainties as estimates of the expected errors (i.e., 1 σ), then the expectation that all of the varied rate coefficients will depart at least as far from the "best" values as those used in a test model, and in the same sense, will be roughly $(0.16)^n$ where n is the number of adjusted rate coefficients. However, because the model is insensitive to many of the rate coefficients and very sensitive to a few, this methodology provides only a lower limit to the expectation of a model with a sensitivity at least as divergent from the "best" model as the model tested. If many of the parameters varied are insensitive, this lower limit would be so extreme as to be meaningless.

The basic model used for these experiments was the LLL one-dimensional model used in the CIAP documentation (Grobecker et al. 1974, Grobecker 1975). Its structure has been described elsewhere (Chang et al. 1974). This model includes the chemical reactions given in Table 1. It treats the following species dynamically (by parameterized vertical transport) as well as photochemically: O, O_3, NO, NO_2, HNO_3, HO, HO_2, H_2O_2, N_2O. Steady-state approximations are made for $O(^1D)$, N, and H, and the concentration profiles of H_2O and CH_4 are prescribed.* The various species concentrations are solved numerically at 44 levels extending to an altitude of 55 km. In this study both the carbon cycle (except insofar as methane is a source of HO_x) and the halogen cycles were omitted. The response of the model to the choice of eddy diffusion profile was examined by Chang (1974). For this study we used the LLL diffusion profile derived in the earlier study (Chang et al. 1974). (See Fig. 2.) Nine sets of rate coefficients were examined:

*The reactions examined were K6, K10, K11, K12, K14, K18, K19, K20, K26, and the reactions of $O(^1D)$ with N_2, O_2, and CO_2. Only relative rates were compared for the $O(^1D)$ reactions with species other than CO_2, which were the source of absolute rate data in Hampson and Garvin.

*This version of the basic model is chosen specifically to provide continuity with the CIAP Report.

Table 1. Reactions and rate parameters for the various models used.

Reaction		Photolysis rates at the indicated altitudes for Model A_2		
Formula	Number	55 km	30 km	15 km
$O_2 + h\nu \rightarrow 2O$	J1	7.76×10^{-10}	1.90×10^{-11}	8.42×10^{-16}
$O_3 + h\nu \rightarrow O + O_2$	J2	2.80×10^{-4}	2.41×10^{-4}	2.07×10^{-4}
$O_3 + h\nu \rightarrow O(^1D) + O_2$	J3	4.79×10^{-3}	5.85×10^{-5}	7.90×10^{-6}
$NO_2 + h\nu \rightarrow NO + O$	J4	5.03×10^{-3}	4.85×10^{-3}	4.74×10^{-3}
$N_2O + h\nu \rightarrow N_2 + O(^1D)$	J5	4.14×10^{-7}	2.89×10^{-8}	1.44×10^{-15}
$NO + h\nu \rightarrow N + O$	J6	1.35×10^{-6}	8.90×10^{-10}	7.30×10^{-37}
$HNO_3 + h\nu \rightarrow OH + NO_2$	J7	6.38×10^{-5}	4.78×10^{-6}	3.21×10^{-7}
$H_2O_2 + h\nu \rightarrow 2OH$	J8	8.25×10^{-5}	6.39×10^{-6}	2.22×10^{-6}
$HO_2 + h\nu \rightarrow OH + O$	J9	1.98×10^{-4}	3.40×10^{-6}	1.70×10^{-10}
$NO_3 + h\nu \rightarrow NO + O_2$	$J10_1$	(Either $J10_1$ or $J10_2$ is assumed to be the only fate of NO_3 as is indicated by model subscript.)		
$NO_3 + h\nu \rightarrow NO_2 + O$	$J10_2$			

Reaction		Arrhenius A-factor[a] for indicated model			
Formula	Number	A	B	C	Temperature dependence[b]
$O + O_2 + M \rightarrow O_3 + M$	K1	1.07×10^{-34}	0.91×10^{-34}	1.26×10^{-34}	+ 510.
$O + O_3 \rightarrow 2O_2$	K2	1.9×10^{-11}	1.5×10^{-11}	2.4×10^{-11}	-2300.
$O_3 + NO \rightarrow NO_2 + O_2$	K3	9×10^{-13}	11.6×10^{-13}	$7. \times 10^{-13}$	-1200.
$O + NO_2 \rightarrow NO + O_2$	K4	9.1×10^{-12}	10.4×10^{-12}	7.9×10^{-12}	–
$N_2O + O(^1D) \rightarrow N_2 + O_2$	K5	1.1×10^{-10}	0.7×10^{-10}	1.74×10^{-10}	–
$N_2O + O(^1D) \rightarrow 2NO$	K6	1.1×10^{-10}	0.7×10^{-10}	1.74×10^{-10}	–
$N + O_2 \rightarrow NO + O$	K7	1.1×10^{-14}	0.7×10^{-14}	1.74×10^{-14}	-3150.
$N + NO \rightarrow N_2 + O$	K8	2.7×10^{-11}	2.1×10^{-11}	3.4×10^{-11}	–
$N + NO_2 \rightarrow 2NO$	K9	6×10^{-12}	6×10^{-12}	0.	–
$O(^1D) + H_2O \rightarrow 2OH$	K10	3.5×10^{-10}	2.8×10^{-10}	4.4×10^{-10}	–
$O(^1D) + CH_4 \rightarrow OH + CH_3$	K11	$4. \times 10^{-10}$	3.2×10^{-10}	5×10^{-10}	–
$O_3 + OH \rightarrow HO_2 + O_2$	K12	1.6×10^{-12}	0.8×10^{-12}	3.2×10^{-12}	-1000.
$O + OH \rightarrow O_2 + H$	K13	4.2×10^{-11}	2.7×10^{-11}	6.7×10^{-11}	–
$O_3 + HO_2 \rightarrow OH + 2O_2$	K14	1.0×10^{-13}	0.5×10^{-13}	2.0×10^{-13}	-1250.
$O + HO_2 \rightarrow OH + O_2$	K15	8×10^{-11}	2×10^{-11}	$32. \times 10^{-11}$	- 500.
$H + O_2 + M \rightarrow HO_2 + M$	K16	2.08×10^{-32}	2.44×10^{-32}	1.77×10^{-32}	+ 290.
$H + O_3 \rightarrow OH + O_2$	K17	1.23×10^{-10}	1.0×10^{-10}	1.55×10^{-10}	- 562.
$HO_2 + HO_2 \rightarrow H_2O_2 + O_2$	K18	3×10^{-11}	6×10^{-11}	1.5×10^{-11}	- 500.
$HO_2 + OH \rightarrow H_2O + O_2$	K19[c]	2×10^{-11}[c]	2×10^{-10}	1.5×10^{-11}	–
$OH + NO_2 \xrightarrow{M} HNO_3$	K20[d]	4×10^{-12}	2×10^{-12}	8×10^{-12}	–[d]
$OH + HNO_3 \rightarrow H_2O + NO_3$	K21	8.9×10^{-14}	4.5×10^{-14}	1.8×10^{-13}	–
$H_2O_2 + OH \rightarrow H_2O + HO_2$	K22	1.7×10^{-11}	2.7×10^{-11}	1.1×10^{-11}	- -910.
$N_2 + O(^1D) + M \rightarrow N_2O + M$	K23	2.8×10^{-36}	5.6×10^{-36}	1.4×10^{-36}	–
$N + NO_2 \rightarrow N_2O + O$	K24	9×10^{-12}	9×10^{-12}	1×10^{-12}	–
$NO + O + M \rightarrow NO_2 + M$	K25	3.96×10^{-33}	2×10^{-33}	8×10^{-33}	+ 940.
$NO + HO_2 \rightarrow NO_2 + OH$	K26	2×10^{-13}	6.3×10^{-14}	6.3×10^{-13}	–
$OH + OH \rightarrow H_2O + O$	K27	1×10^{-11}	1.6×10^{-11}	0.63×10^{-11}	- 550.
$N + O_3 \rightarrow NO + O_2$	K28	5.7×10^{-13}	1.8×10^{-12}	1.8×10^{-13}	–
$NO_2 + O_3 \rightarrow NO_3 + O_2$	K29	1.23×10^{-13}	1.55×10^{-13}	$1. \times 10^{-13}$	-2470.
$OH + CH_4 \rightarrow H_2O + CH_3$	K30	2.36×10^{-12}	2.15×10^{-12}	2.6×10^{-12}	-1710.
$OH + OH + M \rightarrow H_2O_2 + M$	K31	2.5×10^{-33}	$4. \times 10^{-33}$	1.6×10^{-33}	+2500.
$H_2O_2 + O \rightarrow OH + HO_2$	K32	2.75×10^{-12}	2.34×10^{-12}	3.23×10^{-12}	-2125.
$O(^1D) + M \rightarrow O + M$	K33	5.85×10^{-11}	4.14×10^{-11}	8.26×10^{-11}	–
$CH_3 \xrightarrow{O_2} 2HO_2 + CO$		(Assumed to be the only fate of CH_3.)			

[a] Constant A in $K = A \exp(C/T)$ in units of cm^3/s (cm^6/s for three-body processes).

[b] Constant C in $K = A \exp(C/T)$.

[c] Model A' differs from A only in that K19 is set to 2×10^{-10}, the value used in most of the CIAP experiments.

[d] K20 is pressure-dependent. In our model $K20 = K[M]/(1.12 \times 10^{18} + [M])$ where K is value tabled above. This is a fit to the altitude-dependent expression given by Hampson and Garvin (1975).

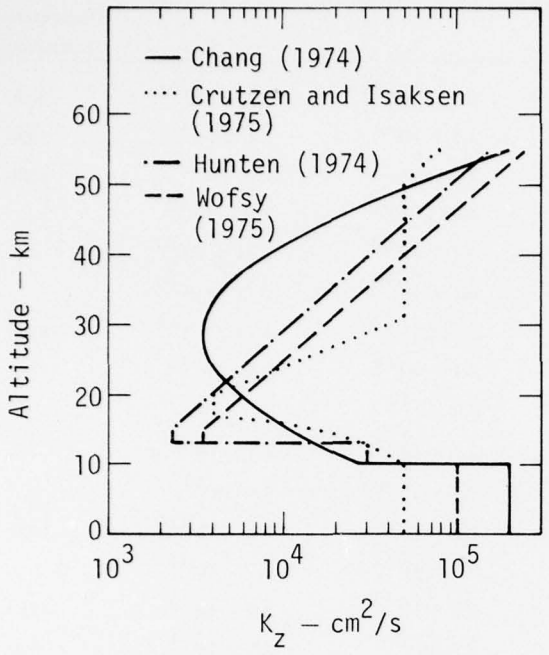

Fig. 2. K_z profiles that have been used by various investigators. The Chang (1974) profile was used to examine the nine sets of rate coefficients described in the text.

1. Model A_1 used the rate coefficients given in Hampson and Garvin (1975) with the rate coefficient for the reaction $HO + HO_2 \rightarrow H_2O + O_2$ (K19) set to 2×10^{-11} cm^3/s. This is the low end of the range quoted, and the value currently preferred by us (Kaufman 1975, Lloyd 1974). Branch 1 was assumed for J10.

2. Model A_2 differed from model A_1 in that branch 2 was assumed for J10.

3. Model A'_1 differed from model A_1 in that K19 was set to the high end of the range, i.e., 2×10^{-10}, the value used for most of the CIAP computations. Branch 1 was assumed for J10.

4. Model A'_2 differed from model A'_1 by assuming branch 2 for J10.

5. Model B assumed all the rate coefficients were in error by the estimated uncertainty indicated by Hampson and Garvin (1975)* and were varied within this range with the intent of maximizing the destruction of O_3 by a given amount of NO_x, minimizing the destruction of O_3 by ambient O_x and HO_x, and minimizing the ambient concentrations of NO_x and HO_x. Branch 1 was assumed for J10.

*When a rate constant was reported to be known with higher accuracy, but only at room temperature, and the room-temperature rate constant was less than 10^{-12} cm^3/s, a ±3-fold uncertainty was assumed.

6. Model C_1 varied all rate coefficients within the same range of uncertainty with the intent of minimizing the destruction of O_3 by a given quantity of NO_x, maximizing O_3 destruction by ambient O_x and HO_x, and maximizing the ambient concentrations of NO_x and HO_x. Branch 1 was assumed for J10.

7. Model C_2 differed from model C_1 by assuming branch 2 for J10.

8. In an attempt to identify the reactions most responsible for the change in model behavior, a model C'_1, analogous to model C_1, was developed in which only a limited set of rate coefficients was adjusted. Branch 1 was assumed for J10.

9. Model C'_2 differed from model C'_1 by assuming branch 2 for J10.

It should be noted that the uncertainties in the photodissociation rates, which are probably even larger than the uncertainties in thermal rate coefficients, were not treated here. Several approximations are involved in the calculation of photodissociation rates, and these approximations are the subject of concurrent research.

The following computations were carried out:

1. An ambient condition was computed for each of the models.

2. The condition after 300 years of NO_x injection at 2000 molecules/cm^3·s throughout a 1-km-thick layer at 17 km altitude, the average cruise altitude of the Concorde SST, hereafter designated as NO_x-17.*

3. All models were used to compute the condition after 300 years with the above NO_x injection at 20 km, a possible cruise altitude for an "advanced" SST (NO_x-20).

4. Same as cases 2 and 3 with injection at 35 km (NO_x-35).

5. Ambient conditions (case 1) were recomputed for all models with the water column increased by 10%, roughly the magnitude of the increase in stratospheric water content expected from the hypothetical fleet of 500 Boeing SST's (Grobecker 1975) ($1.1 \times H_2O$).

6. Case 2 was repeated with the water column increased by 10% ($1.1 \times H_2O$, NO_x-17).

The calculated O_3 columns and the percent of O_3 deviation (ΔO_3) from the respective ambient conditions are given in Table 2. The effect of the choice of diffusion profile was examined for cases 1 and 2 and the results are summarized in Table 3. The K_z profiles studied are given in Fig. 2.

*This emission rate corresponds to a very large Concorde fleet, numbered in thousands of planes. For comparison we examined a few cases assuming a tenfold smaller injection rate and found the resultant perturbations to be about ninefold smaller, suggesting an almost linear relationship between injection rate and resultant perturbation.

Table 2. Calculated ambient and perturbed O_3 column densities ($10^{18}cm^{-2}$) and percent deviation from the respective ambient O_3 column densities (ΔO_3) for the perturbation cases 1-6 as described in the text. See text for description of models

Case		CIAP model (high value of K19) A'_1 J10 yields $NO + O_2$	CIAP model (high value of K19) A'_2 J10 yields $NO_2 + O$	"Best" model (low value of K19) A_1 J10 yields $NO + O_2$	"Best" model (low value of K19) A_2 J10 yields $NO_2 + O$	Maximized response to NO_x B J10 yields $NO + O_2$	Minimized response to NO_x C_1 J10 yields $NO + O_2$	Minimized response to NO_x C_2 J10 yields $NO_2 + O$	Response to NO_x minimized on four rates C'_1 J10 yields $NO + O_2$	Response to NO_x minimized on four rates C'_2 J10 yields $NO_2 + O$
1. Ambient	O_3	7.765	7.993	7.422	7.555	7.577	6.893	6.997	7.338	7.415
2. NO_x–17	O_3	7.428	7.712	7.292	7.467	6.996	7.013	7.152	7.383	7.490
	ΔO_3	-4.34%	-3.52%	-1.75%	-1.16%	-8.06%	+1.74%	+2.22%	+0.61%	+1.01%
3. NO_x–20	O_3	7.005	7.316	7.035	7.250	6.370	7.004	7.182	7.323	7.467
	ΔO_3	-9.79%	-8.47%	-5.21%	-4.03%	-15.92%	+1.61%	+2.64%	-0.20%	+0.70%
4. NO_x–35	O_3	6.426	6.767	6.377	6.614	5.674	6.450	6.663	6.663	6.837
	ΔO_3	-17.24%	-15.34%	-14.06%	-12.46%	-25.11%	-6.42%	-4.77%	-9.20%	-7.80%
5. 1.1 × H_2O	O_3	7.767	7.992	7.408	7.539	7.588	6.857	6.959	7.312	7.387
	ΔO_3	+0.03%	-0.01%	-0.14%	-0.21%	+0.15%	-0.52%	-0.54%	-0.35%	-0.38%
6. 1.1 × H_2O, NO_x–17	O_3	7.435	7.715	7.282	7.454	6.979	6.978	7.114	7.357	7.462
	ΔO_3	-4.25%	-3.48%	-1.88%	-1.34%	-7.89%	+1.23%	+1.67%	+0.26%	+0.63%

Table 3. Calculated ambient (case 1) and perturbed (case 2) O_3 column densities ($10^{18}cm^{-2}$) and percent deviation from the respective ambient O_3 column densities (ΔO_3) for four eddy diffusion coefficient profiles as described in the text. See text for description of models

Eddy diffusion coefficient profile	Model A_1	Model A_2	Model B	Model C_1	Model C_2
Chang (1974):					
Case 1–ambient	7.422	7.555	7.577	6.893	6.997
Case 2–NO_x-17	7.292	7.467	6.966	7.613	7.152
ΔO_3	-1.75%	-1.16%	-8.06%	+1.74%	+2.22%
Crutzen (1975):					
Case 1–ambient	7.444	7.648	7.267	7.102	7.271
Case 2–NO_x-17	7.346	7.575	6.896	7.150	7.345
ΔO_3	-1.32%	-0.95%	-5.10%	+0.68%	+1.02%
Wofsy (1975):					
Case 1–ambient	7.845	8.090	7.577	7.474	7.675
Case 2–NO_x-17	7.462	7.814	6.460	7.509	7.835
ΔO_3	-4.88%	-3.41%	-14.74%	+0.47%	+2.08%
Hunten (1974):					
Case 1–ambient	7.463	7.713	7.090	7.272	7.497
Case 2–NO_x-17	6.964	7.358	5.888	7.149	7.572
ΔO_3	-6.68%	-4.60%	-16.95%	-1.69%	+1.00%

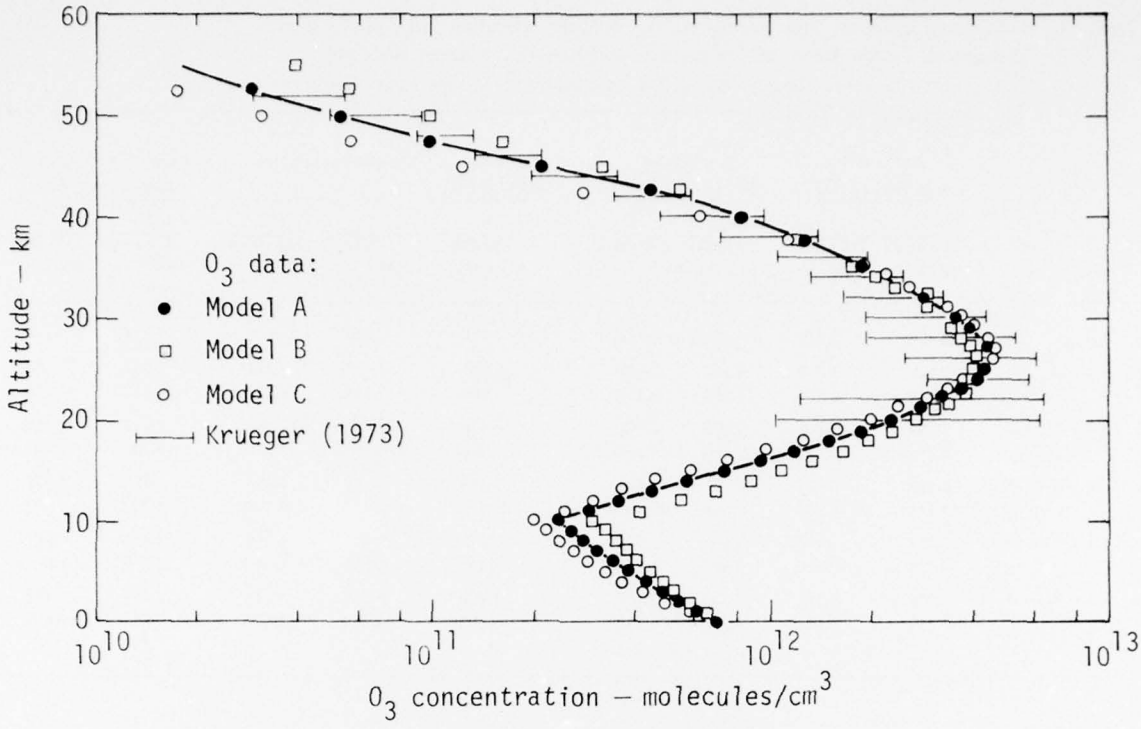

Fig. 3. Calculated equilibrium concentration profiles for O_3 compared with observations from Krueger (1973). Note that for Figs. 3-7 all surface concentrations are input, not calculated.

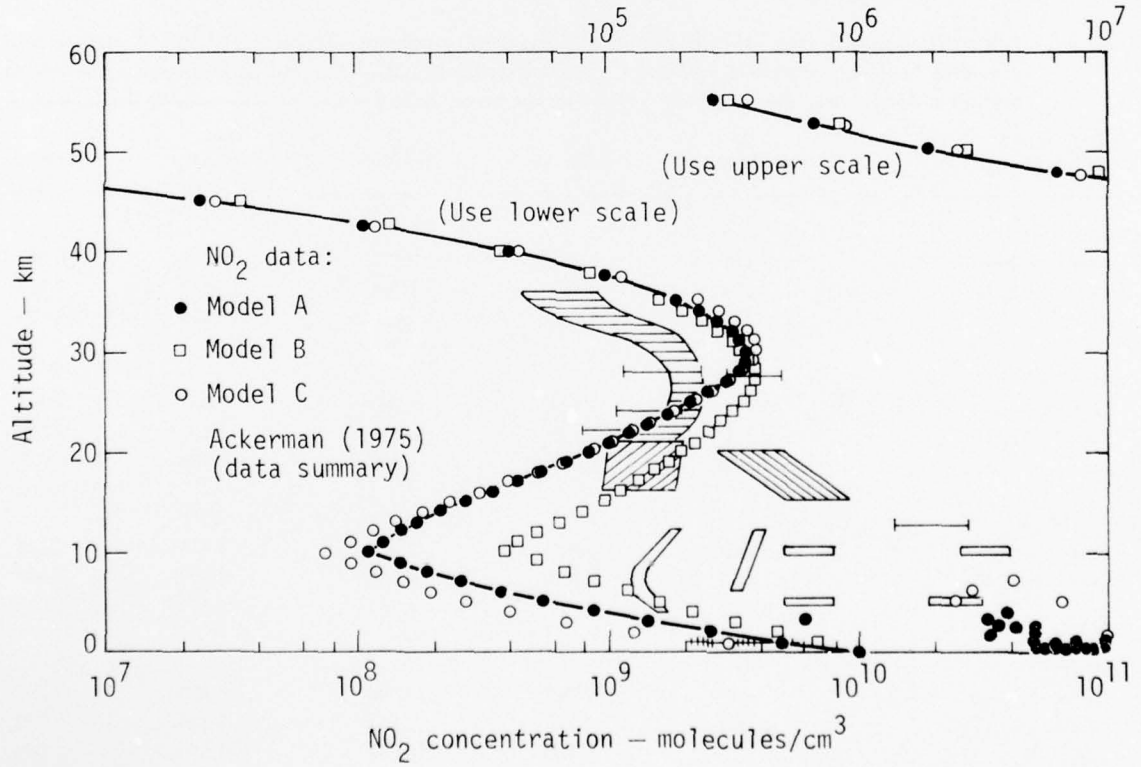

Fig. 4. Calculated equilibrium concentration profiles for NO_2 compared with data summary of Ackerman (1975).

The computed ambient concentration profiles are compared with observations in Figs. 3-7 for models A_1, B, and C_1. (For most species model A′ closely resembled model B and model C′ resembled model C. Differences due to the J10 branch were barely detectable on these semilog plots.) Only profiles for species for which we could find measurements are given here.

As can be seen, the computed ambient states for the species that have been measured in the stratosphere are rather similar for all three models (labeled simply as A, B, and C in the figures). The concentrations plotted represent diurnally averaged conditions as parameterized by a "half sun" condition (the photolysis rates used are one-half of the noontime rate as calculated by the model). Only for the OH measurements of Anderson (1976) can computed concentration profiles be said to disagree with measurement by more than the spread in recent measurements. From Fig. 7 model B would be the most likely to be judged inadequate. However, in order to be more definitive, one must carry out detailed sensitivity analyses involving diurnal models on the details of HO_x chemistry since OH variations are highly time-dependent.

Based on present kinetics data, models B and C are highly improbable. The fact that they gave computed profiles agreeing as well as model A with present observations indicates that such agreement is insufficient to validate a model. This seems to suggest that for observational data to be used to discriminate among models the concentrations must be known within a factor of two at the very least. If, as seems probable, many trace species vary substantially in time and space, the above statement pertains to the accuracy with which the concentration distribution must be known, a much more expensive undertaking than a single measurement.

Perturbations in the O_3 column computed for a 17-km injection of NO_x (case 2) are plotted on a

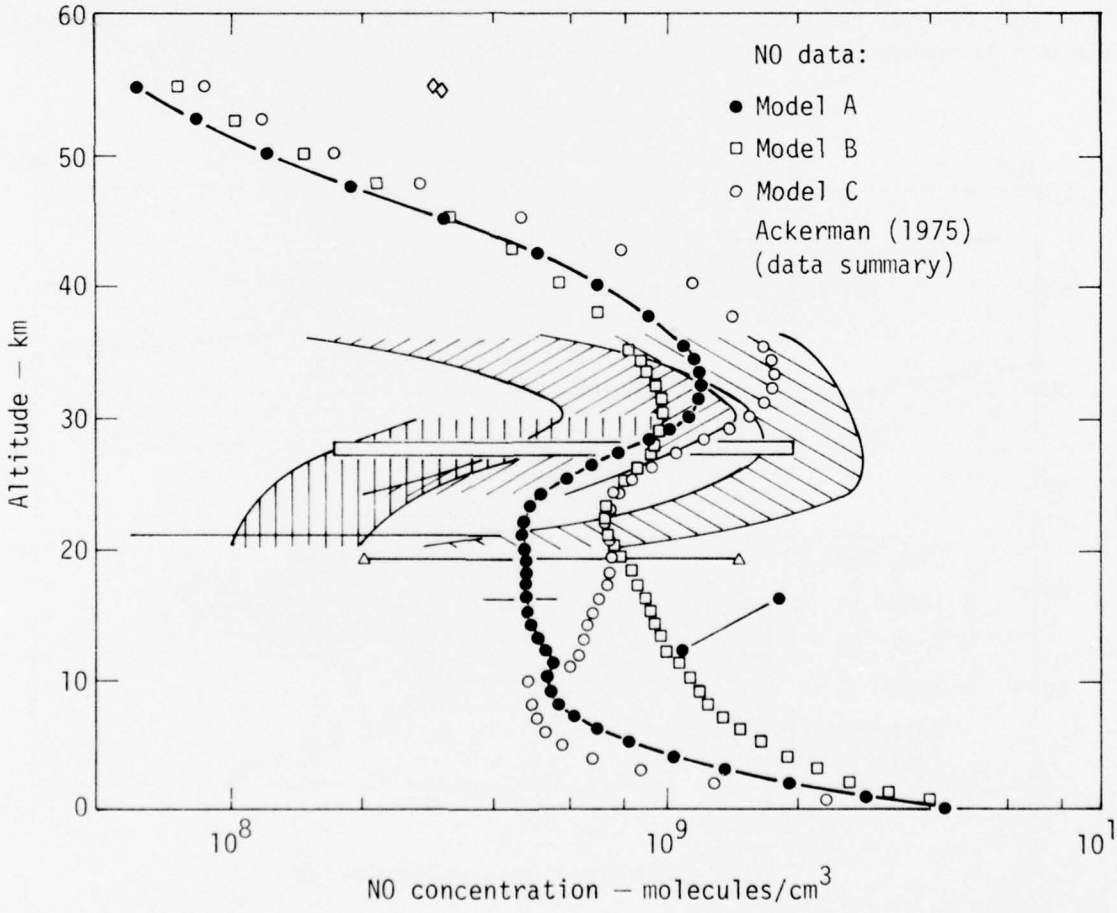

Fig. 5. Calculated equilibrium concentration profiles for NO compared with data summary of Ackerman (1975).

linear scale in Fig. 8. As can be seen, the tropospheric perturbations, largely influenced by the CH_4 and NO_x smog reactions (Chameides and Walker 1973, Johnston and Quitevis 1974), are quite small compared to the stratospheric perturbations. This is in part due to our use of fixed concentrations as a surface boundary condition. We have experimented with the lower boundary condition sufficiently to demonstrate that this type of surface boundary condition has a negligible effect on computed stratospheric profiles, although the tropospheric sensitivities are significantly affected by the boundary conditions.

The opinion has been expressed that model predictions of O_3 destruction for a given NO_x injection are accurate to within a factor of 2 or 3 (Grobecker et al. 1974). As can be seen in Table 2, the perturbations in the O_3 column calculated from the base case (model A) and the most sensitive case (model B) differed by a factor of roughly 5 for a 17-km injection, 3 for a 20-km injection, and only 1.6 for a 35-km injection. Thus, in the case of maximizing the effect of an NO_x injection the uncertainty is comparable to that expected, and is not severe. Further, more than half the computed difference resulted from the variation of K19 (compare models A and A′ for case 2). However, in the case of minimizing O_3 destruction (model C), an NO_x injection at 17 km resulted in an *increase* in O_3 equal to about 25% of the decrease in the base case. For a 35-km injection of NO_x all of the models predicted an O_3 decrease, the model C decrease being about 40% as large as that of model A. Thus, the range of predicted effects is small for a high altitude injection, and the uncertainty is modest for maximizing the effect of an NO_x injection; however, the uncertainty is very substantial (encompassing a reversal of the effect) in the case of minimizing the effect of a given NO_x injection at low altitudes.

If it were necessary to vary all 33 thermal rate coefficients to the limit of their uncertainty in order to obtain this reversal, the expectation of its being realized would be almost nonexistent. However, we examined the results of the model C computation and were able to identify several key parameters that are responsible for the reversal of the calculated effect. We found in model C that at low altitudes O_3 is regulated primarily by the HO_x cycle and that the most important parameters were those regulating the HO_x concentrations, the reactions of HO_x with odd oxygen, and the reactions

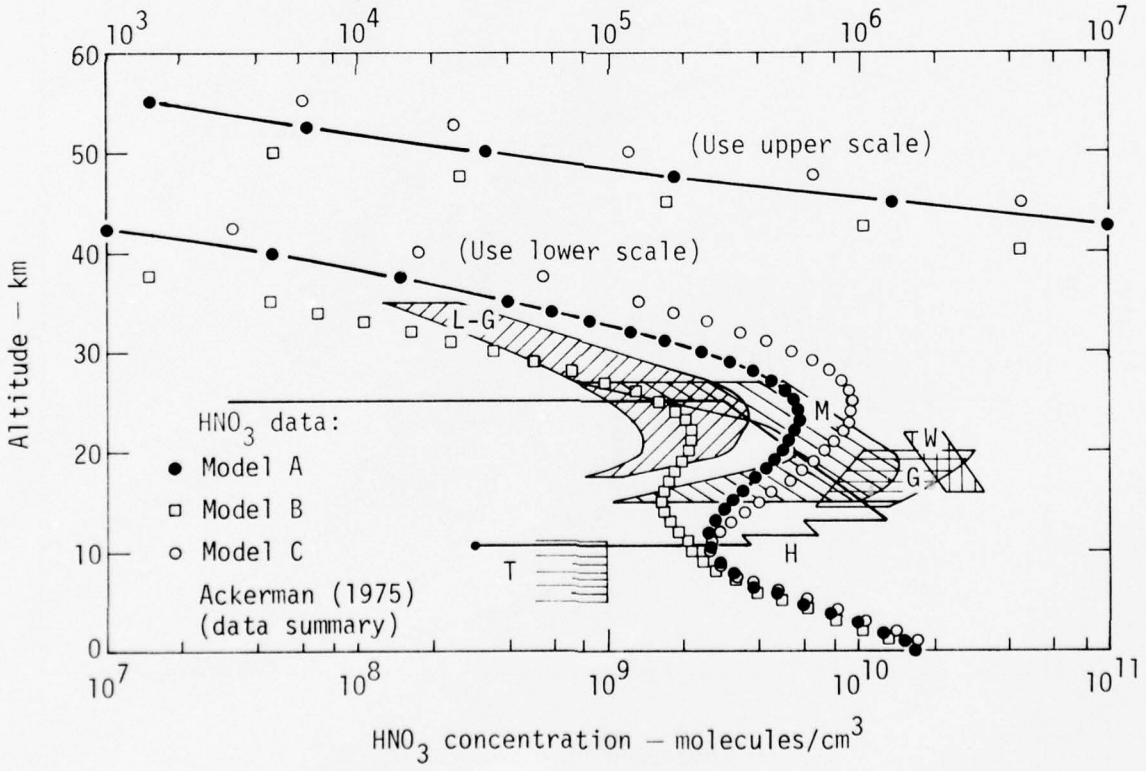

Fig. 6. Calculated equilibrium concentration profiles for HNO_3 compared with data summary of Ackerman (1975).

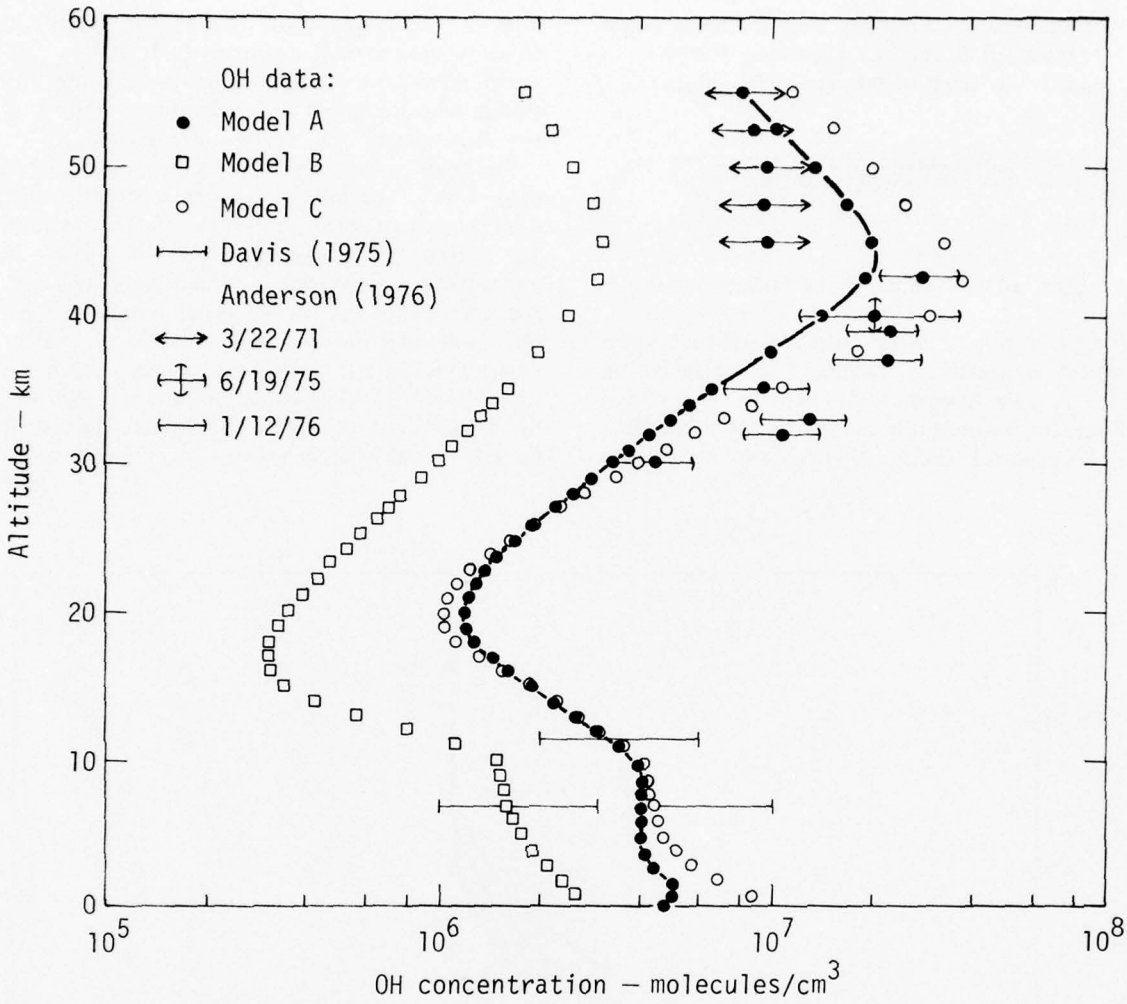

Fig. 7. Calculated equilibrium concentration profiles for OH compared with observations by Anderson (1976) and Davis (1975). Most of Anderson's data were taken at high zenith angles, whereas Davis's data were taken at low zenith angles. Thus, the "half-sun" correction should not be applied in making comparisons with the Anderson data.

$$HO_2 + NO \rightarrow NO_2 + HO \qquad \text{(K26)}$$

and

$$HO + NO_2 \xrightarrow{M} HNO_3. \qquad \text{(K20)}$$

These reduce the efficiency of the NO_x and HO_x cycles in the lower stratosphere where the NO_x destruction cycle is already inefficient because NO_2 is usually photolyzed there resulting in the regeneration of odd oxygen.

To improve our understanding we have sought to separate the odd oxygen destruction roles of the Chapman, NO_x, and HO_x cycles. Since the cycles are known to be coupled (e.g., the NO_x and HO_x cycles are coupled through K20, K21, and K26), it is unclear which quantities would be most illuminating. As a beginning we have defined the net odd oxygen destruction rate (D) of each of the cycles as follows:

$$D(\text{Chapman}) \equiv 2K2[O][O_3].$$

(O_2 photolysis is omitted because we wish to compare destruction terms.)

$D(NO_x) \equiv K3\,[NO][O_3] + K4\,[NO_2][O] + K25\,[NO][O][M] + K29\,[NO_2][O_3] - J4\,[NO_2] - J6\,[NO] - K7\,[N][O_2] - K8\,[N][NO] - K24\,[N][NO_2] + K28\,[N][O_3] - J10\,[NO_3]$ (if Branch 1 is assumed).

(All reactions involving [N] are trivial below 50 km, as is also NO photolysis; $J10[NO_3]$ is treated as equal to the rate of NO_3 formation.)

$$D(HO_x) \equiv K12\,[O_3][OH] + K13\,[O][OH] + K14\,[O_3][HO_2] + K15\,[O]\,[HO_2] + K17\,[O_3][H] + K10\,[O^1D][H_2O] - K27\,[OH]^2 - J9\,[HO_2]$$

(The last two terms are of little significance.)

Vertical profiles of these quantities evaluated under ambient or equilibrium conditions of models A_2, B, and C_2 are compared in Fig. 9. The largest differences between the models appear in $D(HO_x)$, in D(Chapman) above 40 km, and in $D(NO_x)$ below 27 and above 45 km. Table 4 was prepared to reflect these differences quantitatively. It gives for each model the relative fraction of the integral (over the altitude range indicated) of the odd oxygen destruction rate ascribable to each of the three cycles.

The model most comparable to the models used in CIAP is A'_1. The instantaneous rates widely quoted from Johnston (1975) are included for comparison. The differences in results reflect differences in methodology and definitions as well as differences in rate coefficients and species concentration profiles. Our results were obtained from a 1-D time-dependent model with coupled kinetics and transport extending from 0 to 55 km using photolysis rates averaged over the diurnal cycle by taking half the rates calculated for a 45° zenith angle. Johnston's values were obtained

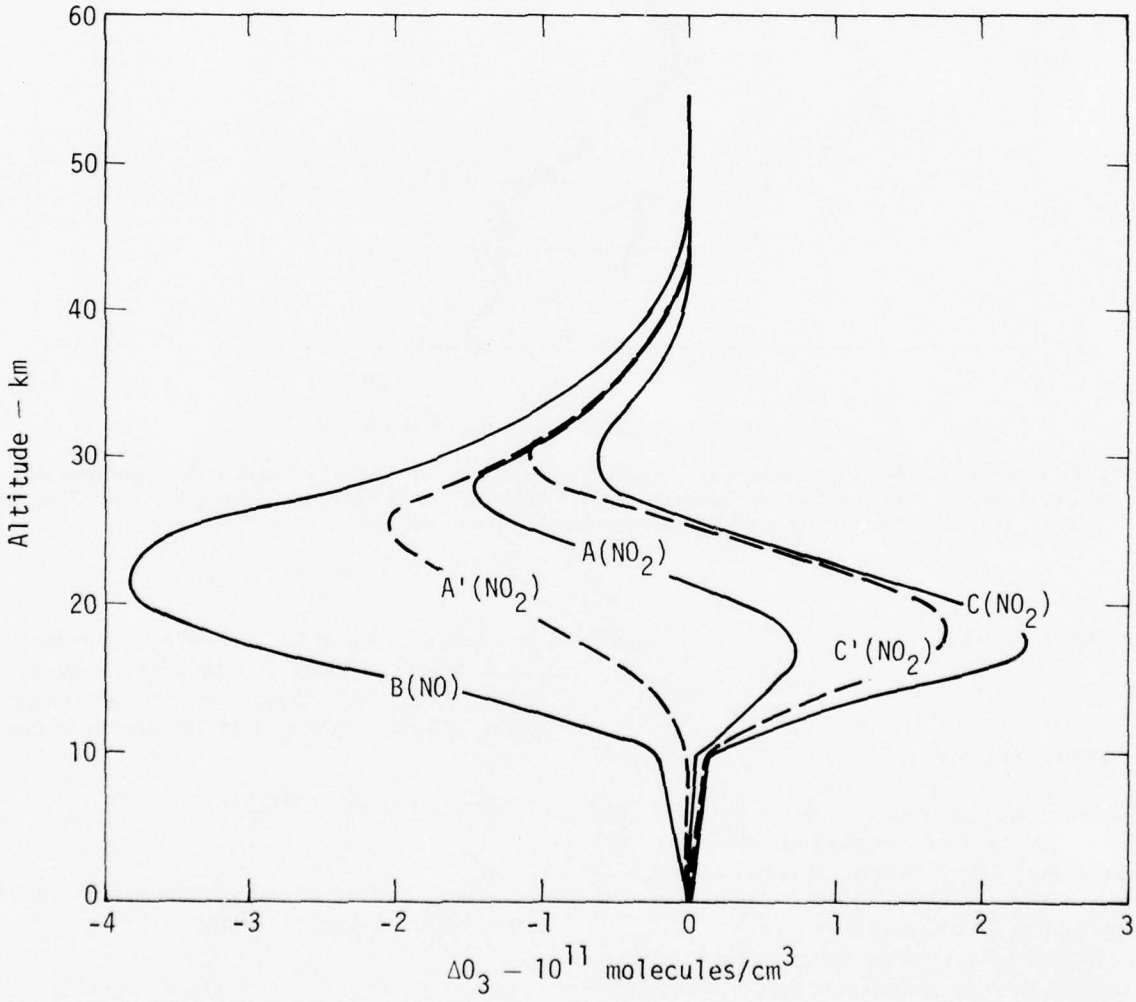

Fig. 8. Calculated perturbations in the O_3 profile for a 17-km injection of NO_x (case 2) plotted as departures from the ambient profiles (case 1) of the models indicated.

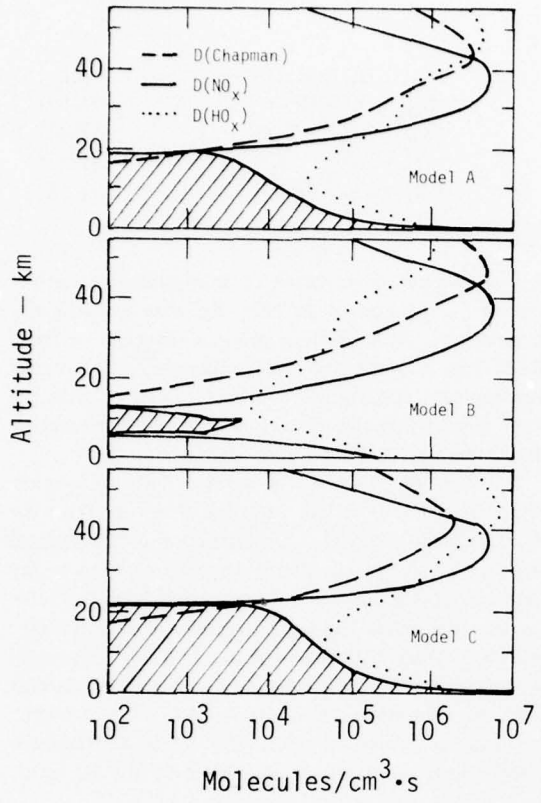

Fig. 9. Calculated equilibrium profiles of odd oxygen destruction rates as defined in text for models A, B, and C. Where $D(NO_x)$ forms cusps at the left border, it changes sign. Regions of net ozone production by NO_x are shaded.

from a nondynamic model integrated between "tropopause" and 45 km, but using photolysis rates for specific altitudes, latitudes, and times of day. Little quantitative significance should be attached to these integrated destruction rates since they do not accurately reflect the relative importance of the various processes in determining total O_3. In an effort to estimate the relative importance of these processes in determining total column densities, we have weighted the various local destruction rates by the product of the local O_3 concentration and the local lifetime* for each level and integrated the results from 11 to 55 km. These weighted loss rates are insensitive to the choice of the integration limits so long as the top is above 45 km and the bottom is below 12 km.

In an effort to identify the most sensitive reactions we generated additional models by varying smaller subsets of the 33 K's listed in Table 1. We found that varying as few as three rates, K14, K18, and K26, was sufficient for an NO_x injection at 17 km to produce an increase rather than a decrease in the O_3 column. Model C' uses the values of the three K's cited above plus K20 from model C and the rest from model A. As seen in Table 2 this is sufficient for a 17-km injection of NO_x to produce an O_3 increase more than one-third as large as that produced in model C.

We also examined the effect of increased stratospheric water vapor both alone and in

*The local O_3 lifetime was defined as the ratio of the local O_3 concentration to the arithmetic sum of the net chemical loss rates and the flux of O_3 through each level.

Table 4. Relative fractions of integrated odd oxygen destruction rates ascribable to the Chapman, NO_x, and HO_x cycles for various models over the indicated domains. For "weighted" integrations the loss terms for each level were multiplied by the local O_3 concentration and the local lifetime (lifetime determined by both chemistry and transport)

Model	D (Chapman)			D (NO_x)			D (HO_x)		
	11-50 km	11-45 km	Weighted 11-55 km	11-50 km	11-45 km	Weighted 11-55 km	11-50 km	11-45 km	Weighted 11-55 km
B	0.37	0.26	0.05	0.58	0.71	0.90	0.05	0.03	0.05
A_2'	.36	.29	.06	.50	.62	.81	.15	.09	.13
A_1	.24	.23	.07	.43	.53	.66	.33	.24	.27
A_2	.24	.23	.07	.43	.52	.64	.33	.24	.29
C_2'	.25	.23	.09	.40	.50	.50	.35	.27	.41
C_2	0.13	.14	0.07	0.32	.38	0.45	0.55	.48	0.49
Johnston (1975)[a]	–	0.17	–	–	0.70	–	–	0.12	–

[a]Johnston used a nondynamic model to simulate a three-dimensional system. His integration was between a variable tropopause and 45 km.

combination with an NO_x injection at 17 km. As can be seen in Table 2 (case 5 compared to case 1), a 10% increase in stratospheric water vapor increased the O_3 column in model B and decreased it in A, C', and C. When the increased water vapor was imposed on a 17-km NO_x injection, the effects on the O_3 column were almost additive (case 6 compared to cases 2 and 5).

These experiments have led us to the following conclusions:

1. A value of 2×10^{-11} cm^3/s for K19 leads to an O_3 reduction due to a fixed NO_x injection less than half that predicted during the CIAP program.

2. The matching of computed profiles of species concentration against observations does not at present provide a definitive criterion for choosing between models, even for models as different in their response as those described here. However, HNO_3, OH, and HO_2 differ most between the models and thus would provide the sharpest discriminators if observational data were of equal quality for all species. The observed OH data are more easily consistent with the lower value for K19.

3. Species concentration profiles must be known to better than a factor of 2 before they can be used to discriminate between models differing widely in sensitivity to NO_x injections.

4. The reactions

$$HO_2 + HO \rightarrow H_2O + O_2, \quad (K19)$$
$$HO_2 + O_3 \rightarrow HO + 2O_2, \quad (K14)$$
$$HO_2 + HO_2 \rightarrow H_2O_2 + O_2, \quad (K18)$$
$$HO_2 + NO \rightarrow NO_2 + HO, \quad (K26)$$
$$HO + NO_2 \xrightarrow{M} HNO_3 \quad (K20)$$

are of greatest importance in determining the effect on the O_3 column of an NO_x injection in the lower stratosphere. None of these processes (except, perhaps, K20) has a well-established rate coefficient under stratospheric conditions. The best chance of reducing these uncertainties is through very accurate laboratory determinations of these rate coefficients.

5. Finally, it is worth noting that uncertainty resulting from imperfect knowledge of the rates for the Chapman and NO_x O_3 destruction cycles is small (less than a factor of 2); the largest variations in the model results arose from the uncertainty in the rates for the HO_x cycle and the processes coupling the NO_x and HO_x cycles. It is also suggested in Table 2 (case 5, models A and C) that for sets of rate coefficients that tend to minimize the response to NO_x, a major injection of water vapor in the lower stratosphere could significantly reduce the depth of the O_3 layer.

2.2 SENSITIVITY OF OZONE REDUCTION FROM CHLOROFLUOROMETHANES TO PARAMETER UNCERTAINTIES

Since the effect of chlorofluoromethanes (CFM's) on atmospheric ozone was initially predicted by Molina and Rowland (1974), a number of papers have been published (for example, Wofsy et al. 1975, Crutzen and Isaksen 1975, Turco and Witten 1975) describing investigations of these effects made with various one-dimensional models of the stratosphere. In this study, we examined the sensitivity of one such 1-D stratospheric model to uncertainties in some of the important parameters used in it. In particular, we examined the sensitivity of the effect of $CFCl_3$ and CF_2Cl_2 on total global ozone due to changes in key chemical rates and diffusion coefficients.

The calculations in this study were made with LLL's one-dimensional time-dependent model of the troposphere and stratosphere. In this model 92 chemical (and photochemical) reactions are used to dynamically describe the stratospheric vertical distributions of 20 minor atmospheric species ($O(^3P)$, O_3, NO, NO_2, N_2O, HNO_3, OH, HO_2, H_2O_2, Cl, Cl_2, ClO, ClO_2, OClO, ClNO, $ClNO_2$, HCl, CCl_4, CF_2Cl_2, and $CFCl_3$) while three (H, N, $O(^1D)$) are assumed to be in instantaneous equilibrium. Vertical distributions of N_2, O_2, H_2O, CH_4, and H_2 were assumed constant throughout the calculations.

The chemical rates for six reactions important to the chlorine cycle are shown in Table 5. Other reaction rates in the model are based on the review by Hampson and Garvin (1975). Solar flux, absorption cross sections, and the calculation of photodissociation rates are as described by Gelinas (1974).

Sensitivity to Diffusion Coefficients

The vertical transport in a one-dimensional "globally" averaged model of the stratosphere is parameterized through the so-called eddy diffusion coefficient. There does not yet exist a unique approach for the derivation of a suitable set of eddy diffusion coefficients, and each modeler has his own justification for choosing a particular diffusion profile. Because there are no unambiguous reasons for choosing one profile over another, the sensitivity of the model to that choice must be examined. The various diffusion coefficients used in this study are shown in Fig. 2.

Table 5. Rates used for key reactions

Reaction	Rate	Source
$Cl + O_3 \rightarrow ClO + O_2$	$2.97 \times 10^{-11} \exp(-243/T)$	Average of Davis et al. (1975) and Anderson et al. (1975)
$ClO + O \rightarrow Cl + O_2$	5.3×10^{-11}	Watson (1974)
$Cl + CH_4 \rightarrow HCl + CH_3$	$5.4 \times 10^{-12} \exp(-1133/T)$	Davis et al. (1975)
$OH + HCl \rightarrow H_2O + Cl$	$2.0 \times 10^{-12} \exp(-310/T)$	Anderson et al. (1975)
$ClO + NO \rightarrow Cl + NO_2$	$2.6 \times 10^{-11} \exp(-50/T)$	Anderson et al. (1975)
$OH + HO_2 \rightarrow H_2O + O_2$	2×10^{-11}	Low value quoted by Hampson and Garvin (1975)

For each of the three diffusion coefficients (Chang 1974, Crutzen and Isaksen 1975, and Wofsy 1975), the following series of calculations was carried out: (1) a natural atmosphere containing no chlorine, (2) a natural atmosphere containing chlorine assuming an HCl mixing ratio of 10^{-9} by volume at the surface and a constant CCl_4 flux at the surface, and (3) model 2 plus the fluorocarbons $CFCl_3$ and CF_2Cl_2 introduced at the surface starting in 1950 and running through 1975 based on world fluorocarbon production data (McCarthy 1974).

In addition possible scenarios beyond 1975 have been examined with model 3: (3a) continued growth in fluorocarbon production at a rate of 10% per year, (3b) continued constant production at the 1973 production levels, (3c) continued constant production at one-half of the 1973 production level, (3d) constant production at 1973 level until a sharp cutoff in 1978 or in 1983 (model 3e).

In comparing the calculations for the three diffusion profiles, it was found that when compared to their respective chlorine-free atmospheres the inclusion of chlorine caused a reduction of total ozone of 0.50% for the Chang profile, 0.56% for the Crutzen profile, and 0.62% for the Wofsy profile. With the chlorofluoromethanes (model 3) at the end of 1975 there is a calculated reduction in total ozone (relative to the respective chlorine-containing atmospheres, model 2) of 0.77% with the Chang profile, 1.08% with the Crutzen profile, and 1.00% with the Wofsy profile. These results indicate an uncertainty due to choice of eddy diffusion profiles of approximately a factor of 0.83 to 1.17 from the mean in the ozone reduction predicted at the end of 1975. Inclusion of other natural sources of stratospheric chlorine omitted in this model would only alter the baseline level of O_3 and have minimal effect on the predicted perturbations due to chlorofluoromethanes, especially with respect to this relative uncertainty.

The differences in predicted effects using the different diffusion profiles can be attributed to the different rates at which free chlorine (created by the photodissociation of $CFCl_3$ and CF_2Cl_2 mostly above 30 km) is transported to levels below 30 km. The Crutzen and Wofsy profiles allow more rapid transport of the free radical chlorine to levels where the chlorine catalytic cycle has its strongest effect on stratospheric ozone.

Figure 10 shows the reduction in total ozone calculated for the case of a continued growth in $CFCl_3$

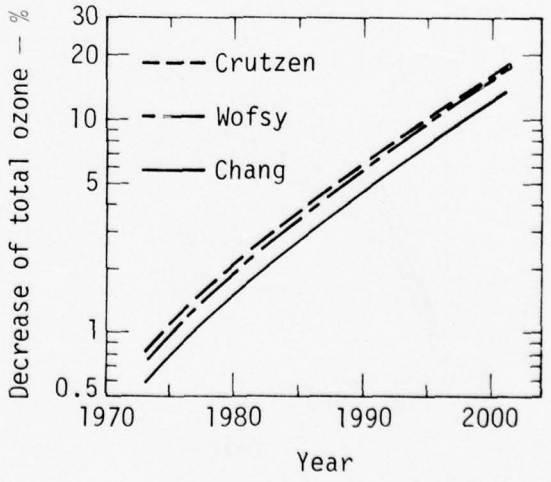

Fig. 10. Sensitivity to the diffusion profile assumed is shown in these calculations of the decrease in total ozone that would result from a continued growth of 10% per year in chlorofluoromethane production beyond 1975.

and CF_2Cl_2 production beyond 1975 of 10% per year (model 3a) which corresponds to approximately a seven-year doubling time. As is expected, all predicted perturbations increase exponentially. For this scenario, the reduction of global total ozone is 5.0 to 6.92% by the end of 1990 and 13.6 to 17.8% by the year 2000. It is significant to note that there is only a three-year difference among the predictions as to the time when a given reduction in ozone is reached.

A constant production rate at 1973 levels for the chlorofluoromethanes (model 3b) was assumed in the calculated total ozone reductions shown in Fig. 11. The shaded area shows the range of ozone projections as a function of time when the 1973 production rate is used. The time after 1975 to reach a total ozone depletion of 5% ranges from 23 to 33 years, depending on the choice of diffusion profile. By the year 2000, there is a range of uncertainty of 1.3% (5.3%, Wofsy; 4%, Chang) in the predicted reduction in total ozone. Also shown in Fig. 11 is the calculated ozone depletion resulting from a constant production rate at one-half the 1973 level (model 3c). At this lowered release rate, a meaningful uncertainty range can be assigned to the projected steady-state values as well as the times needed to approach them. The different eddy diffusion models lead to ultimate ozone depletions of 6.5% (Chang) to 7.8% (Wofsy). For both scenarios the characteristic times differ very little; the time needed to reach one-half the final equilibrium depletion is 38 years for the Chang diffusion and 34 years for the Wofsy diffusion.

The effect of stopping production of the chlorofluoromethanes is shown in Fig. 12. For this case (model 3d) constant production at 1973 levels was assumed until the end of 1978 when all releases were assumed to cease. For each of the tested diffusion profiles, the destruction of ozone continues for some time following the stopping of production. This happens because the troposphere, acting as a reservoir, continues to furnish a source of $CFCl_3$ and CF_2Cl_2 to the stratosphere. The minimum in the total ozone level occurs approximately at 8 to 13 years after production is halted, depending on the choice of the diffusion profile. At the peak reduction in ozone, there was a calculated range of 0.60-0.83% additional ozone destroyed from the 1978 levels, resulting in a peak ozone reduction ranging from 1.75 to 2.32%. As seen in Fig. 12, it takes 55 to 75 years (i.e., until 2033 or 2053) to return to the already reduced ozone levels of 1978 (when production was halted). For the three diffusion profiles studied, if the release of chlorofluoromethanes were halted in 1978, ozone reduction would continue for another decade (with an uncertainty of ±3 years) to a peak ozone reduction a factor of 1.5 greater than the 1978 reduction, and it would take 55-75 years to return to the 1978 ozone concentrations.

With production at 1973 levels continued until the end of 1983, total ozone continues to fall for 7-10 years with a peak reduction ranging from 2.4 to 3.2% (approximately 30% greater than the 1983 values), and it would take 33-50 years to return to

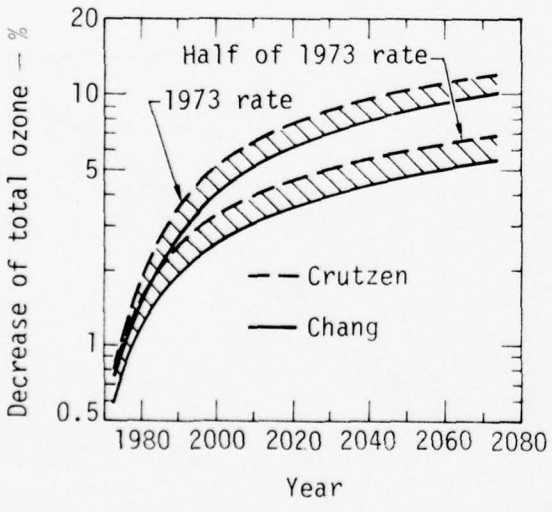

Fig. 11. Calculated decrease in total ozone that would result from a constant production of chlorofluoromethanes at the 1973 rate and at one-half the 1973 rate. Shaded bands show range of values resulting from assumption of different diffusion profiles.

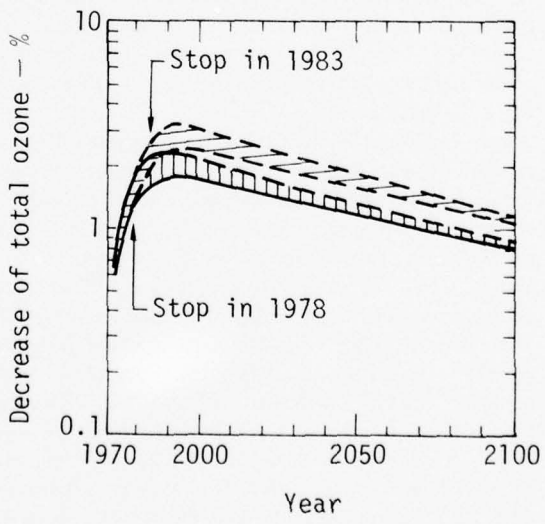

Fig. 12. Calculated decrease in total ozone that would result if chlorofluoromethane production were stopped in 1978 or in 1983. Shaded bands show range of values resulting from assumption of different diffusion profiles.

the reduced 1983 ozone levels. Consequently, a five-year delay in halting production of chlorofluoromethane would entail an increase in peak ozone reduction by a factor of 1.4 lasting over an additional period of 30-50 years.

Sensitivity to Reaction Rates

Another uncertainty to be examined is the sensitivity to key reaction rate coefficients important to stratospheric chlorine chemistry. For each of six reactions, currently used rates were changed to test the sensitivity to potentially controversial rate choices. As a reference case the diffusion profile labeled Chang was used in each of these calculations. Because of this, it is the ratio of the change in O_3 relative to the standard case rather than the absolute magnitude that is of interest. It is reasonable to expect that similar fractional changes would hold for the other diffusion profiles, although the actual reductions would be somewhat different.

For the reaction $Cl + O_3 \rightarrow ClO + O_2$, the currently used value in the model is an average of two recent measurements by Davis et al. (1975) and Anderson et al. (1975). Both of these measurements agree quite well at stratospheric temperatures. However, until recently the value used for this reaction in most models (e.g., in the model of Wofsy et al. 1975) was 1.85×10^{-11}, the value given in the Watson (1974) chlorine chemistry review. Using this rate in our model, we found that the reduction in ozone by the end of 1975 increased by a factor of 1.56. Since the rates examined have a ratio of approximately 1.7 at stratospheric temperatures, the change in the ozone perturbation was nearly proportional to the increase in the rate of this reaction.

To study the sensitivity to the reaction $ClO + O \rightarrow Cl + O_2$, we varied the reaction rate coefficient from the value in Watson (1974) of 5.3×10^{-11} to a value approximately 17% lower, 4.4×10^{-11}. The reason for choosing this lower value is that it represents a recent preliminary measurement for this reaction at the University of Pittsburgh (Kaufman, private communication, 1975). With the lower value the 1975 calculated reduction in ozone was reduced by a factor of 0.88.

The rate coefficient for the reaction $ClO + NO \rightarrow Cl + NO_2$ currently used in our model, $2.6 \times 10^{-11} \exp(-50/T)$, is based on recent measurements at the University of Pittsburgh (F. Kaufman, private communication, 1975). Until recently, the rate coefficient recommended in Watson (1974), 1.7×10^{-11}, was used. With the value of 1.7×10^{-11}, the calculated reduction in total ozone for the end of 1975 increased by a factor of 1.13.

The measurement by Davis et al. (1975) of $5.4 \times 10^{-12} \exp(-1133/T)$ for the rate coefficient of the reaction $Cl + CH_4 \rightarrow HCl + CH_3$ is the value currently used in our model. However, there is still uncertainty regarding this quantity. It differs from the earlier measurement recommended by Watson (1974), $5.6 \times 10^{-11} \exp(-1790/T)$. This rate coefficient has a large effect on the 1975 reduction of total ozone, the old value leading to an ozone reduction about a factor of 1.4 greater than the new value used in our base case.

The $OH + HCl \rightarrow H_2O + Cl$ reaction rate coefficient of $2 \times 10^{-12} \exp(-310/T)$ measured by Anderson et al. (1975) is the one currently used in our model. It agrees well at stratospheric temperatures with the value of $2.8 \times 10^{-12} \exp(-410/T)$ recommended in Watson (1974). Using the Watson rather than the Anderson et al. value changes the 1975 reduction in ozone by a factor of 0.96.

The reaction $OH + HO_2 \rightarrow H_2O + O_2$ is extremely important in determining the amount of stratospheric hydroxyl, OH. The OH distribution likewise is important in determining the conversion rate of HCl to atomic chlorine available for the ozone-destroying catalytic cycle. Though the rate coefficient for this reaction has not been directly measured, there are data which support a range of values (as recommended in Hampson and Garvin 1975), from 2×10^{-11} to 2×10^{-10}. Theory and combustion experiments tend to support the lower part of the range, although the lower temperature experiments support the high end of the range. If the range of values for this rate coefficient are used in the 1-D model, it is found that the 1975 reduction in total ozone is reduced by a factor of 0.32 for the faster rate of 2×10^{-10}. The range of uncertainty for the reaction $Cl + HO_2 \rightarrow HCl + O_2$ may also be large, but was not examined in this study. Only the estimated rate of 3×10^{-11} cm^3/s was used (this rate coefficient has not been measured).

Another sensitivity that is of interest is the possible presence of synergistic effects when several rate coefficients are varied. One test of this is to study the cumulative uncertainty in the rates of these reactions by choosing the rates of the six reactions such that they would maximize or minimize the effect on total ozone. Using the previously discussed values, the rates were chosen in the following manner:

	Maximize	Minimize
$Cl + O_3$	HI	LO*
$ClO + O$	HI*	LO
$ClO + NO$	LO	HI*
$Cl + CH_4$	LO	HI*
$OH + HCl$	HI*	LO
$OH + HO_2$	LO*	HI

*Indicates base case rates shown in Table 5.

HI and LO refer respectively to the faster and slower rate at stratospheric temperatures. An approximate factor of 9 was found for the ratio of predicted 1975 ozone reduction in the two extreme cases. This agrees well with the bounds obtainable through direct multiplicative superposition of the individual sensitivity factors, i.e., (1.56)(1.42)(1.13) = 2.5 versus the direct maximum factor of 2.3 and (0.88)(0.96)(0.31) = 0.26 versus the direct minimum factor of 0.25. Consequently, we conclude that there is no important synergistic effect among these six reaction rates. It should be emphasized that this max-min uncertainty range was obtained by taking some extreme values in reaction rate coefficients and does not represent the "most probable" range of uncertainty. In fact, using the individual sensitivity factors as reported above and some reasonable estimates for the expected uncertainty in individual rate coefficients, one could derive a "most likely" uncertainty range that could be significantly smaller than the present max-min range.

All of the above uncertainty analysis applies to the calculation of the ozone reduction in 1975. This provides a basis for estimating the uncertainty in the steady-state ozone reduction that is calculated in a constant-production scenario. With a constant rate of injection of CFM's into the atmosphere, the approach to the steady state of percent ozone reduction is shown in Fig. 11. These curves are well described by an exponential expression of the form $A(1 - e^{-\lambda t})$. The time-dependent term, $e^{-\lambda t}$, represents the atmospheric residence time. For the CFM's this residence time, $1/\lambda$, depends predominantly on the eddy diffusion coefficients (which determine the rate of CFM injection into and the HCl removal from the stratosphere) and on the rate of CFM photolysis. For ozone reductions less than 15%, $1/\lambda$ depends only weakly on the chemical rate constants since the amount of HCl in the stratosphere is nearly unaffected by changes in these constants. On the other hand, these rate constants strongly affect the catalytic chain length for ozone destruction, which appears in the multiplicative constant A. This implies that a change in rate constant has, to a good approximation, the effect of a linear scaling of the entire time-dependent curve. Thus, the relative uncertainties estimated for the 1975 ozone reductions are applicable to the steady state limit of a constant-production scenario.

It should be noted that these experiments did not examine the full range of uncertainties associated with the chemical rate inputs to the model. Each of the other 86 reactions in the model has some uncertainty, and numerous reactions are omitted from the model either because there are no available data or because the reactions are considered insignificant. A "maximum" and "minimum" analysis for the complete reaction set could lead to unrealistic profiles for many species in the ambient atmosphere. Such simulations have not been carried out. The sensitivity of the model to omitted processes (e.g., heterogeneous reactions, ionic reactions) remains at present an uninvestigatable problem, and potentially a serious source of error in stratospheric models.

Among the reactions that were studied, $OH + HO_2 \rightarrow H_2O + O_2$ stands out as the most critical. Since the stratospheric OH concentration is very sensitive to the precise value of this reaction rate coefficient and since direct laboratory measurements of this rate coefficient are very difficult, a good *in situ* measurement program may provide some very useful, although indirect, data to narrow the range of uncertainties involved.

2.3 SOLAR ABSORPTION IN A STRATOSPHERE PERTURBED BY NO_x INJECTION

While much attention has been directed toward nitrogen dioxide as a chemical reactant capable of reducing the ozone layer of the stratosphere, little attention has been directed toward its role as an absorber of solar radiation. Solar absorption by nitrogen dioxide had not been expected to be significant compared with solar absorption by ozone because many radiative equilibrium models have generated reasonable stratospheric temperature profiles without including nitrogen dioxide (e.g., Manabe and Strickler 1964). However, as will be shown, the increase in solar absorption by nitrogen dioxide may counteract a significant fraction of the decrease in solar absorption by ozone following stratospheric injection of NO_x (oxides of nitrogen).

The radiative transfer model used for these calculations assumes a cloudless, plane-parallel atmosphere in which there is molecular multiple scattering and gaseous absorption above an isotropically scattering ground. The wavelength region between 187.2 and 735 nm, in which molecular oxygen, ozone, and nitrogen dioxide are the dominant gaseous absorbers, is divided into 119 spectral intervals. The atmosphere between 0 and 55 km is divided into 43 layers, which are 1 km thick up to 35 km and 2.5 km thick from 35 to 55 km. Each atmospheric layer is divided into sublayers which have an optical depth, including scattering and absorption, of less than 0.02. There may be as many as 500 sublayers depending upon the total optical depth of the

atmosphere. The Gauss-Seidel iterative scheme is used to solve the radiative transfer equation to obtain the radiative intensity at increments of 6° in the local zenith angle at each level. Components of the radiative intensity are then integrated over the upper and lower hemispheres to obtain the diffuse fluxes.

The absorption cross sections were derived from a variety of sources described in Gelinas (1974). The vertical profiles of temperature, pressure, and oxygen concentration correspond to the U.S. Standard Atmosphere (1962), and the concentration profiles for O_3 and NO_2 were derived from transport-kinetics calculations.

The two cases considered are NO_x injections (as NO_2) at 17 or 20 km at the rate of 2000 molecules/cm^3·s uniformly distributed over a 1-km-thick layer. This injection rate (2.5×10^{12} g/year) corresponds to that of a fleet of several thousand supersonic transports (Grobecker et al. 1974). The stratospheric column densities of O_3 and NO_2 for each of the three cases are shown in Table 6. The unperturbed O_3 profile corresponds to

Table 6. Stratospheric column densities (above 13 km) for O_3 and NO_2 (molecules/cm^2)

Case	O_3	NO_2
Unperturbed	7.92×10^{18}	4.06×10^{15}
17-km injection	7.50×10^{18}	5.43×10^{15}
20-km injection	7.03×10^{18}	6.80×10^{15}

0.305 atm·cm of O_3. The 17-km injection corresponds (by model calculation) to a 5.3% reduction in stratospheric O_3 and a 33.7% increase in stratospheric NO_2, whereas the 20-km injection corresponds to an 11.2% reduction in O_3 and a 67.5% increase in NO_2. In each case, the fractional change in the NO_2 column density is approximately six times the fractional change in the O_3 column density.

For each of the three sets of concentration profiles, O_3 and NO_2 solar absorption rates were computed for values of the solar zenith angle θ ranging from 0° to 78° and values of the surface albedo a_s ranging from 0 to 1. For the unperturbed case, the stratospheric O_3 absorption ranged from 2.95% ($\theta = 0°$, $a_s = 0$) to 7.23% ($\theta = 78°$, $a_s = 1$) of the incoming solar radiation. For the unperturbed case, the stratospheric NO_2 absorption ranged from 0.072% ($\theta = 0°$, $a_s = 0$) to 0.365% ($\theta = 78°$, $a_s = 1$) of the solar radiation incident at the top of the atmosphere. This result verifies that the solar absorption by NO_2 is normally only a small fraction (0.024 to 0.050) of the solar absorption by O_3.

The ratio of the increase in stratospheric solar absorption by NO_2 (with respect to the unperturbed case) to the decrease in absorption by O_3 is given in

Table 7. The ratio of the increase in NO_2 absorption to the decrease in O_3 absorption for a surface albedo of 0.25

Case	Solar zenith angle			
	0°	30°	60°	78°
17-km injection	0.38	0.40	0.45	0.50
20-km injection	0.35	0.37	0.41	0.47

Table 7 for selected solar zenith angles and a surface albedo of 0.25. This ratio varies significantly with solar zenith angle but only slightly with surface albedo. The ranges of this ratio for the 17- and 20-km injections indicate that the increase in NO_2 absorption significantly compensates (30-50%) for the decrease in O_3 absorption.

The change in stratospheric composition increases the solar radiation transmitted to the troposphere, resulting in increased tropospheric heating. More radiation is scattered upward from the troposphere and a larger fraction of this radiation escapes to space because of the increased transmission of the stratosphere. This leads to an increase in the planetary albedo and a decrease in the net solar heating of the atmosphere/earth system. An analysis of the perturbed solar radiation budget for the 20-km injection case is shown in Fig. 13 for a solar zenith angle of 60°. The increase in stratospheric absorption by NO_2, the increase in tropospheric heating, and the increase in radiation lost to space combine to equal the decrease in stratospheric absorption by O_3. The relative magnitudes of these various components vary with surface albedo. For small values of surface albedo, most of the net decrease in stratospheric heating goes into increased tropospheric heating. For large values of surface albedo, most of the net decrease in stratospheric heating is lost to the system as radiation scattered to space. The increase in NO_2 absorption is approximately a constant fraction of the decrease in O_3 absorption for all values of surface albedo, as was previously mentioned.

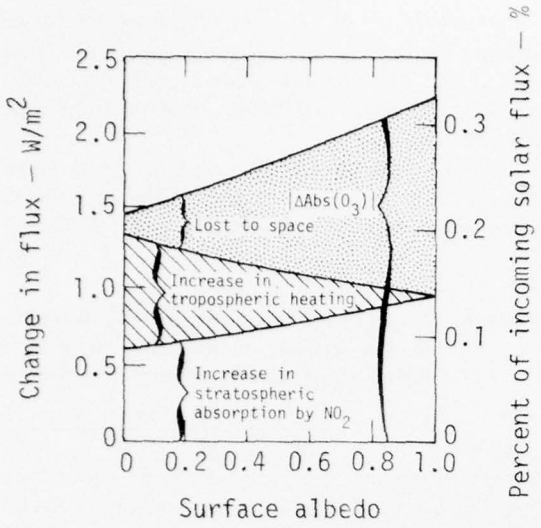

Fig. 13. Calculated decrease in stratospheric absorption by O_3 (upper curve) and the three components that make up this quantity as a function of surface albedo. This example is for the 20-km injection case and a solar zenith angle of 60°.

Although perturbations to the stratospheric composition due to NO_x injection lead to increased solar heating of the troposphere, it does not necessarily follow that these perturbations cause an increase in surface temperature. Perturbations to the longwave (IR) radiation budget must also be considered when computing changes in surface temperature. Because of the reduction in solar heating of the stratosphere, the stratospheric temperature will decrease. This reduction in emitting temperature combined with the reduction in ozone concentration results in a decrease in the downward longwave radiative flux entering the troposphere. This cooling effect tends to counteract the increased solar heating of the troposphere. Ramanathan et al. (1975) found that the longwave effect dominates the solar effect for global mean conditions. Using a radiative-convective model and a perturbation similar to the 20-km injection case, they computed a change in surface temperature of −0.1 K.

At biologically important wavelengths (280-320 nm), solar absorption by NO_2 has only a small effect on the amount of solar radiation reaching the earth's surface. In this spectral region the optical thickness of O_3 is several orders of magnitude greater than the optical thickness of NO_2; thus the flux of UV-B radiation incident at the earth's surface is much more sensitive to changes in O_3 column density. Neglecting solar absorption by NO_2 leads to a slight overestimate of the biological effects from stratospheric injection of NO_x. For the 17- and 20-km injection cases considered, neglecting solar absorption by NO_2 caused the change in UV-B radiation at the earth's surface to be overestimated by 2%.

The fact that a significant fraction of the decrease in net stratospheric heating is lost to the system as radiation scattered to space has important implications for radiative equilibrium models and climatic models dependent on radiative energy balance calculations. The effect on planetary albedo of changes in atmospheric composition must be included to accurately compute the perturbed solar radiation budget. Not including the albedo effect may even lead to predicted changes in surface temperature of the wrong sign (Ramanathan et al. 1975). The effect of solar absorption by NO_2 should also be included in these models for case studies involving significant changes in NO_2 column density. Other species, such as water vapor and aerosols, should also be included in more complete analyses of SST effects, but they would not affect the qualitative results presented here.

2.4 EFFECT OF NO PHOTOLYSIS ON NO_y MIXING RATIOS

It has been suggested that the only significant sink for odd nitrogen in the stratosphere is through transport of HNO_3 to the troposphere. As a result, if NO were to be injected in the middle or lower stratosphere, the change in odd nitrogen ($NO_y \equiv NO + NO_2 + HNO_3 + N$) mixing ratio above the height of injection would be nearly constant (National Academy of Sciences 1975b, pp. 114-119).

Photolysis of nitric oxide and the subsequent reactions of nitrogen atoms with nitric oxide act as a sink for odd nitrogen in the upper stratosphere. This paper reports an investigation of the importance of this net NO_y sink by means of a one-dimensional transport-kinetics model (Chang et al. 1974). In this model the reactions

$$NO \xrightarrow{h\nu} N + O,$$
$$N + NO \rightarrow N_2 + O,$$
$$N + NO_2 \rightarrow N_2O + O$$

provide a chemical sink for odd nitrogen in the upper stratosphere. Using the Chang (1974) eddy diffusion profile, a parameterization of NO photolysis as shown by Cieslik and Nicolet (1973), and the chemical reactions used by Duewer et al. (1976), we carried out the following experiments:

1. We computed an ambient NO_y mixing ratio and a perturbed NO_y mixing ratio due to an injection of NO at a rate of 2000 molecules/cm^3·s in a 1-km-thick layer centered at 17 km using our standard chemistry (with the rate constant for OH + HO_2 → H_2O + O_2 equal to 2×10^{-11} cm^3/s). We then repeated the calculation with the rates of the NO photolysis sink set equal to zero.

2. Both of the above sets of calculations were repeated for the Hunten eddy diffusion profile (Climatic Impact Committee 1975, p. 42) and for the Crutzen eddy diffusion profile (Crutzen and Isaksen 1975).

The NO_y mixing ratios resulting from the above calculations are given in Fig. 14. A comparison of the results with and without the NO photolysis sink implies that this sink for NO_y is responsible for both decreasing $[NO_y]$ at all altitudes and for a decrease in NO_y mixing ratio with altitude above about 30 km.

It is worth noting, however, that for the perturbed cases the changes in mixing ratio are not constant with altitude even when the photolysis sink (the only chemical sink for NO_y in the model) is removed. This is a result of a change in the net rate of the "natural" production of NO_y from the reaction

$$N_2O + O(^1D) \rightarrow 2NO.$$

This source term changes because the ozone concentration changes. The ozone reduction leads to a decrease in $O(^1D)$ concentrations at high altitudes where the proportional change in solar flux is less than the change in ozone concentration, and an increase in $O(^1D)$ at low altitudes where the change in solar flux density more than compensates for the change in ozone. The changes in N_2O (because of altered solar flux) are relatively minor. The net change in the production of NO_y from $O(^1D)$ + N_2O in the model with NO photolysis suppressed is given in Fig. 15 for the three diffusion profiles.

The net changes in the ozone column for the above calculations are given in Table 8. In examining the ozone reductions it should be noted that the rate coefficients used in the current calculations are the recommended values from Hampson and Garvin (1975), with 2×10^{-11} cm^3/s for OH + HO_2. Thus, there are numerous minor changes and one major change in the rate coefficients used here compared to those used to generate the CIAP findings (Grobecker et al. 1974). Although omission of the N atom sink for NO_y makes a very substantial difference in the NO_y mixing ratio above 30 km, it causes only a minor increase in the percentage ozone perturbation for NO_x injections. This results because both the ambient and perturbed NO_y mixing ratios are reduced by the sink. The ozone perturbation is more strongly affected for the Hunten profile, which was used in the formula developed by NAS (National Academy of Sciences 1975b, p. 42), than for the other diffusion profiles considered.

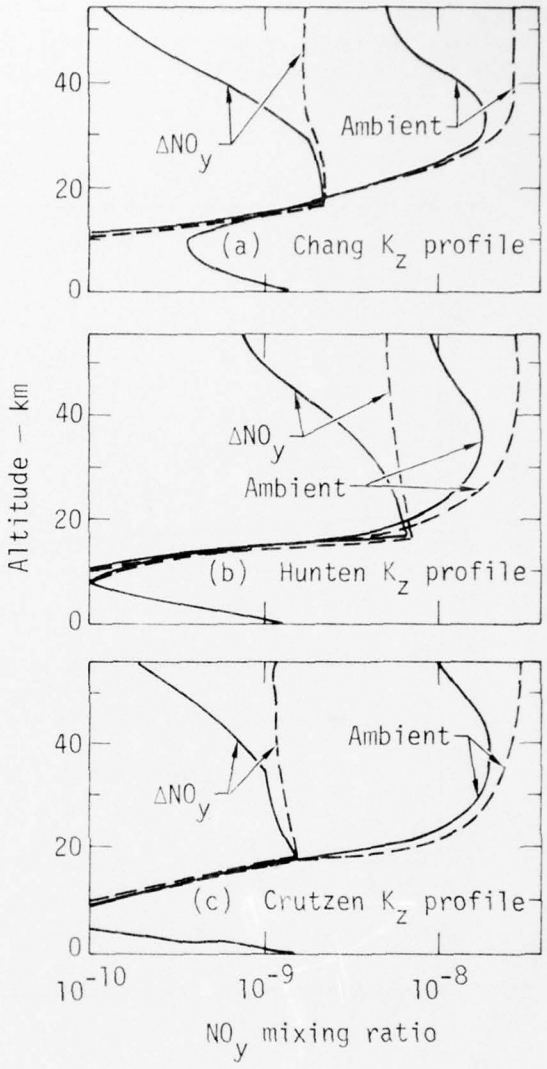

Fig. 14. Plots of calculated ambient NO_y mixing ratio (ambient) and changes in NO_y mixing ratio (ΔNO_y) after a 17-km NO_x injection as described in the text. Solid curves are calculations with the normal model, dashed curves are calculations with the NO photolysis sink suppressed.

The effect of the N atom reactions on the O_3 response of the model to a ClO_x injection is opposite in sign and larger than their effect on the O_3 response to an NO injection. We find that the stratosphere is substantially less sensitive to chlorofluorocarbons when the N atom sink is removed from our model than when

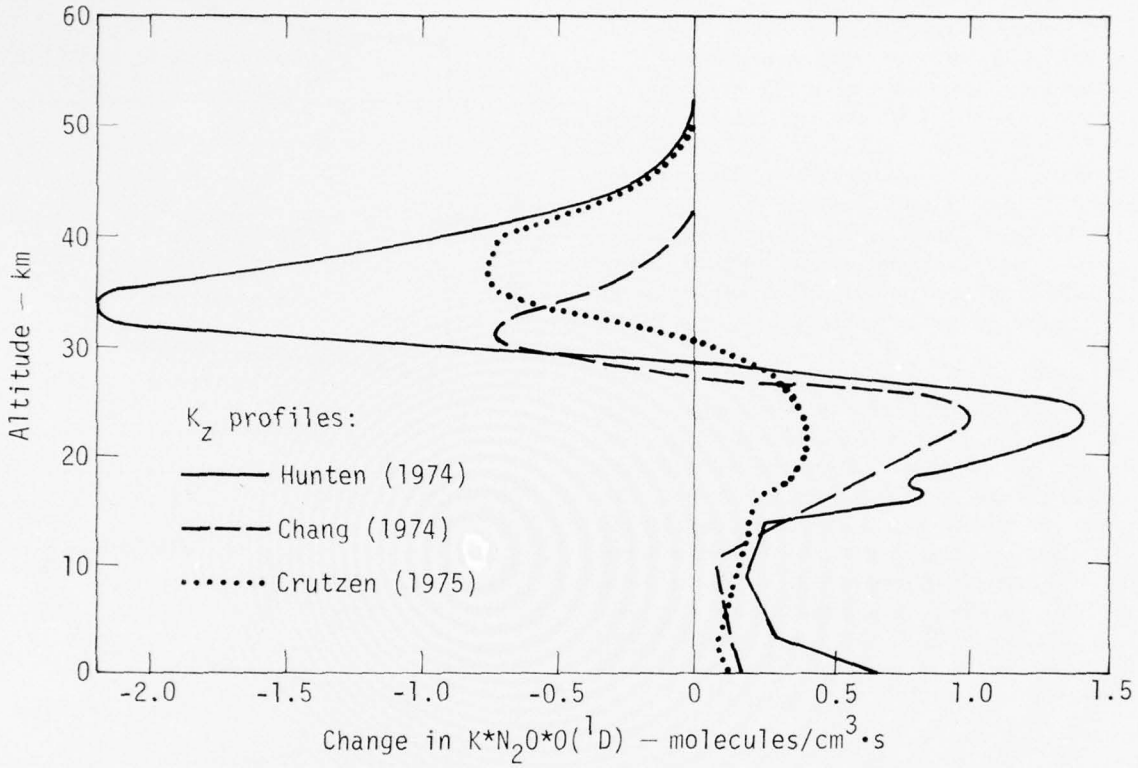

Fig. 15. Calculated change in the odd nitrogen production rate in models with the NO photolysis sink suppressed.

Table 8. Ozone columns (molecules/cm^2) and percent deviations

	Chang K_z	Hunten K_z	Crutzen K_z
Normal, ambient O_3	7.4334×10^{18}	7.4627×10^{18}	7.4437×10^{18}
Normal, 17-km NO source	7.2920×10^{18}	6.9644×10^{18}	7.3459×10^{18}
ΔO_3	-1.75%	-6.68%	-1.31%
No N atom, ambient O_3	7.2752×10^{18}	7.148×10^{18}	7.1165×10^{18}
No N atom, 17-km NO source	7.1467×10^{18}	6.630×10^{18}	7.0195×10^{18}
ΔO_3	-1.77%	-7.25%	-1.36%

it is included. A model that computed a 0.51% reduction in ozone due to chlorofluorocarbons in 1976 using our full chemistry computed only a 0.30% ozone reduction in 1976 when NO photolysis was neglected. This effect occurs because the reaction

$$NO + ClO \rightarrow NO_2 + Cl$$

reduces the efficiency of both the chlorine and NO_x ozone destruction cycles, and the effect of this reaction is especially dependent on the NO_x mixing ratio above 35 km.

Thus, although models of the effects of NO_x injections on the stratosphere are not very sensitive to the NO photolysis sink for NO_x, inclusion of this sink is quite important for models of the effects of chlorofluorocarbons in the stratosphere. Indeed, the concentration of NO above 35 km is an important and poorly validated quantity in current models.

2.5 OTHER INVESTIGATIONS USING THE 1-D TRANSPORT-KINETICS MODEL

Transient Effects in the Transport-Kinetics Model

When the time-dependent response of the LLL one-dimensional model to a constant NO_x injection is computed, there is an initial period when the model computes an increase or very slowly growing decrease in total ozone. An initial increase in total ozone is obtained when the rate of the reaction of OH with HO_2 is taken to be near 2×10^{-11} cm^3/s (model A, described earlier in Sec. 2.1) and the injection altitude is 17 km or less.

This behavior arises because, in the region below about 20 km, a local increase in NO_x results in an increase in the local concentration of ozone in that model, and if the injection altitude is much below 20 km, ozone is increased, until injected NO_x is transported up into the region above 20 km where it causes ozone destruction.

The increase in ozone at lower altitudes results from a combination of three factors. Given the rate coefficient used, the most important of these (in terms of the total ozone column) is the interference in HO_x cycle destruction of ozone caused by NO_x. The intimately related methane smog reaction has a similar effect, and is the major source of the tropospheric ozone increase. The effect of high altitude reductions in ozone on the radiation reaching the lower stratosphere results in an increase in lower stratospheric ozone at later times, but has little effect on the early transient behavior.

The LLL treatment of methane oxidation uses the following reactions:

$$CH_4 + OH \rightarrow H_2O + CH_3,$$
$$CH_4 + O(^1D) \rightarrow OH + CH_3,$$
$$CH_3 \xrightarrow{O_2,\ NO} 2HO_2 + CO \text{ (assumed to occur rapidly).}$$

This shortcut mechanism yields roughly the correct amount of HO_2 production while underestimating O_3 production by about one-third. It avoids an increase in the number of species, and produces significant errors only in the troposphere, which is controlled by boundary conditions in any case.

The transient behavior calculated using the Chang (1974) eddy diffusion profile (Fig. 2) for a 17-km injection of NO_x at a rate of 2000 molecules/$cm^3 \cdot s$ in a 1-km-thick layer is illustrated in Fig. 16, and the transient behavior for a 10-km NO_x injection of equal magnitude is illustrated in Fig. 17. The references to branch 1 or branch 2 concern the assumed products of NO_3 photolysis. In calculating the curves labeled branch 1, NO_3 photolysis was assumed to yield NO + O_2, and in calculating those labeled branch 2, NO_2

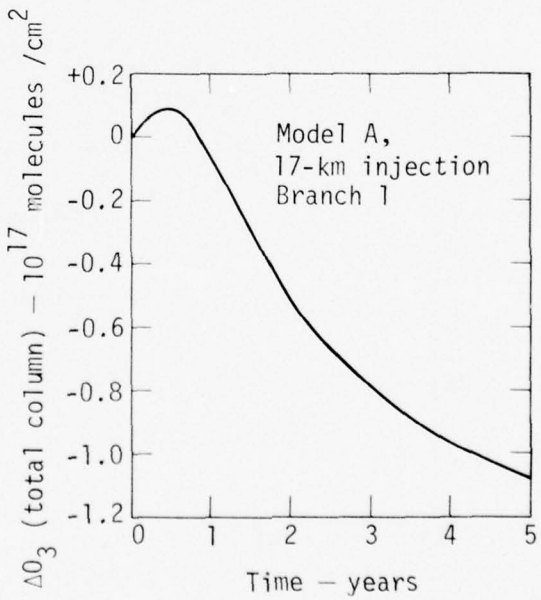

Fig. 16. Calculated change in the total O_3 column vs time as a result of an NO_x injection (as NO_2) of 2000 molecules/$cm^3 \cdot s$ in a 1-km-thick layer centered at 17 km.

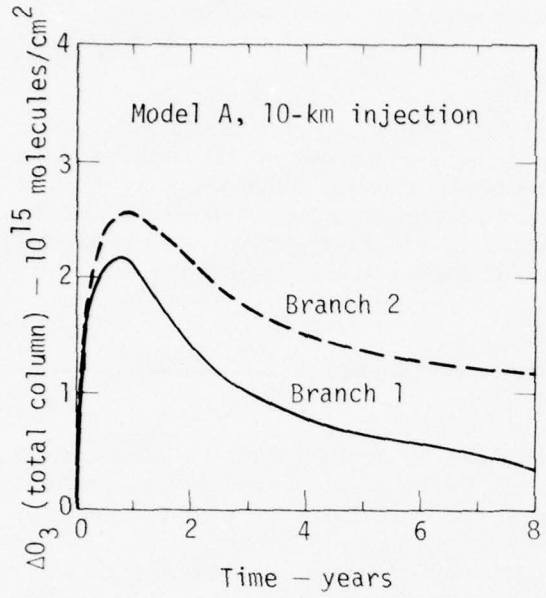

Fig. 17. Calculated change in the total O_3 column vs time as a result of an NO_x injection (as NO_2) of 2000 molecules/cm^3·s in a 1-km-thick layer centered at 10 km.

+ O were the assumed products. Figure 18 presents the altitude-dependent change in ozone concentration after 0.2, 0.8, 2, 5, and 10 years for the 10-km NO_x injection assuming branch 1.

The results described here are of qualitative significance. They are sensitive to the choice of poorly known rate constants, and are expected to be quite sensitive to the eddy diffusion profile. The greatest uncertainty is associated with low altitude injections of NO_x. Thus, the qualitative results should be treated cautiously.

New Eddy Diffusion Coefficient Profile

A new vertical eddy diffusion coefficient profile has been derived for the 1-D transport-kinetics model. This profile was designed to improve the fit with methane and nitrous oxide measurements in the upper stratosphere. It was necessitated by the requirement for improved representation of transport in the upper stratosphere where the distribution of chlorofluoromethanes becomes important. The new eddy diffusion coefficient profile (shown in Fig. 19) provides for increased transport in the upper stratosphere.

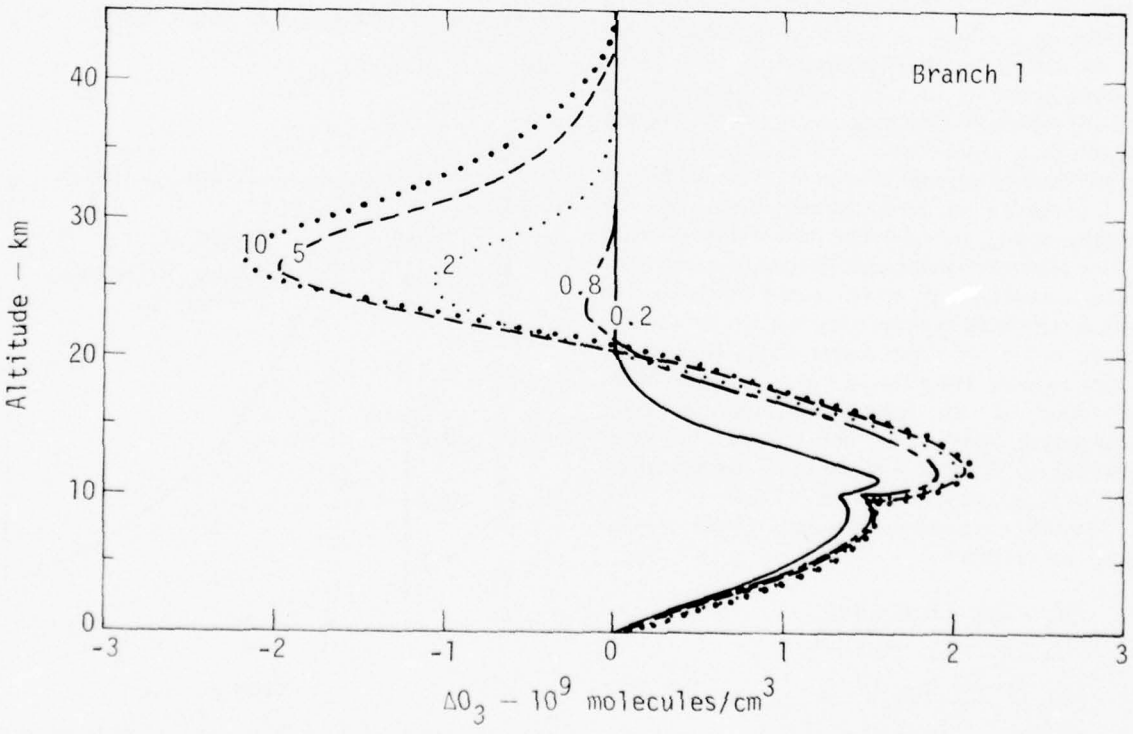

Fig. 18. Calculated change in ozone concentration vs altitude after 0.2, 0.8, 2, 5, and 10 years for the 10-km NO_x injection of Fig. 17.

Effect of $ClONO_2$ in the Stratospheric Model

The effect of adding $ClONO_2$ to the 1-D transport-kinetics model is shown in Table 9. The actual reaction rate for formation of $ClONO_2$ is unknown at present, but preliminary measurements (Kaufman 1976, Birks 1976, DeMore 1976, all private communication) have indicated the rate coefficient is between 0.05 and 0.1 times that for formation of HNO_3. Case 0 refers to the model without $ClONO_2$. In case 1 the $ClONO_2$ production rate was assumed to be 0.1 times that of HNO_3, and in case 2 the $ClONO_2$ production rate was assumed to be 0.05 times that of HNO_3. A reaction rate of 2×10^{-13} cm^3/s (Davis 1976, private communication) was used for the $ClONO_2 + O(^3P)$ in cases 1 and 2. The photolysis rate calculated in the model for $ClONO_2$ includes the recently revised absorption cross sections from Spencer, Molina, and Rowland (1976), and the new Chang diffusion profile (Fig. 19) was used in all calculations.

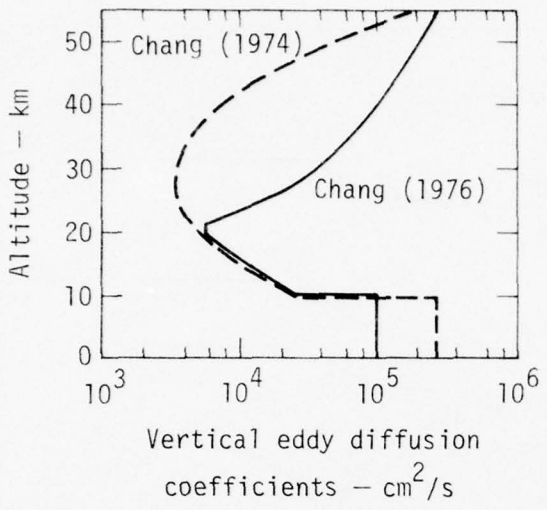

Fig. 19. New vertical eddy diffusion coefficient profile (Chang 1976) compared with the previously used profile (Chang 1974).

As seen in Table 9, the effect of $ClONO_2$ is to reduce the effectiveness of the ClO_x released by the chlorofluoromethanes by approximately a factor of 2. With constant production of the chlorofluoromethanes at 1973 levels, the ozone reduction by the year 2176 changes from 13.68% without $ClONO_2$ to 7.47% for case 2 which has $ClONO_2$ produced at 0.05 times the rate of HNO_3. In the model, the effect of $ClONO_2$

Table 9. Percent change in total ozone from ambient atmosphere (containing CCl_4 and CH_3Cl) due to chlorofluoromethanes

	1974	1976	2176 (constant production at 1973 levels)
Case 0 (without $ClONO_2$)	0.61	0.86	13.68
Case 1 (with $ClONO_2$ = 0.1 HNO_3)	0.23	0.30	4.87
Case 2 (with $ClONO_2$ = 0.05 HNO_3)	0.38	0.51	7.47
Case 2 (with $ClONO_2$ and rate change):			
$OH + HO_2 \rightarrow H_2O + O_2$ (2×10^{-11}; 2×10^{-10})	0.02	0.03	–
$Cl + O_3 \rightarrow ClO + O_2$ ($2.97 \times 10^{-11} e^{-243/T}$; 1.85×10^{-11})	0.43	0.59	–
$ClO + O \rightarrow Cl + O_2$ ($3.38 \times 10^{-11} e^{75/T}$; 5.3×10^{-11})	0.38	0.53	–
$ClO + NO \rightarrow Cl + NO_2$ ($1.13 \times 10^{-11} e^{200/T}$; 1.7×10^{-11})	0.40	0.55	–
$Cl + CH_4 \rightarrow HCl + CH_3$ ($5.4 \times 10^{-13} e^{-1133/T}$; $5.6 \times 10^{-11} e^{-1790/T}$)	0.41	0.56	–
$OH + HCl \rightarrow H_2O + Cl$ ($2.0 \times 10^{-12} e^{-310/T}$; $2.8 \times 10^{-12} e^{-410/T}$)	0.33	0.45	–

occurs primarily below the altitudes of importance for the ClO_x catalytic cycle. The peak concentration of $ClONO_2$ occurs at approximately 25 km. At this altitude, the effect of $ClONO_2$ is primarily to reduce the available NO_x (for the NO_x-O_3 cycle) in a region where O_3 removal is dominated by NO_x, thus compensating somewhat for the reduction of ozone occurring above due to ClO_x. The peak concentrations

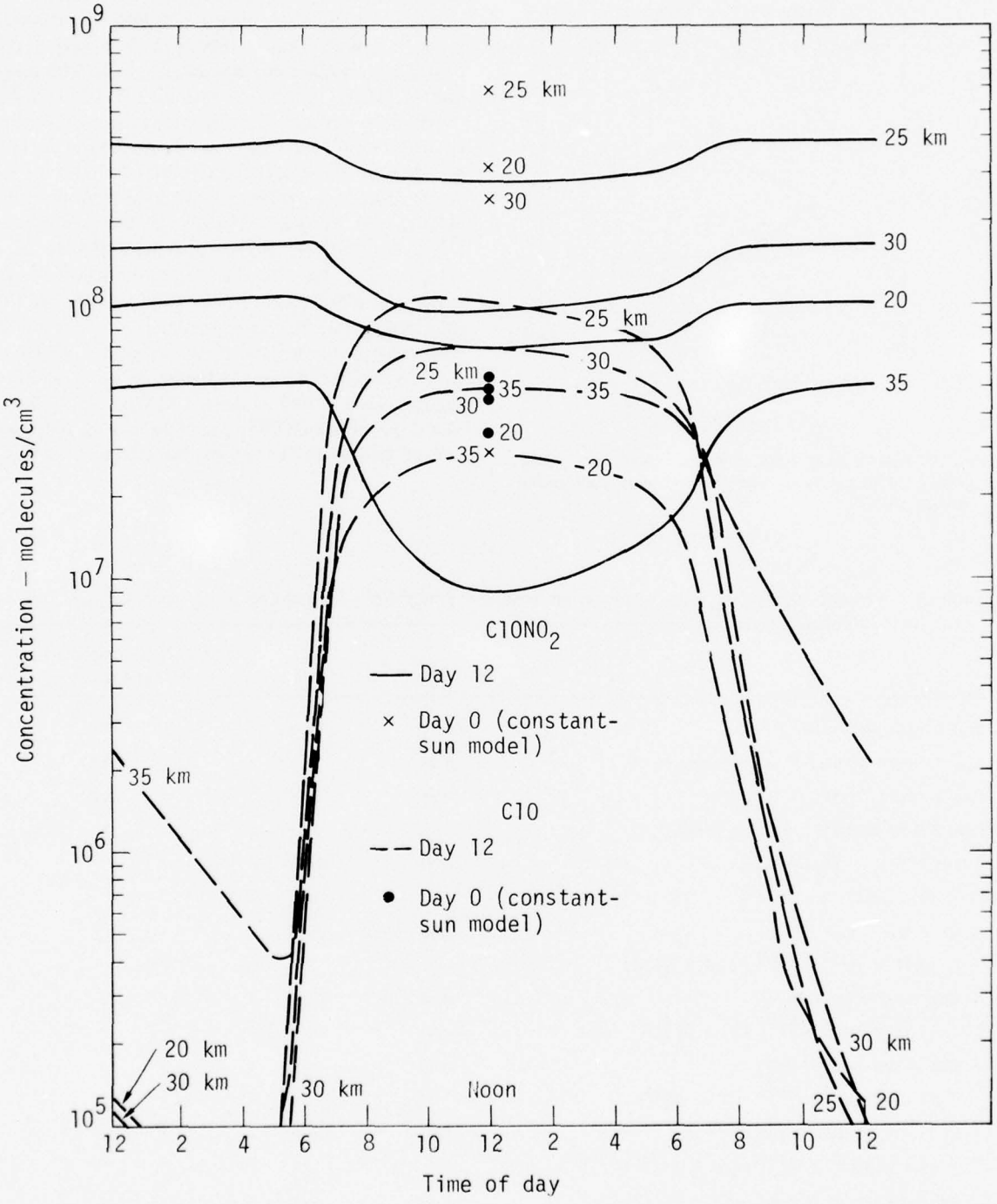

Fig. 20. Calculated concentrations of ClO and $ClONO_2$ at various altitudes vs time of day, based on diurnally varying model and constant-sun model.

of $ClONO_2$ for both cases 1 and 2 are less than the upper limit of 10^9 molecules/cm^3 given by Murcray (1976).

Also shown in Table 9 is the effect of varying the same six reactions discussed above when $ClONO_2$ is included in the model. The rates shown in parentheses indicate the rates normally used in the model (on the left) and the rates used to test the model's sensitivity (on the right). Whereas changing the rate coefficient for $OH + HO_2$ from 2×10^{-11} to 2×10^{-10} cm^3/s had reduced the effectiveness of ClO_x by a factor of 3.1 without $ClONO_2$, the effect with $ClONO_2$ is to reduce the change in total ozone by a factor of 17 (from 0.51% to 0.03%) for the year 1976. This increased sensitivity is attributed to $ClONO_2$ tying up NO_x in an atmosphere where O_3 is predominantly controlled by NO_x when $OH + HO_2$ is 2×10^{-10} cm^3/s (this rate will reduce the OH available to react with NO_2 to produce HNO_3, resulting in increased NO and NO_2 levels relative to when the rate is 2×10^{-11}).

Diurnal calculations have also been carried out for the model containing $ClONO_2$. The diurnal variations of ClO and $ClONO_2$ after the 12th day (starting from the constant-sun model results) are shown in Fig. 20. The diurnal calculation shows less diurnally averaged $ClONO_2$ as compared with values from the constant-sun calculation (see crosses in Fig. 20). This is due to conversion of some of the $ClONO_2$ to HCl through the diurnal variation of NO_x and ClO_x species.

Effects of $O_3 \xrightarrow{h\nu} O(^1D) + O_2$ Quantum Yields Near Threshold

In comparing our model results with similar results from the Michigan and NCAR groups, we found that the LLL model yielded about half the total stratospheric NO_x contained in the other models. The reason was that the other modeling groups were assuming a unit quantum yield for $O(^1D)$ production from ozone photolysis at wavelengths shorter than 310 nm and zero at longer wavelengths (as recommended by Hampson and Garvin 1975), whereas we were using the formulation

$$\phi(O(^1D)) = 1 - \frac{1}{1 + e^{(\lambda - 303)/1.6}} \quad \text{for } \lambda < 305 \text{ nm},$$

$$\phi(O(^1D)) = \frac{1}{1 + e^{(\lambda - 303)/4.8}} \quad \text{for } 305 < \lambda < 330 \text{ nm},$$

which was recommended by Johnston (1973). Use of Johnston's expression reduces the lower stratospheric $O(^1D)$ production by about a factor of 2 relative to the 310-nm step function and accounts for most of the differences in NO_x between the LLL model and the other models. Because an abrupt threshold is theoretically unlikely and seems incompatible with recent results, we believe the form of expression used in our model to be superior to the 310-nm step function. However, we recognize that the temperature dependence and precise value of $O(^1D)$ in the 300-to-315-nm range is quite uncertain. Thus the expression used is significantly uncertain. The sensitivity of stratospheric NO_x to an incremental NO_x injection is fairly sensitive to the ambient NO_x concentration (in an atmosphere with doubled NO_2 the response of total ozone in model A to a 17-km NO_x injection changed from a base case 1.75% decrease to a 1.35% decrease). Also, depending on the importance of chlorine nitrate, the response of ozone to a source of stratospheric chlorine may be quite sensitive to the ambient NO_x concentration.

2.6 COMPARISON OF MODEL RESULTS WITH OBSERVATIONS

Catalytic Destruction of Ozone

We have been collecting observational data believed to have a bearing on the validity of the catalytic destruction of stratospheric O_3. The data qualitatively confirm the current theory for short-period responses of O_3 at levels above 30 km to polar cap absorption events (PCA's) and changes in solar flux. Above 30 km the stratosphere is in photochemical equilibrium, and ozone should be controlled by photochemistry in this region. The data reveal that dynamics may be the dominant controlling process affecting long-term trends in ozone below 30 km.

Specific examples of differences between model results and observational data are cited below. These differences reveal areas where we have limited understanding about the processes that may be affecting ozone. Further research is needed to satisfactorily explain these differences.

1. O_3 and nuclear tests. Since 1962, total O_3 has increased to mean levels higher than observed before atmospheric nuclear testing. Consequently catalytic destruction of ozone by NO_x generated during nuclear tests could not be the only controlling mechanism affecting ozone during this period.

2. O_3 and PCA's. There is no apparent dose response relationship either in terms of the relative

intensities of the PCA's of 1959, 1960, 1966, and 1972 or in terms of the colatitude of the O_3 data.

3. Correlation of O_3 with sunspots. One method in which ozone might be affected by solar activity adopts the following argument (Ruderman and Chamberlain 1975): An increase in sunspot activity → increased solar wind → decreased cosmic ray flux into the upper atmosphere → decreased NO production → increased ozone. This theory is not consistent with the observed variations of total ozone. O_3 oscillations decreased in amplitude as the sunspot amplitude increased up to 1969. Total O_3 increased from a peak sunspot maximum of 1957 to the very low sunspot maximum of 1969. Before 1954, O_3 oscillations lagged sunspots by about three years; after 1963 the variations appear almost in phase. O_3 amplitudes exceed amplitudes computed from the Ruderman and Chamberlain (1975) theory by about tenfold. There are rather large hemispheric differences in the apparent 11-year oscillations in O_3.

4. Seasonal changes in total O_3. The area with the best long-period O_3 data, Western Europe, shows between 1955 and 1970 a 14% increase in winter O_3 and only 4% in summer O_3. This suggests processes other than photochemistry.

5. High O_3 mixing ratios in polar night. Heath (1974) reported BUV observations of a 4-mbar O_3 mass mixing ratio of 23 ppm at 70°N on 2 January 1971, 44% above the maximum of 16 ppm normally observed in the tropical stratosphere. Unless the high O_3 measurement is due to instrument difficulties, this is highly suggestive of a nonphotochemical O_3 source not included in any current models.

6. Total O_3 following Agung eruption. Uniform global mixing of the estimated 1-MT stratospheric injection of Cl is computed (Ryan and Mukherjee 1975) to cause a decline in total O_3 of approximately 5%. If the bulk of the Cl from Agung remained in the southern hemisphere as did the bulk of the Agung dust, even larger changes in O_3 should have occurred there. O_3 observations show, if anything, an increase in total O_3 following the eruption.

Due to the sparseness and possible unreliability of some of the data, most of these differences cannot be resolved at the present time. We have indicated, however, several areas in which more data of a reliable nature would be very helpful.

Effect of Sudden Stratospheric Warmings on Global Ozone

To simulate and facilitate further investigation of the possibility that variation in the global ozone amount is caused by sudden stratospheric warmings (SSW's), observed SSW's were tabulated by year, date, and measure of intensity. It was noted that in the winters having major SSW's (1962-63 and 1967-68), total O_3 not only rose to higher levels sooner but also remained above the minor SSW winter of 1966-67 throughout the following spring and summer. The data since 1955 indicate that a minor SSW is the normal situation in the northern hemisphere and only the major warmings are abnormal. One can then hypothesize that the O_3 trend since 1958, down until 1962 and up since 1963, is due to major SSW's alone. This would also explain why the trend in the southern hemisphere appears to be much weaker or even reversed, since fewer and weaker SSW's occur in the southern hemisphere. Christie's (1973) O_3 analysis fits this hypothesis very well, as shown in Fig. 21, where the years with major SSW's have been circled. The fit with O_3 trend analyses of others is not so good, but this appears to be a problem plaguing all current theories. Later analysis suggests that late-season major SSW's culminating after the end of January have little effect on mean annual O_3 for the following year, e.g., the major SSW of 19 January through 6 February 1957. Admittedly, some of these arguments are speculative, but it is hoped that these ideas will stimulate further research and exchange of ideas which might clarify this possible climatic mechanism.

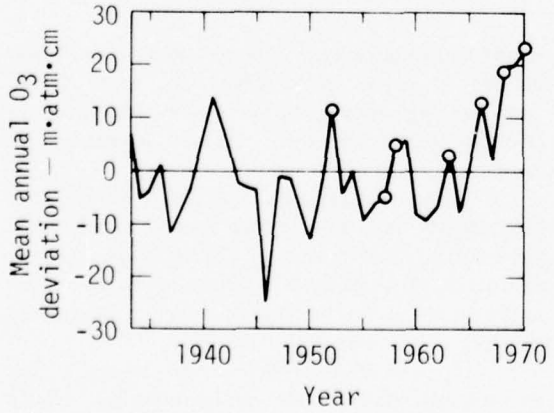

Fig. 21. Time series of annual mean values of ozone deviation. Circles indicate years with major sudden stratospheric warmings. (After Christie 1973.)

2.7 POSSIBLE CAUSE OF THE PRE-1970 INCREASE IN OZONE

The upward trend in total O_3 in the northern hemisphere from about 1957 to 1970 might be attributable to a change in the general circulation. Those proposing such explanations (e.g., Komhyr et al. 1971, Crutzen 1972) have tended to be nonspecific as to what changes have occurred, since we are lacking in understanding in this area. Empirical deduction seems to indicate that a weakening of the Hadley circulation and consequently of the exchange of air between the troposphere and the stratosphere would lead to an increase in stratospheric O_3. This conclusion rests strongly on the opinion prevailing prior to the unveiling of the NO_x catalytic cycle that the troposphere was the major sink for stratospheric O_3. Current theory is remarkably consistent in showing that in the extratropical lower stratosphere, O_3 concentrations are in excess of those predicted by photochemical equilibrium. A slowdown in tropospheric-stratospheric exchange would appear to allow more time for O_3 in this region to decay to the photochemical equilibrium concentrations, but that effect may well be overpowered by other effects. A slowdown in tropospheric-stratospheric exchange also reduces the upward rate of transfer of N_2O to the 25-to-30-km level, where it is oxidized to NO by $O(^1D)$, and allows more time on the way up for the N_2O to be photodissociated, producing N_2 rather than NO. And secondly, since the Hadley cell is driven by tropical convection which in turn maintains upward pressure on the tropical tropopause, any weakening can be expected to allow a lowering and warming of the tropical tropopause. This in turn would allow a higher mixing ratio of H_2O through the cold trap of the tropical tropopause.

Thus a weakening of the Hadley circulation with resultant slowing of the tropospheric-stratospheric exchange has at least three consequences, all of which appear to lead to increases in the stratospheric reservoir of O_3:

1. It reduces the rate of transfer of O_3 from the storage region of the lower stratosphere to underlying well-mixed troposphere and O_3-destroying surface boundary layer (i.e., it reduces the tropopause value of the K_z of the 1-D model). This should result both in a reduction in the tropospheric concentration and surface destruction rate of O_3 and an increase in total O_3 in the storage reservoir of the lower stratosphere.
2. It slows the upward flux of N_2O, thus allowing more time for photodissociation and reducing the fraction that is oxidized by $O(^1D)$ to form NO. It also presumably allows more time for operation of the unknown tropospheric sink, thus assuring that an even smaller fraction survives to produce NO in the stratosphere.
3. It allows a lowering and warming of the tropical tropopause, which in turn allows a higher H_2O mixing ratio to pass through the tropical tropopause cold trap and to increase the humidity of the stratosphere. This in turn ties up a larger fraction of stratospheric NO_y as HNO_3, reducing the fraction capable of attacking O_3 catalytically.

There remains the nagging problem that the pre-1970 increase in total O_3 appears to have been a phenomenon only of the northern hemisphere while the Hadley cell is usually regarded as a global phenomenon. This is not necessarily an insurmountable problem. We know that the northern hemisphere (winter) Hadley cell is stronger than the southern hemisphere (summer cell) – twice as strong according to Reed and Vlcek (1969), and almost ten times as strong according to Dütsch (1972) – and that the tropical tropopauses of both hemispheres vary in unison on an annual cycle, i.e., highest and coldest in January and February (pushed up by the northern-hemisphere Hadley cell) and lowest and warmest in July and August when the weak southern-hemisphere Hadley cell is operative (Smith 1963). This seems to indicate that the Hadley circulation and its control of the tropical tropopause and troposheric-stratospheric exchange is strongly asymmetric, due presumably to both the distribution of land and sea and the eccentricity of the earth's orbit; the former amplifies latitudinal temperature gradients to strengthen the northern-hemisphere Hadley cell, and the latter causes the received solar flux in January to exceed that of July by nearly 7%, again strengthening the northern hemisphere cell. Thus, restriction to the northern hemisphere of the pre-1970 increase in O_3 becomes an additional argument supporting a relationship between the increase and the tropospheric-stratospheric exchange rate since the latter and the nuclear test hypothesis are the only ones proposed which would lead to a hemispheric as opposed to a global phenomenon.

Finally, it is necessary to establish that there was a progressive weakening of the Hadley circulation and a slowdown in tropospheric-stratospheric exchange for approximately a decade prior to 1970-71. This is attested to by the following evidence.

1. Angell and Korshover (1974) found a 5-to-7-mbar/decade increase in tropical tropopause pressure which appeared to have begun about 1957. Associated with it was a warming of the tropical tropopause at Singapore and Gan of approximately 1 K/decade, which they suggested might be related to the increase in H_2O mixing ratio in the lower stratosphere observed by Mastenbrook (1971) over Washington, D.C., between 1964 and 1970.

2. Measurements of Junge layer stratosphere aerosols by both airborne collectors and remote sensing reported a minimum and virtual disappearance of the layer in mid-1971 (Fox et al. 1973). While the major thinning of the layer from 1963 to this time has been related to the Mt. Agung and subsequent volcanic eruptions, the 1971 levels represented a significant decline over the pre-Agung values reported by Junge and Friend. This is even more apparent after application to the pre-Agung data of the 5-to-6-fold correction for impactor collection efficiency which now appears appropriate (Cadle and Grams 1975). Since gaseous sulfur and particulates, like all other material not episodically injected into the stratosphere (as by volcanoes, etc.), must enter through the Hadley circulation, the pre-Agung-to-1971 thinning of the Junge layer suggests a weakening of the Hadley circulation.

3. Winstanley (1973) reported for the Sahel strip of Africa and India a continuing decline in summer monsoonal rainfall since the late 1920's, apart from a temporary reprieve in the early 1950's. The recent drought was the result of the cumulative effects of a decade of below-average monsoon rainfall with less and less rain each year through 1970.

Since tropical convection cells penetrating the tropical tropopause are likely to decrease even more than summer ITCZ (intertropical convergence zone) and monsoonal rainfall in general, Winstanley's data also indicates a progressive weakening (from about 1957 to 1970) of the Hadley circulation and, thus, of tropospheric-stratospheric exchange.

The above, of course, does not constitute proof, but does appear to indicate rather strongly that a progressive 10-to-13-year-long weakening of the Hadley cell and of tropospheric-stratospheric exchange is responsible for the progressive northern-hemisphere increases in total O_3 observed up through 1970.

2.8 WORK IN PROGRESS

Temperature Feedback in a Stratospheric Model

Perturbations to the stratospheric composition affect the stratospheric temperature profile via the solar and longwave radiation balance. Changes in temperature affect chemical reaction rates, which in turn feed back on stratospheric composition. The temperature feedback mechanism has long been recognized as potentially important in mitigating perturbations to the ozone concentration, but it has only recently been included in stratospheric models. Barnett et al. (1975) have investigated the temperature dependence of ozone concentration near the stratopause, and they showed that a decrease in temperature tends to increase the ozone concentration.

In order to investigate the effect of temperature feedback on the concentration of ozone, LLL's one-dimensional transport-kinetics model was coupled to a stratospheric radiative transfer model. The temperature profile is determined using a radiative equilibrium calculation with convective adjustment. The model includes solar absorption and longwave interaction by O_3, H_2O, and CO_2 along with solar absorption by NO_2. The techniques adopted for treating longwave radiative transfer are the same as those described by Ramanathan (1974). A band absorptance formulation is used to treat the 9.6-μm band of O_3 and the fundamental and several weak bands of CO_2 and its isotopes in the 15-μm region. An emissivity formulation is used to treat longwave radiative transfer by H_2O. Solar absorption by O_3 is treated using the empirical formulation given by Lindzen and Will (1973). Band absorptance formulations are also adopted for treating solar absorption by H_2O and CO_2. The empirical formulation of Luther (1976) is used for solar absorption by NO_2. Solar absorption by O_3 and NO_2 are treated independently because absorption by these species is weak in the region where their absorption bands overlap. Solar radiation scattered from the troposphere is included assuming an albedo of 0.3.

A single cloud layer is included at 6.5 km with 42% cloud cover as suggested by Cess (1974). The lapse rate within the troposphere is assumed to be wet adiabatic (6.5 K/km), and the temperature at the earth's surface is specified to be 288 K. The tropopause height and the temperature profile within the stratosphere are computed by the model. The CO_2 mixing ratio is assumed to be 320 ppm by volume.

The temperature profile generated by the radiative equilibrium model is shown in Fig. 22. This profile is similar to temperature profiles observed at tropical latitudes. The temperature profile from the *U. S. Standard Atmosphere* (1962), which represents a midlatitude average, is shown for comparison since this profile is frequently assumed for transport-kinetics calculations which neglect temperature feedback. The unperturbed temperature profile, which we will hereafter refer to as the "ambient," is similar in shape to the standard atmosphere but is a few degrees warmer above 20 km. The higher temperature is related to the model-generated ozone concentration. There is excellent agreement when the midlatitude ozone profile from the *U. S. Standard Atmosphere Supplements* (1966) is used to generate an ambient

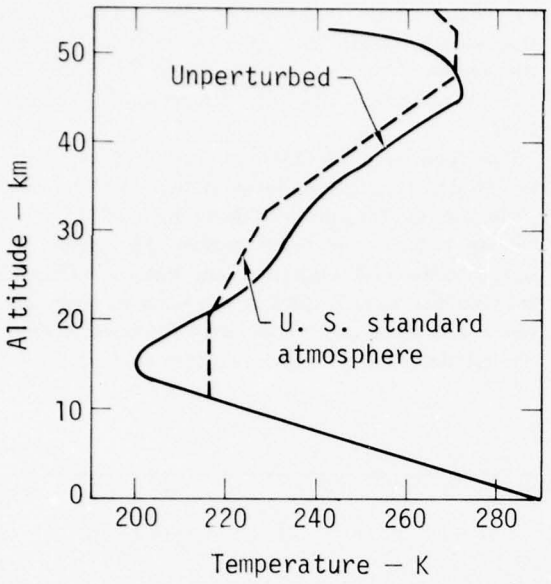

Fig. 22. Temperature profile derived by the model for unperturbed conditions compared with the U. S. Standard Atmosphere temperature profile.

temperature profile. Large-scale dynamical processes are neglected in the determination of the temperature profile. The processes have a significant effect on the temperature profile near the tropopause at midlatitudes. Including these effects would likely lessen the temperature gradient above the tropopause.

The model was applied to two perturbations to test the significance of temperature feedback on ozone concentration. The perturbations considered were stratospheric injection of NO_x and fluorocarbon production.

Stratospheric Injection of NO_x. The effect of stratospheric injections of NO_x by supersonic transports (SST's) on ozone concentration was computed for four cases:

1. No temperature feedback; *U. S. Standard Atmosphere* (1962) temperature profile assumed.
2. No temperature feedback; ambient temperature profile from radiative equilibrium model assumed.
3. With temperature feedback.
4. Temperature feedback without including solar absorption by NO_2.

The first case is an assumption frequently made in transport-kinetics calculations. The second case is the reference condition for comparison with the temperature feedback calculation, which is the third case. The fourth case is included to indicate the significance of neglecting solar absorption by NO_2. These calculations are not intended to imply the effect of a particular fleet of SST's since they do not include the injection of other species such as H_2O and SO_2. Once the significance of temperature feedback is determined for the NO_x perturbation alone (which can be compared with other calculations), then the case of temperature feedback with multiple perturbations will be considered.

The reduction in the ozone column caused by the stratospheric injection of NO_x is shown in Fig. 23 for the case with temperature feedback. The NO_x injection rate as NO_2 represents a global average value uniformly distributed over a 1-km-thick layer centered at the indicated altitude. The ozone reduction is a steady state value obtained from a time-dependent calculation as it approached equilibrium. Relatively large levels of injection of NO_x are required to reduce the ozone column more than a few percent. The ozone reduction values in Fig. 23 are smaller than previously reported (Chang 1975) by about a factor of 2 due to changes in the chemistry, especially the $OH + HO_2$ reaction rate. The reaction rate presently used for $OH + HO_2$ is 2×10^{-11} cm^3/s, whereas previously we used the upper limit 2×10^{-10} cm^3/s (Hampson and Garvin 1975).

The ratio of the ozone reduction for each given case to the ozone reduction with temperature feedback is

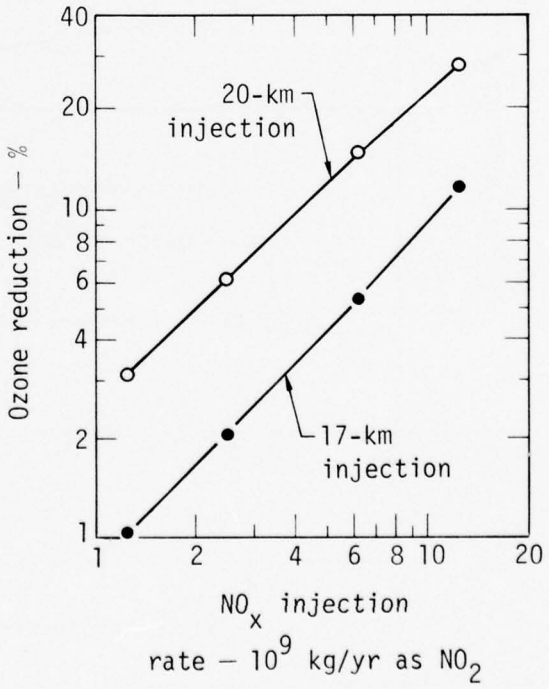

Fig. 23. Calculated ozone reduction vs NO_x injection rate for 17- and 20-km injection heights.

shown in Fig. 24 for the 17-km injection. There are significant differences between the various cases for small NO_x injection rates. The two cases without temperature feedback demonstrate the sensitivity of the calculation to the assumed temperature profile. The ozone reduction using the *U. S. Standard Atmosphere* (1962) temperature profile is as much as 13% greater than for the ambient temperature profile, the difference decreasing with increasing NO_x injection rate.

The ozone reduction with temperature feedback but without solar absorption by NO_2 is substantially less than for the other cases. Neglecting solar absorption by NO_2, which is important for the perturbed stratosphere, leads to an overestimate of the stratospheric temperature change and, consequently, an overestimate of the temperature feedback effect.

The results for the 20-km injection case are shown in Fig. 25. Although the range of NO_x injection rates is the same as in the previous figure, the range of ozone column reduction is much greater. The results are similar to the 17-km injection case, but the difference between the various cases is not quite as large. The ozone reduction with temperature feedback is about 5% less than that with fixed ambient temperature for

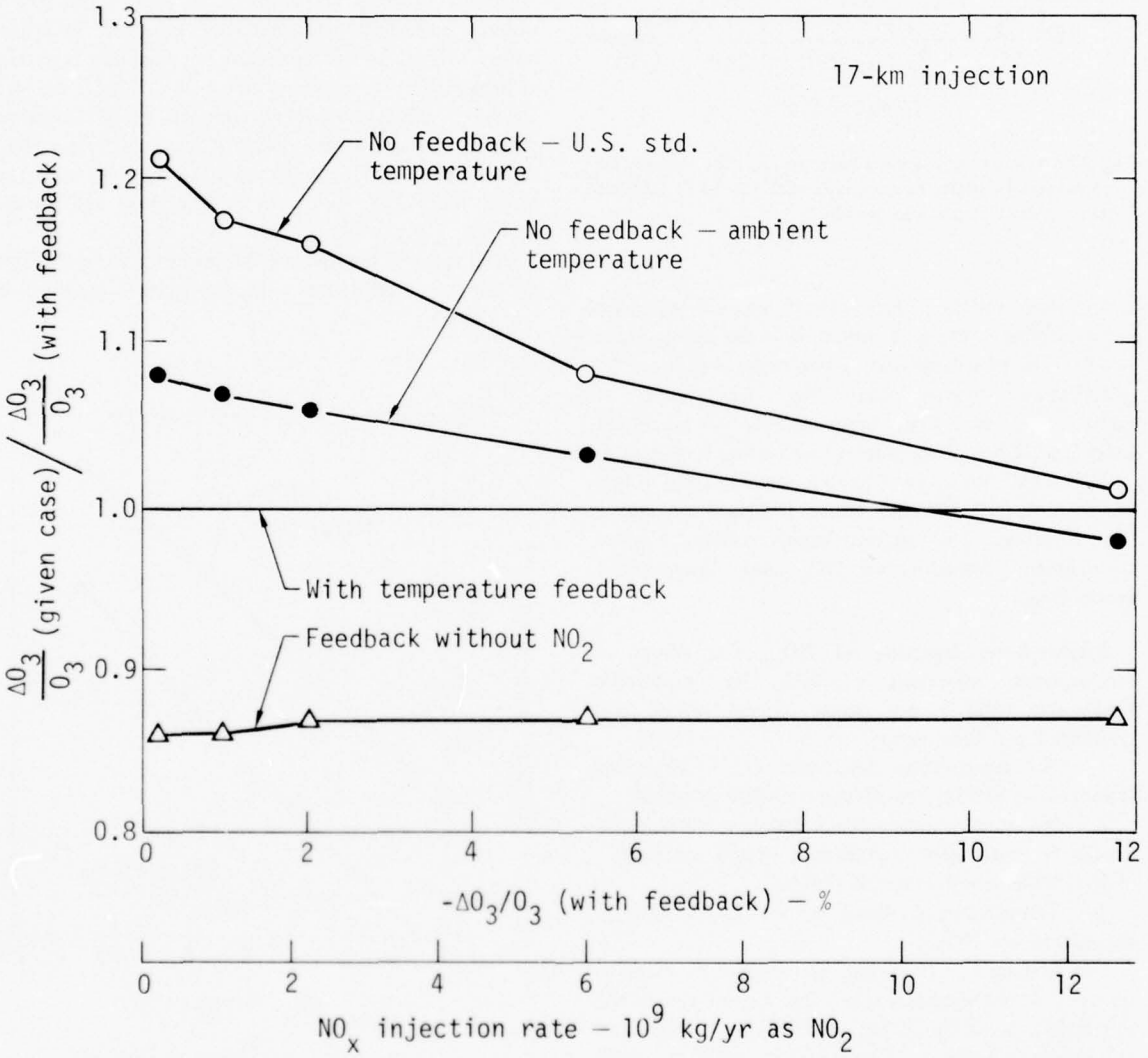

Fig. 24. Calculated ratio of ozone reduction for a given case to ozone reduction with feedback vs NO_x injection rate for a 17-km injection height. Calculation assumes the NO_x injection is uniformly distributed in a 1-km-thick layer centered at the injection height.

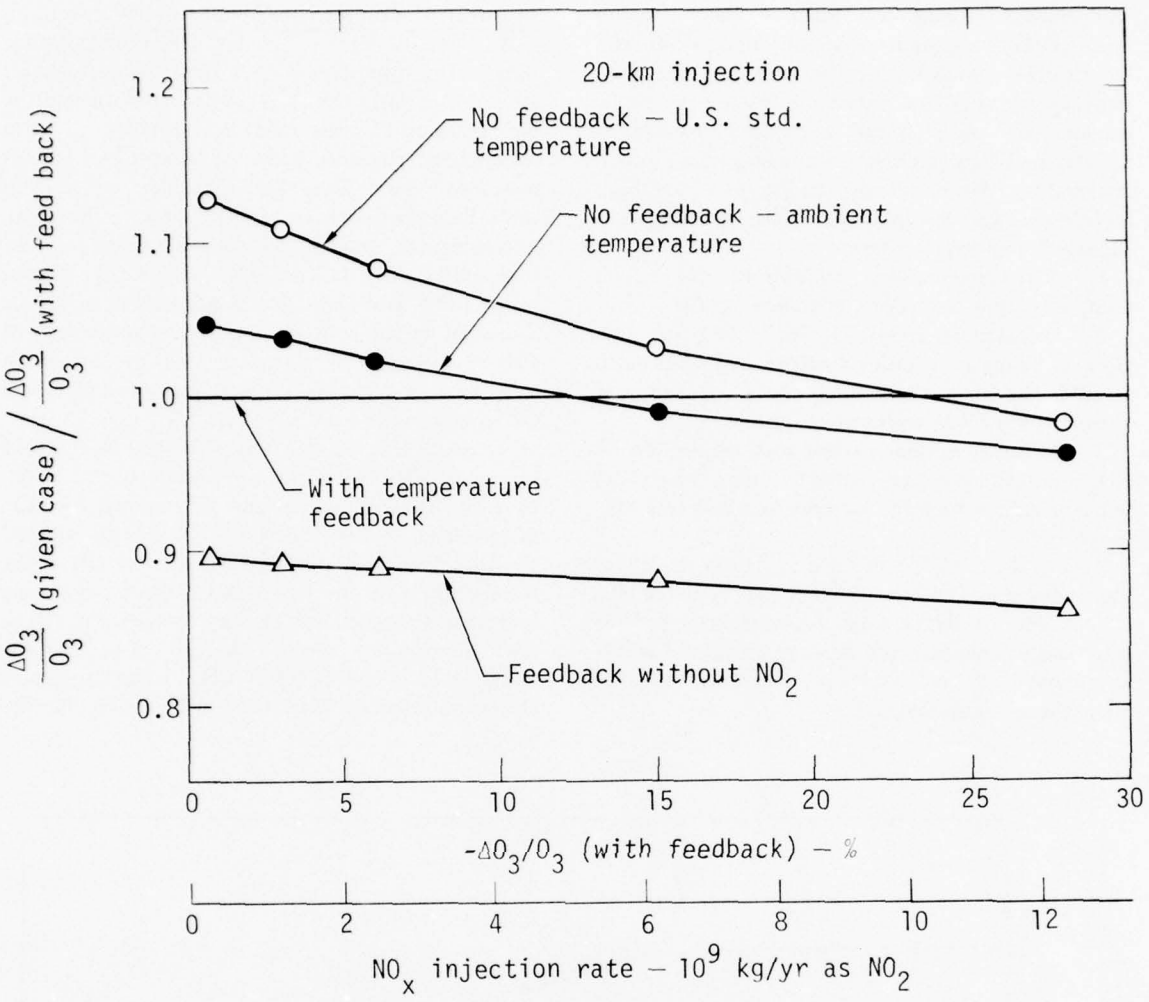

Fig. 25. Calculated ratio of ozone reduction for a given case to ozone reduction with feedback vs NO_x injection rate for a 20-km injection height.

small NO_x injection rates, and the crossover occurs near 14% ozone reduction.

Fluorocarbon Production. The natural atmosphere for these calculations contained HCl with an assumed mixing ratio of 10^{-9} by volume at the earth's surface and a constant CCl_4 flux at the surface. The fluorocarbons $CFCl_3$ and CF_2Cl_2 were introduced at the surface starting in 1950 and running through 1975 based on world fluorocarbon production data (McCarthy 1974). The computed reduction in the ozone column resulting from the atmospheric release of fluorocarbons during this period of time is shown in Fig. 26.

The reduction in the ozone column at the end of 1975 is 0.62% for the case with temperature feedback. The ozone reduction for the fixed-temperature calculation using the ambient temperature profile is a factor of 1.09 greater than for the case with temperature feedback. With the *U. S. Standard Atmosphere* (1962) temperature profile, the ozone reduction is a factor of 1.18 greater. As in the case of NO_x injection, the results are sensitive to the assumed temperature profile for the fixed-temperature calculations, and temperature feedback significantly mitigates the ozone reduction. Temperature feedback reduces the maximum percentage change in ozone, which occurs near 40 km. The maximum change in absolute concentration occurs at 28 km.

Summary of Temperature Feedback Investigations. The effect of temperature feedback on ozone concentration has been investigated for two perturbations to the atmospheric composition.

Temperature feedback was found to have a similar effect for both the stratospheric injection of NO_x and fluorocarbon production. In both cases temperature feedback had a 5-10% restoring effect on the ozone column for small ozone reductions. Comparing calculations based on either fixed-temperature profiles, temperature feedback, or temperature feedback neglecting solar absorption by NO_2 revealed these additional important points:

1. Fixed-temperature calculations are quite sensitive to the assumed temperature profile.
2. Calculations of $\Delta O_3/O_3$ due to NO_x injection alone including temperature feedback may be as much as 20% less than those using the *U. S. Standard Atmosphere* (1962) temperature profile.
3. Calculations that neglect solar absorption by NO_2 significantly overestimate the effect of temperature feedback for perturbations involving NO_x injection.

As the chemical kinetics and transport models of the stratosphere continue to improve in detail, the effects due to temperature feedback will become increasingly important and must be considered in any assessment of potential perturbations to the atmospheric composition.

Variation of Tropospheric Minor Species

We are examining the latitudinal and diurnal variations of tropospheric minor species with particular attention to OH. This is an initial effort to improve the transport-kinetics model's capability to treat tropospheric residence times for modeling of aircraft injections and also for possible replacement chlorofluoromethanes in aerosols and refrigeration. According to model calculations, most of the tropospheric OH is contained within the tropical region (±30° latitude). Diurnal calculations indicate a sinusoidal variation in the daytime concentration of OH at tropospheric altitudes, with the maximum concentration occurring at noon. Very small nighttime OH concentrations are predicted.

Since the HO_x species (OH, HO_2, and H_2O_2) have very short lifetimes in the troposphere (on the order of a few seconds for OH and 10^4 seconds for HO_x as calculated by the model), it is possible to calculate the altitudinal and latitudinal variation of OH in the troposphere with the 1-D model without considering horizontal transport. The primary formation of OH in the troposphere comes through the reactions $O(^1D) + H_2O$ and $O(^1D) + CH_4$, while the loss of OH is controlled by $OH + CO$ and $OH + CH_4$. Profiles

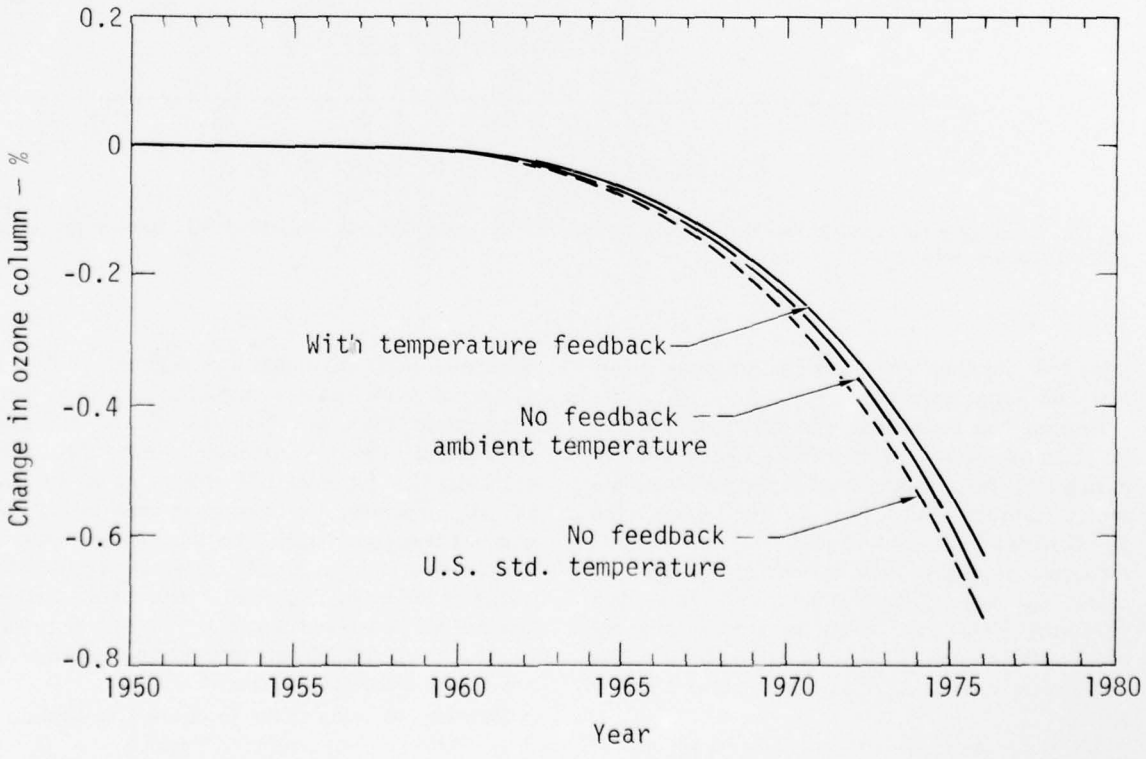

Fig. 26. Calculated change in ozone column due to fluorocarbon production between 1950 and 1976.

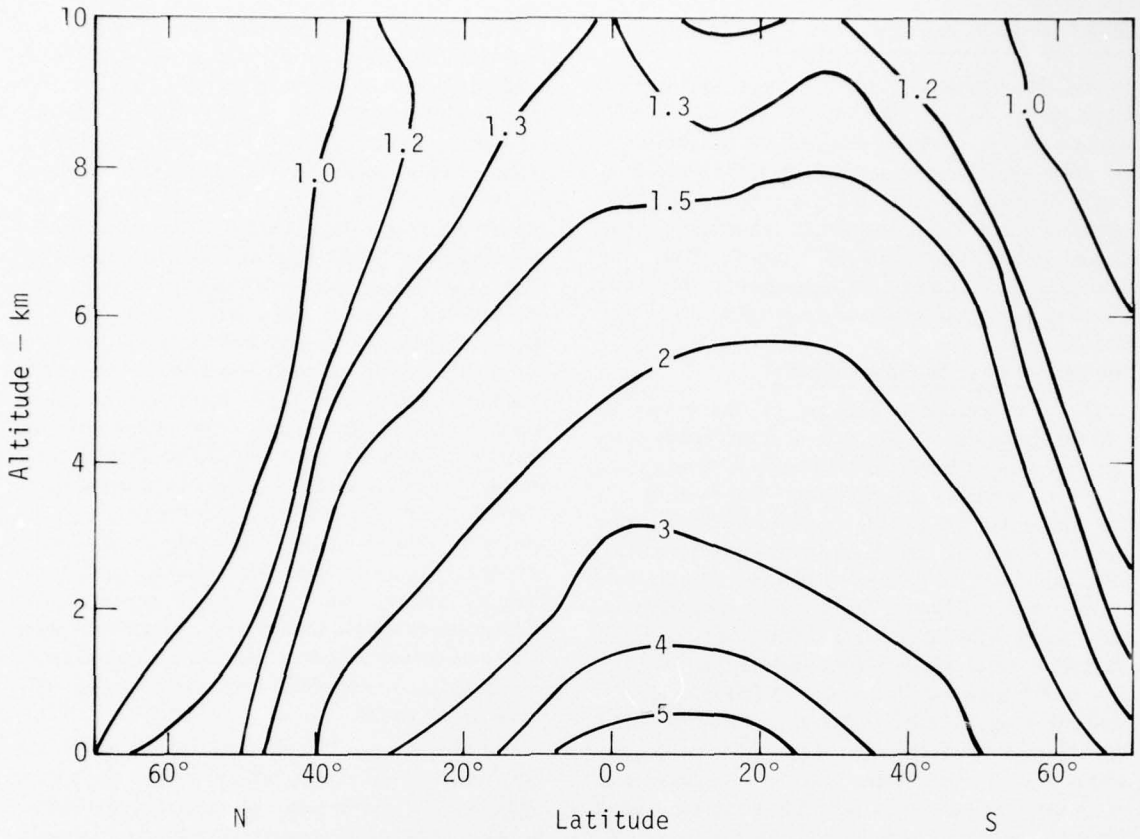

Fig. 27. Diurnally and seasonally averaged values of OH concentration vs latitude and height in the troposphere. Contour values are concentrations (10^6 molecules/cm^3).

of temperature, H_2O, CH_4, CO, and O_3 (through photolysis to provide $O(^1D)$) were specified in the model and varied with latitude according to available measurements. The latitudinal distribution of water vapor was taken from Oort and Rasmussen (1971), the O_3 data are from Dütsch (1969), the temperature profiles versus latitude are from Louis (1974), and the CO data are from Seiler (1974). The model was then used to calculate the diurnal OH concentrations for various seasons and latitudes. A comparison of these calculations with the available measured OH distribution derived from the model is shown in Fig. 27. As indicated above, 71% of the tropospheric OH is contained within the band 30°S–30°N.

The derived OH concentrations were used to determine the tropospheric chemical lifetime for a number of fluorocarbon species based on chemical degradation via OH radical. The calculated lifetimes are shown in Table 10. The reaction rates for these species with OH are based on measurements by Davis (1976). The tropospheric residence time of these species is important in determining whether their future use will lead to an impact on stratospheric ozone.

Table 10. Estimated tropospheric chemical lifetimes for some fluorocarbons

Fluorocarbon	Lifetime (years)
CH_3Cl	0.4
CH_2Cl_2	0.2
CCl_3H	0.2
CH_3Br	0.5
CH_2FCl	0.5
CHF_2Cl	4.6
$CHFCl_2$	0.7
CH_3CF_2Cl	7.1
C_2Cl_4	0.2
CH_3Cl_3	1.4

Model Sensitivity to Tropospheric N_2O Concentrations

We have investigated the effect of doubling the tropospheric N_2O concentrations in our standard model and in models designed to maximize or minimize the effect of an N_2O increase. We found ozone decreases of 2.6% (minimum reduction), 7.5% (standard), and 11.2% (maximum reduction) for the Chang (1974) eddy diffusion profile. Thus, the response to a doubling of tropospheric N_2O was moderate, and the range of uncertainties was not drastic.

Nuclear Weapons Sensitivity Studies

The time-dependent response of the model to massive injections of NO_x such as might result from the explosion of hundreds to thousands of megatons of nuclear weapons was calculated. This work is still incomplete and will not be described in detail at this time. However, one significant finding was that a pulse injection of NO_x in the lower stratosphere comparable to that expected from a few hundred megatons total yield using 1-to-3-Mt devices resulted in a transient increase in total ozone when models A_1, A_2, C_1, C_2, C'_1, or C'_2 (described in Sec. 2-1 of this report) were used. This suggests that single test clouds might result in local ozone increases after a few days, making the results of such studies even harder to interpret as tests of theory. We are currently regenerating the coding necessary to study single clouds.

Two-Dimensional Transport-Kinetics Model Development

During the last year, numerous changes were made in the two-dimensional transport-kinetics model of the earth's atmosphere, in the mean wind and eddy diffusion coefficient data, in the chemical kinetics data, and in the various computer codes used to process input and output data. Numerous runs have been made to verify the behavior of the transport-kinetics model, and to verify the transport model by comparison with experimental data for several passive tracers. Current work is under way to improve the accuracy of the latitudinal dependence of photodissociation.

The seasonal average mean wind data of Louis was fitted with Fourier series to provide a full global time-dependent mean wind. The eddy diffusion data of Luther was modified to improve accuracy in the stratosphere. Global multipliers were added to allow modification of the mean wind and eddy diffusion coefficients. A capability of simulating particulate settling, using the Stokes-Cunningham formula, was added to allow comparison of the model with experimental measurements for various natural and artificial tracers for which particulate settling may be significant.

The transport equations were replaced with a new mass-consistent formulation, which is much better behaved when the mean wind field is not mass-consistent, as when horizontal or vertical components are modified by the global multipliers. A variable input parameter was added which allows choice of any weighted combination of first-order (upstream) or second-order (central) spatial differencing to model advection by the mean wind. This allows testing and partial control of the effects of numerical diffusion and dispersion. An option to keep concentrations fixed at any selected altitude was added. The upper boundary condition was modified to improve stability and avoid negative concentrations which could result from certain combinations of steep gradients and wind direction. These changes were tested in a tracer version of the 2-D model with no chemical kinetics and a single passive tracer, with a variety of runs simulating periods up to three years and with different initial and boundary conditions. Stability and accuracy were greatly improved, and correct steady-state solutions were obtained for those cases with known solutions. The full transport-kinetics model was run to simulate a six-month period, with encouraging results.

The tracer code was used to simulate the distribution of plutonium-238 released by the burnup of a SNAP-9A nuclear power source in the stratosphere in April 1964, which was described by Telegadas (1968). Various combinations of the particle size and density were used to model settling. It appears that settling significantly affected the actual distribution, and could not be modeled quantitatively with a single particle size.

The tracer model was also used to simulate the distribution of excess carbon-14 in the atmosphere released by atmospheric nuclear tests. The several simulations began with the measured distribution in March-May 1963, reported by Telegadas (1971), and simulated up to three years using various multipliers for components of the mean wind and eddy diffusion coefficients. The model-predicted distribution of excess carbon-14 for July 1964 is shown in Fig. 28, and the measured distribution is shown in Fig. 29. Good quantitative agreement was obtained for the maximum mixing ratio and for the integrated total load in the whole atmosphere, the troposphere, the stratosphere, and in the northern hemisphere. All were within 18% of the measured values. Agreement with measured concentrations at particular locations was qualitatively good in general and quantitatively good at lower latitudes. The main differences were occurrence of the maximum mixing ratio at about 25 km instead of 20 km, and concentration contours displaced toward higher altitudes in the polar regions.

The best overall agreement was obtained by multiplying Louis's mean wind data by 0.5 and Luther's horizontal eddy diffusion coefficients by 0.5. A different vertical profile of the vertical eddy diffusion coefficient with smaller values in the stratosphere would probably reduce the altitude error in the maximum mixing ratio and polar concentration contours.

The tracer model was also used to simulate the distribution of tungsten-185, as described in Stebbins (1961), resulting from a release of about 10 MCi at 18 km, 10°N latitude, on August 15, 1968. Several runs were made beginning with the distribution described for December 1968. Fair agreement with the measured distributions and with Louis's simulations was obtained for the first eight months of the simulation. For longer times, results diverged, probably due to the lack of a model for rainout of the tungsten-185 in the troposphere. The best results for the first few months were obtained with Louis's mean wind values reduced in half. The vertical profiles again indicated that the vertical eddy diffusion coefficients should be reduced in the stratosphere.

The full transport-kinetics code is presently being tested with new chemical reaction rates and a full annual variation of the solar zenith angle for each latitude. Rapid changes in concentrations at the boundary of the terminator near the winter pole may require modifications in the model to avoid the use of prohibitively small time steps or failure of the differential equation solver to converge.

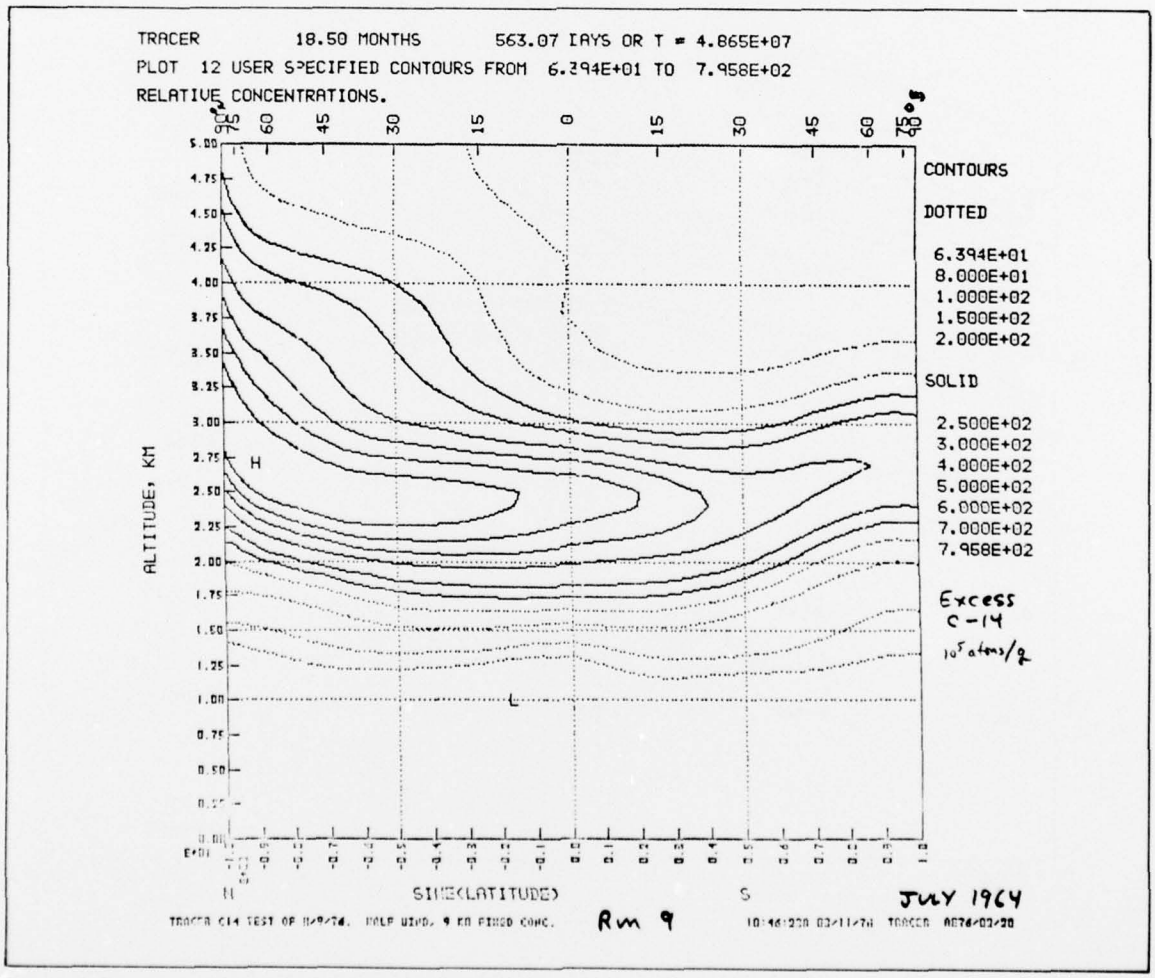

Fig. 28. Distributions of excess carbon-14 for July 1964 as calculated with the two-dimensional model.

Uncertainties in the Odd Nitrogen Budget of the Stratosphere

In an effort to improve our understanding of current stratospheric models, including their uncertainties and limitations, a review was undertaken of the odd nitrogen budget of the stratosphere as computed by the models. This review has revealed: (1) an uncertain consensus that $N_2O + O(^1D)$ is the principal, if not the only, source of stratospheric NO_x; (2) estimates of the strength of the N_2O source published since 1970 vary by more than an order of magnitude (0.2 to 4 $\times 10^8$ *molecules/cm*^{2}·*s*); (3) additional NO_x sources

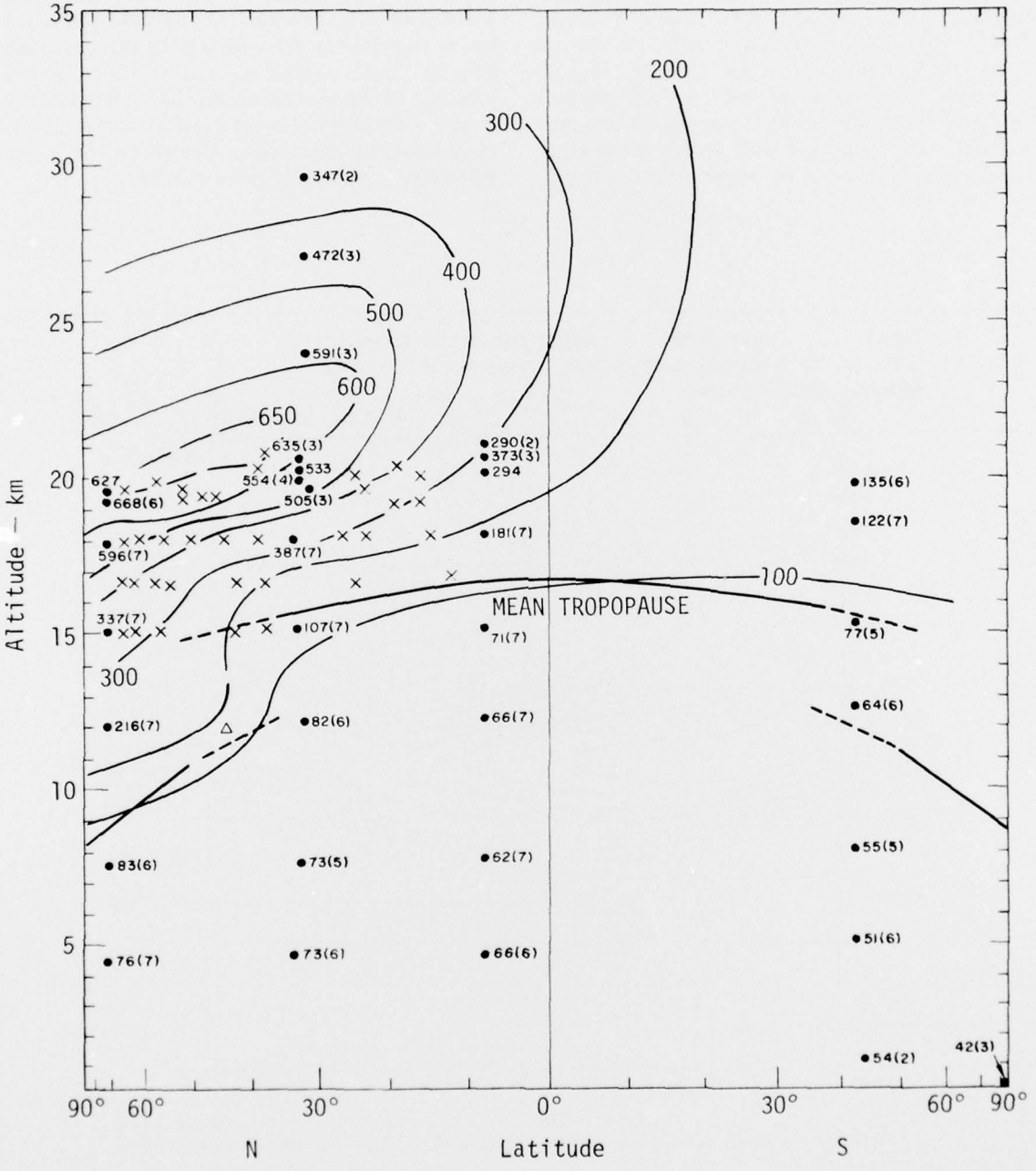

Fig. 29. Measured distribution of excess carbon-14 for June-August 1964. Values are in units of 10^5 atoms per gram of air; number of samples the value is based on is shown in parentheses.

which have been proposed include cosmic rays, downward transport from the thermosphere, oxidation of NH_3 (which alternatively may be an NO_x sink), and upward transport of NO_2 through the tropopause, as well as surmised but yet to be identified sources.

Aerosols and the Radiation Budget: One-Wavelength Versus Full-Flux Calculations

We have compared one-wavelength solar radiation calculations with full-flux calculations (0.285 to 2.5 μm) in order to assess the limitations and uncertainty of the results when only one wavelength in the visible is used. Comparisons were made for a standard atmosphere with tropospheric and stratospheric aerosols. Calculations at 0.55 μm greatly overestimate Mie scattering, but good agreement with the full-flux calculation has been obtained by scaling the aerosol optical depth to the flux-weighted aerosol optical depth.

In the past, assessments of the solar radiative effects of aerosols have been made using one-wavelength calculations in the visible spectrum. One-wavelength calculations have the advantage that they require much less computer time than the full-flux calculations. Their disadvantage is that they are less accurate than the full-flux calculations. If a method could be found for correcting the one-wavelength calculation, then extensive calculations on the solar effects of stratospheric aerosols could be undertaken at a reasonable cost.

Two corrections must be made to the one-wavelength calculation. One correction applies to the fact that the radiative properties of the aerosol at the given wavelength (usually 0.55 μm) are not representaive of the full-flux radiative properties. This can be corrected to a large degree for weakly absorbing aerosols by scaling the one-wavelength results for the changed fluxes by the ratio of the flux-weighted aerosol optical depth to the optical depth at 0.55 μm. The second correction applies to the difference in the solar flux incident on the aerosol. In the case of stratospheric aerosols, the total downward flux incident from above is accurate to within a few percent of the full-flux value. However, the one-wavelength calculation overestimates the flux reaching the earth's surface. Consequently, the error in the flux incident on the aerosols from below depends upon the surface albedo. In the case of tropospheric aerosols the downward flux and the upward flux incident on the aerosols are overestimated by approximately the same factor, so the error is nearly independent of surface albedo and can be corrected effectively with a constant scaling factor.

The change in the upward-scattered flux at the top of the atmosphere due to a stratospheric aerosol layer between 18 and 22 km is shown in Fig. 30 as a function of solar zenith angle and surface albedo. The solid lines correspond to the full-flux calculation, and the broken lines correspond to the scaled one-wavelength calculation at 0.55 μm. The one-wavelength results have been scaled by a factor of 0.75, which is the ratio of the flux-weighted aerosol optical depth (computed using the total downward flux at 22 km) to the optical depth at 0.55 μm. The aerosol optical depth is 0.05; a zero-order logarithmic size distribution (Toon and Pollack 1976) is assumed; and the wavelength-dependent real and imaginary indices of refraction are taken from Palmer and Williams (1975) for 75% H_2SO_4. The scaled one-wavelength calculation duplicates all of the major features of the full-flux calculation (e.g., regions of increase or decrease in solar heating and the local maximum). There is very good agreement for small surface albedo.

The change in the net downward flux at 12 km due to the stratospheric aerosol layer is shown in Fig. 31. A decrease in the net flux indicates a decrease in the solar heating of the troposphere. The calculations show that this particular aerosol layer can lead to an increase in the solar heating for small solar zenith angles and large surface albedo.

The significant variation of the change in solar heating with solar zenith angle and surface albedo indicates that global mean calculations in which a solar zenith angle of 60° and a surface albedo of 0.3 are assumed may vary significantly from diurnal average calculations. Future assessments of the solar radiative effects of aerosols should take into account diurnal, latitudinal, and seasonal variations (as well as variations in surface albedo).

Climatic Effect of Contrails

A series of experiments to test the climatic effect of increased cirrus clouds due to jet contrails is currently under way using the two-dimensional climate model ZAM2. One experiment consists of increasing the computed cirrus cloudiness at all latitudes by a factor of 1.2. Gary Hunt at the British Meteorological Office has performed a similar experiment, and we will compare our results with his. Results will also be compared with those from the two-dimensional COMESA model, which uses a series of latitudinally arranged one-dimensional radiative equilibrium models similar to those of Manabe and Möller (1961). Another experiment attempts to simulate the global climatic effect of increased cirrus along a flight corridor. In this experiment, the cirrus cloud cover between latitudes 30 and 50°N will be incrementally increased by 0.10.

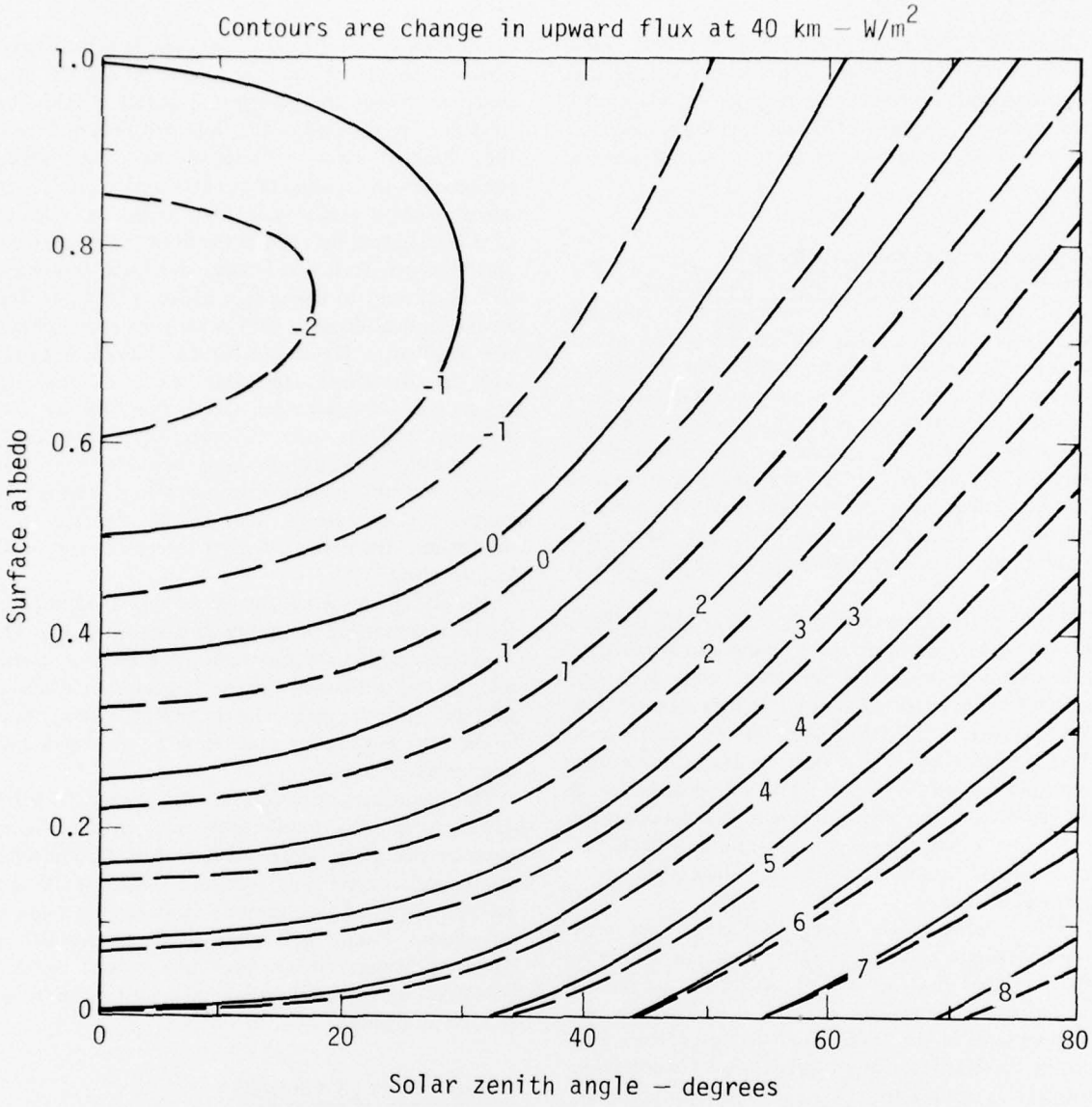

Fig. 30. Calculated change in upward flux at 40-km altitude as a function of surface albedo and solar zenith angle. Solid curves are full-flux calculation, dashed curves are one-wavelength (0.55-μm) calculation.

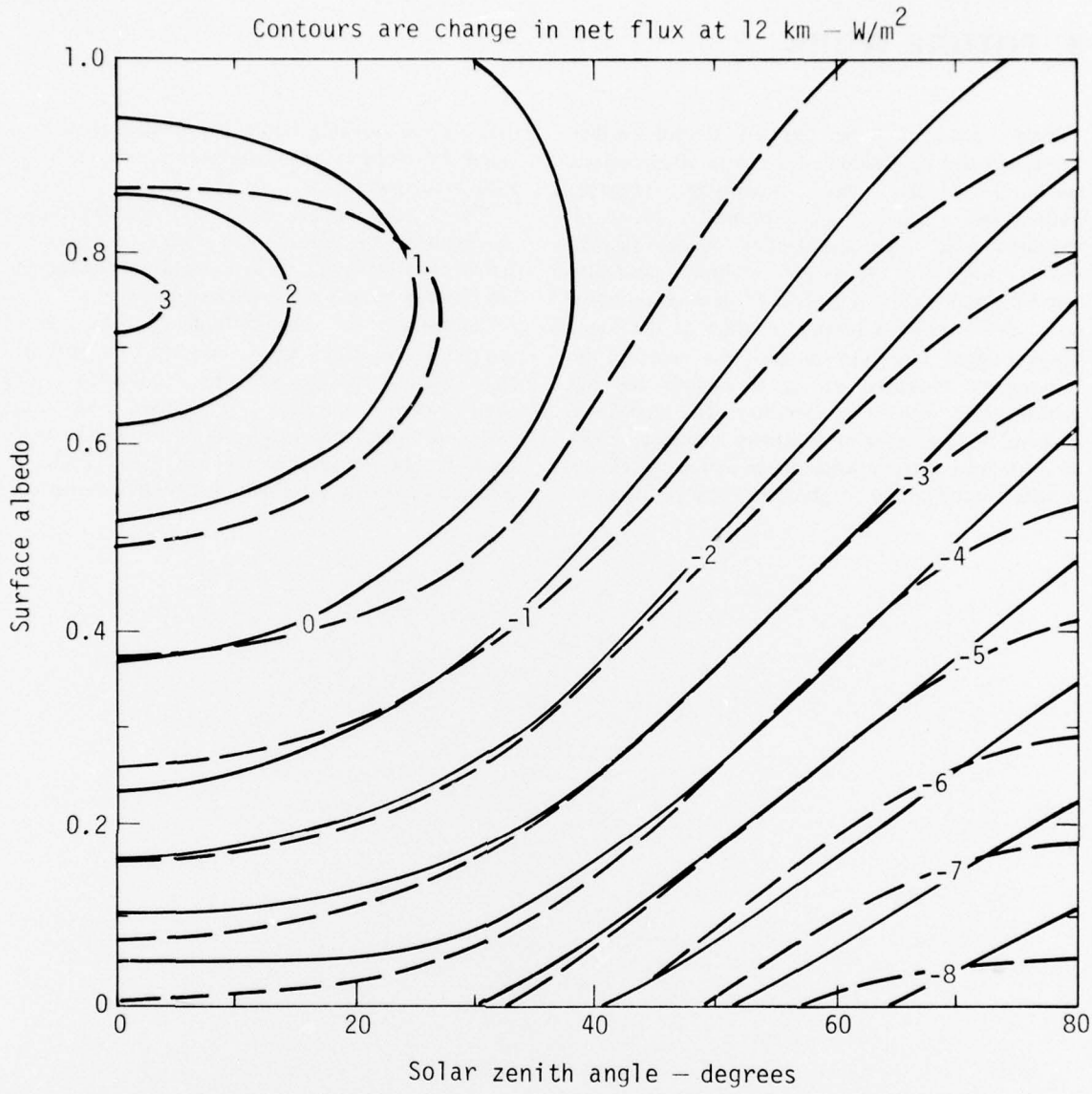

Fig. 31. Calculated change in net flux at 12-km altitude as a function of surface albedo and solar zenith angle. Solid curves are full-flux calculation, dashed curves are one-wavelength (0.55-μm) calculation.

3. FUTURE WORK

Future work will be directed toward further refinement and application of a variety of specialized numerical models and supporting research. Refinements which are planned for the one-dimensional transport-kinetics model include incorporating the effects of multiple molecular scattering and surface reflection on photodissociation rates, incorporating a parameterization of the water vapor budget into the model, and refining the tropospheric chemistry so as to include the full methane cycle and smog chemistry. The model will be used for a number of sensitivity studies to assess the effects of these refinements as well as the effects of new reaction rates or photochemical pathways as data become available. Future perturbation studies will emphasize multiple perturbations (e.g., NO_x and H_2O with background Cl_x).

The two-dimensional model will undergo further development. Additional tracer studies are planned to refine the prescribed transport, and simulation studies are planned to validate model chemistry.

Calculations of the latitudinal and seasonal variations of the solar effects of perturbed stratospheric species will be conducted using concentration profiles generated by the two-dimensional model. Special studies will be made using the two-dimensional climate model ZAM2 to assess the climatic sensitivity to these perturbations.

4. REFERENCES

Ackerman, M. (1975), "NO, NO_2, and HNO_3 Below 35 km in the Atmosphere," *J. Atmos. Sci.* **32**, 1649-1657.

Anderson, J. G. (1975), "The Absolute Concentration of $O(^3P)$ in the Earth's Atmosphere," *Geophys. Res. Lett.* **2**, 231-234.

Anderson, J. G. (1976), University of Pittsburgh, private communication.

Anderson, J. G., F. Kaufman, and M. S. Zahniser (1975), "Kinetics of Some Stratospheric Reactions of Chlorine Species," paper presented at the American Chemical Society National Meeting, Philadelphia, Pa., April 6-11, 1975.

Angell, J. K., and J. Korshover (1974), "Quasi-Biennial and Long-Term Fluctuations in Tropopause Pressure and Temperature, and the Relation to Stratospheric Water Vapor Content," *Mon. Weather Rev.* **102**, 29-34.

Atherton, R. W., R. B. Schainker, and E. R. Ducot (1975), "On the Statistical Sensitivity Analysis of Models for Chemical Kinetics," *AIChE J.* **21**, 441-448.

Bacastow, R., and C. D. Keeling (1973), "Atmospheric Carbon Dioxide and Radiocarbon in the Natural Carbon Cycle: II. Changes from A. D. 1700 to 2070 as Deduced from a Geochemical Model," in *Carbon and the Biosphere*, G. M. Woodwell and E. V. Pecan, Eds., U. S. Atomic Energy Commission, CONF-720510, pp. 86-135 (Proc. 24th Brookhaven Symposium in Biology, Upton, N. Y., May 16-18, 1972).

Barnett, J. J., J. T. Houghton, and J. A. Pyle (1975), "The Temperature Dependence of the Ozone Concentration Near the Stratopause," *Quart. J. Roy. Meteorol. Soc.* **101**, 245

Birks, J. W. (1976), University of Illinois, Urbana, private communication.

Cadle, R. D., and G. W. Grams (1975), "Stratospheric Aerosol Particles and Their Optical Properties," *Rev. Geophys. Space Phys.* **13**(4), 475-501.

Cess, R. D. (1974), "Radiative Transfer Due to Atmospheric Water Vapor: Global Considerations of the Earth's Energy Balance," *J. Quant. Spectrosc. Radiat. Transfer* **14**, 861-871.

Chameides, W., and J. C. G. Walker (1973), "A Photochemical Theory of Tropospheric Ozone," *J. Geophys. Res.* **78**, 8751-8760.

Chang, J. S. (1974), "Simulations, Perturbations, and Interpretations," in *Proc. 3rd Conf. on CIAP*, U. S. Department of Transportation, Transportation Systems Center, Cambridge, Mass., Rept. DOT-TSC-OST-74-15, pp. 330-341.

Chang, J. S. (1975), "Effect on Ozone of Trace Gases from Propulsion Effluents in the Stratosphere," in *The Stratosphere Perturbed by Propulsion Effluents*, U. S. Department of Transportation, Washington, D. C., Rept. DOT-TST-75-53, Chapter 5.

Chang, J. S., A. C. Hindmarsh, and N. K. Madsen (1973), *Simulation of Chemical Kinetics Transport in the Stratosphere*, Lawrence Livermore Laboratory Rept. UCRL-74823 Preprint.

Chang, J. S., A. C. Hindmarsh, and N. K. Madsen (1974), "Simulation of Chemical Kinetics Transport in the Stratosphere," in *Stiff Differential Systems*, R. A. Willoughby, Ed. (Plenum, New York), pp. 51-65.

Christie, A. D. (1973), "Secular or Cyclic Change in Ozone," *Pure Appl. Geophys.* **106-108**, 1000-1009.

Cieslik, S., and M. Nicolet (1973), "The Aeronomic Dissociation of Nitric Oxide," *Aeronomica Acta A* **112**.

Crutzen, P. J. (1972), "SST's–A Threat to the Earth's Ozone Shield," *Ambio* **1**, 41-51.

Crutzen, P. J., and I. S. A. Isaksen (1975), *The Impact of the Chlorocarbon Industry on the Ozone Layer* (Preprint), University of Stockholm, Stockholm, Sweden.

Cukier, R. I., C. M. Fortuin, K. E. Schuler, A. G. Petschek, and J. H. Schaibly (1973), "Study of the Sensitivity of Coupled Reaction Systems to Uncertainties in Rate Coefficients, I. Theory," *J. Chem. Phys.* **59**, 3873-3878.

Davis, D. D. (1975), University of Maryland, private communication.

Davis, D. D. (1976), University of Maryland, private communication.

Davis, D. D. (1976), *Absolute Rate Constants for Elementary Reactions of Atmospheric Importance: Results from the University of Maryland Gas Kinetics Laboratory*, University of Maryland, Rept. No. 3.

Davis, D. D., E. S. Machado, R. L. Schiff, and R. T. Watson (1975), "The Temperature Dependence of Some Cl Atom Reactions of Stratospheric Interest," paper presented at the American Chemical Society National Meeting, Philadelphia, Pa., April 6-11, 1975.

DeMore, W. B. (1976), Jet Propulsion Laboratory, Pasadena, California, private communication.

Dickinson, R. P., and R. J. Gelinas (1975), *Sensitivity Analysis of Ordinary Differential Equation Systems–A Direct Variational Method*, Lawrence Livermore Laboratory Rept. UCRL-76811.

Duewer, W. H., D. J. Wuebbles, H. W. Ellsaesser, and J. S. Chang (1976), "NO_x catalytic Ozone Destruction: Sensitivity to Uncertainties in Rate Coefficients," paper for presentation at the American Chemical Society Meeting, San Francisco, Calif., August 1976.

Duewer, W. H., D. J. Wuebbles, H. W. Ellsaesser, and J. S. Chang (1976), *NO_x Catalytic Ozone Destruction: Sensitivity to Rate Coefficients*, Lawrence Livermore Laboratory Rept. UCRL-77917 Preprint (submitted to *J. Geophys. Res.*).

Dütsch, H. U. (1969), "Atmospheric Ozone and Ultraviolet Radiation," in *Climate of the Atmosphere* (Elsevier Publishing Co., New York).

Dütsch, H. U. (1972), "The Present Status of Ozone Research: Photochemistry and Observations," in *Proc. 2nd Conf. CIAP, Cambridge, Md., November 14-17, 1972*, U. S. Dept. of Transportation Rept. DOT-TSC-OST-73-4, pp. 106-113.

Foley, H. M., and M. A. Ruderman (1973), "Stratospheric Nitric Oxide Production from Past Nuclear Explosions and Its Relevance to Projected SST Pollution," *J. Geophys. Res.* **78**, 4441-4450.

Fox, R. J., G. W. Grams, and B. G. Schuster (1973), "Measurement of Stratospheric Aerosols by Airborne Laser Radar," *J. Geophys. Res.* **78**(33), 7789-7801.

Gelinas, R. J., R. P. Dickinson, and K. E. Grant (1974), *Solar Flux and Photodissociation Calculations for LLL Atmospheric Physics Programs*, Lawrence Livermore Laboratory Rept. UCRL-74944 Preprint.

Gelinas, R. J., R. P. Dickinson, and K. E. Grant (1974), *Solar Flux and Photodissociation Calculations for LLL Atmospheric Physics Programs*, Lawrence Livermore Laboratory Rept. UCRL-74944 Preprint.

Grobecker, A. J. (Ed.)(1975), *CIAP Monograph 3*, U. S. Department of Transportation, Washington, D. C., Rept. DOT-TST-75-53, pp. 1-38.

Grobecker, A. J., S. C. Coroniti, and R. H. Cannon, Jr. (1974), *CIAP Report of Findings*, U. S. Department of Transportation, Washington, D. C., Rept. DOT-TSC-75-50.

Hampson, R. F. (1976), National Bureau of Standards, Gaithersburg, Md., private communication.

Hampson, R. F., and D. Garvin, Eds. (1975), *Chemical Kinetic and Photochemical Data for Modeling Atmospheric Chemistry*, National Bureau of Standards, Gaithersburg, Md., NBS Technical Note 866.

Heath, D. F. (1974), "Recent Advances in Satellite Observations of Solar Variability and Global Atmospheric Ozone," in *Proc. Intern. Conf. on Structure, Composition, and General Circulation of the Upper and Lower Atmospheres and Possible Anthropogenic Perturbations*, Melbourne, Australia, January 14-25, 1974.

Hoffert, M. I. (1974), "Global Distributions of Atmospheric Carbon Dioxide in the Fossil-Fuel Era: A Projection," *Atmos. Environ.* **8**, 1225-1249.

Johnston, H. S. (1971), "Reduction of Stratospheric Ozone by Nitrogen Oxide Catalysts from Supersonic Transport Exhaust," *Science* **173**, 517-522.

Johnston, H. S. (1973), University of California, Berkeley, private communication.

Johnston, H. S. (1975), "Global Ozone Balance in the Natural Stratosphere," *Rev. Geophys. Space Phys.* **13**(5), 637-649.

Johnston, H. S., and G. Z. Whitten (1973), "Instantaneous Photochemical Rates in the Global Stratosphere," *Pure Appl. Geophys.* **106-108**, 1468-1489.

Johnston, H. S., and E. Quitevis (1974), "The Oxides of Nitrogen with Respect to Urban Smog, Supersonic Transports, and Global Methane," paper presented at the Fifth International Congress of Radiation Research, Seattle, Wash., July 14-20, 1974.

Kaufman, F. (1975), "Hydrogen Chemistry: Perspective on Experiment and Theory," in *Atmosphere of Earth and the Planets*, W. McCormac, Ed. (P. Reidel Publishing Co., Dordrecht, Holland), pp. 219-233.

Kaufman, F. (1976), University of Pittsburgh, private communication.

Komhyr, W. D., E. W. Barrett, E. Slocum, and H. K. Weichmann (1971), "Atmospheric Total Ozone Increase During the 1960's," *Nature* **232**, 390-391.

Krueger, A. J. (1973), "The Mean Ozone Distribution from Several Series of Rocket Soundings to 52 km at Latitudes from 58°S to 64°N," *Pure Appl. Geophys.* **106-108**, 1272-1280.

Lindzen, R. S., and D. I. Will (1973), "An Analytical Formula for Heating Due to Ozone Absorption," *J. Atmos. Sci.* **30**, 513-515.

Lloyd, A. (1974), "Evaluated and Estimated Kinetic Data for Gas Phase Reactions of the Hydroperoxyl Radical," *Intern. J. Chem. Kinet.* **6**, 169-228.

Louis, J. F. (1974), *A Two-Dimensional Transport Model of the Atmosphere*, Ph.D. thesis, University of Colorado, Boulder, Colo.

Luther, R. M. (1976), "A Parameterization of Solar Absorption by Nitrogen Dioxide," *J. Appl. Meteorol.* **15**, 479-481.

MacCracken, M. C., and J. S. Chang (1975), *A Preliminary Study of the Potential Chemical and Climatic Effects of Atmospheric Nuclear Explosions*, Lawrence Livermore Laboratory Rept. UCRL-51653.

Machta, L., and T. Carpenter (1971), "Trends in High Cloudiness at Denver and Salt Lake City," in *Man's Impact on the Climate*, W. H. Mathews, Ed. (MIT Press, Cambridge, Mass.), pp. 410-415.

Manabe, S., and F. Möller (1961), "On the Radiative Equilibrium and Heat Balance of the Atmosphere," *Mon. Weather Rev.* **89**, 503-523.

Manabe, S., and R. F. Strickler (1964), "Thermal Equilibrium of the Atmosphere with a Convective Adjustment," *J. Atmos. Sci.* **21**, 361-385.

Mastenbrook, H. J. (1971), "The Variability of Water Vapor in the Stratosphere," *J. Atmos. Sci.* **28**, 1495-1501.

McCarthy, R. L. (1974), "Fluorocarbons in the Environment," paper presented at the American Geophysical Union Meeting, San Francisco, Calif., December 13, 1974.

McElroy, M. B. (1975), "Testimony Before the Committee on Interstate and Foreign Commerce Subcommittee on Health and the Environment, 11 December 1974," in *Fluorocarbons: Impact on Health and Environment* (U. S. Government Printing Office, Washington, D. C.).

Molina, M. J., and F. S. Rowland (1974), "Stratospheric Sink for Chlorofluoromethanes: Chlorine Atom Catalysed Destruction of Ozone," *Nature* **249**, 810-812.

Murcray, D. G. (1976), University of Denver, private communication.

Murcray, D. G., A. Goldman, F. H. Murcray, W. J. Williams, J. N. Brooks, and D. B. Barker (1973), "Vertical Distribution of Minor Atmospheric Constituents as Derived from Air-Borne Measurements of Atmospheric Emission and Absorption Infrared Spectra," in *Proc. 2nd Conf. on CIAP*, U. S. Department of Transportation, Transportation Systems Center, Cambridge, Mass., Rept. DOT-TSC-OST-73-4, pp. 86-98.

National Academy of Sciences (1975a), *Long-Term Worldwide Effects of Multiple Nuclear Weapons*, National Academy of Sciences–National Research Council, Washington, D. C.

National Academy of Sciences (1975b), *Environmental Impact of Stratospheric Flight*, National Academy of Sciences–National Research Council, Washington, D. C.

Oort, A. H., and E. M. Rasmusson (1971), *Atmospheric Circulation Statistics*, U. S. Dept. of Commerce, Rockville, Md., NOAA Professional Paper No. 5.

Palmer, K. F., and D. Williams (1975), "Optical Constants of Sulfuric Acid: Application to the Clouds of Venus?" *Appl. Opt.* **14**, 208-219.

Ramanathan, V. (1974), "A Simplified Stratospheric Radiative Transfer Model: Theoretical Estimates of the Thermal Structure of the Basic and Perturbed Stratosphere," paper presented at the AMS/AIAA Second International Conference on the Environmental Impact of Aerospace Operations in the High Atmosphere, San Diego, Calif., July 8-10, 1974.

Ramanathan, V., L. Callis, and R. Boughner (1975), paper submitted to *Journal of Applied Meteorology*. These authors also presented a brief description of the model at the 4th CIAP Conference, Cambridge, Mass., February 4-7, 1975.

Reed, R. J., and C. L. Vlcek (1969), "The Annual Temperature Variation in the Lower Tropical Stratosphere," *J. Atmos. Sci.* **26**(1), 163-167.

Ruderman, M. A., and J. W. Chamberlain (1975), "Origin of the Sunspot Modulation of Ozone: Its Implications for Stratospheric NO Injection," *Planet. Space Sci.* **23**, 247-268.

Ruderman, M. A., H. M. Foley, and J. W. Chamberlain (1976), "Eleven-Year Variation in Polar Ozone and Stratospheric-Ion Chemistry," *Science* **192**, 555-557.

Ryan, J. A., and N. R. Mukherjee (1975), "Sources of Stratospheric Gaseous Chlorine," *Rev. Geophys. Space Phys.* **13**, 650-658.

Schaibly, J. H., and K. E. Schuler (1973), "A Study of the Sensitivity of Coupled Reaction Systems to Uncertainties in Rate Coefficients, II. Applications," *J. Chem. Phys.* **59**, 3879-3888.

Schneider, S. H. (1975), "On the Carbon Dioxide-Climate Confusion," *J. Atmos. Sci.* **32**, 2060-2066.

Seiler, W. (1974), "The Cycle of Atmospheric CO," *Tellus* **26**, 116-135.

Seiler, W., and P. Warneck (1972), "Decrease of the Carbon Monoxide Mixing Ratio at the Tropopause," *J. Geophys. Res.* **77**, 3204-3214.

Smith, J. W. (1963), "The Vertical Temperature Distribution and the Layer of Minimum Temperature," *J. Appl. Meteorol.* **2**(5), 655-667.

Spencer, J., M. Molina, and F. S. Rowland (1976), "Revised Chlorine Nitrate ($ClONO_2$) Photochemical Absorption Cross Sections," to be published.

Stebbins, A. D., III, Ed. (1961), *Second Special Report on High Altitude Sampling Program*, Defense Atomic Support Agency Rept. 539B.

Telegadas, K. (1968), "The Seasonal Stratospheric Distribution of Cadmium-109, Plutonium-238, and Strontium-90," in *Fallout Program Quarterly Summary Report, December 1, 1967-March 1, 1968*, U.S.A.E.C. Health and Safety Laboratory, New York, N. Y.

Telegadas, K. (1971), "The Seasonal Stratospheric Distribution and Inventories of Excess Carbon-14 from March 1955 to July 1969," in *Fallout Program Quarterly Summary Report, March 1-June 1, 1971*, U.S.A.E.C. Health and Safety Laboratory, Rept. HASL-243.

Toon, O. B., and J. B. Pollack (1976), "A Global Average Model of Atmospheric Aerosols for Radiation Transfer Calculations," *J. Appl. Meteorol.* **15**, 225-246.

Turco, R. P., and R. C. Witten (1975), "Chlorofluoromethanes in the Stratosphere and some Possible Consequences for Ozone," *Atmos. Environ.* **9**, 1045-1061.

U. S. Standard Atmosphere (1962), U. S. Government Printing Office, Washington, D. C.

U. S. Standard Atmosphere Supplements (1966), U. S. Government Printing Office, Washington, D. C.

Watson, R. J. (1974), *Chemical Kinetics Data Survey: VIII. Rate Constants of ClO_x of Atmospheric Interest*, NBSIR 74-515.

Winstanley, D. (1973), "Rainfall Patterns and General Atmospheric Circulation," *Nature* **245**, 190-194.

Wofsy, S. C. (1975), "Interactions of CH_4 and CO in the Earth's Atmosphere," to be published in *Annual Review of Earth and Planetary Sciences*, Vol. 4 (in press).

Wofsy, S. C., M. B. McElroy, and N. D. Sze (1975), "Freon Consumption: Implication for Atmospheric Ozone," *Science* **187**, 535-537.

Wuebbles, D. J., and J. S. Chang (1975), "Sensitivity of Time-Varying Parameters in Stratospheric Modeling," *J. Geophys. Res.* **80**, 2637-2642.

5. BIBLIOGRAPHY OF PUBLICATIONS PRODUCED IN LLL'S WORK ON THE HIGH ALTITUDE POLLUTION PROGRAM

Chang, J., and D. Wuebbles (1975), "A Study of the Atmospheric Budget for Odd Nitrogen," paper presented at American Geophysical Union Fall Meeting, San Francisco, Calif., December 8-12, 1975. Lawrence Livermore Laboratory, UCRL-77299 Abstract (Sept. 1975).

Chang, J. S., D. J. Wuebbles, and W. H. Duewer (1976), "Sensitivity to Parameter Uncertainties for Ozone Reduction from Chlorofluoromethanes," paper presented at 12th International Symposium on Free Radicals, Laguna Beach, Calif., January 4-9, 1976 (sponsored by University of California, Irvine). Lawrence Livermore Laboratory, UCRL-77432 Preprint (Jan. 1976).

Duewer, W. H., H. W. Ellsaesser, D. J. Wuebbles, and J. S. Chang (1976), "NO Catalytic Ozone Destruction: Sensitivity to Rate Coefficients," paper presented at meeting of American Chemical Society, Division of Environmental Chemistry, San Francisco, Calif., August 1976. Lawrence Livermore Laboratory, UCRL-78038 Abstract (1976).

Duewer, W. H., D. J. Wuebbles, and J. S. Chang (1976), "Effect of NO Photolysis on NO_y Mixing Ratios," paper submitted to *Nature*. Lawrence Livermore Laboratory, UCRL-78613 Preprint (April 1976).

Duewer, W. H., D. J. Wuebbles, H. W. Ellsaesser, and J. S. Chang (1976), "NO_x Catalytic Ozone Destruction: Sensitivity to Uncertainties in Rate Coefficients," paper presented at Symposium on Atmospheric Ozone, International Commission on Atmospheric Ozone/Atmospheric Chemical and Global Pollution of the International Association of Meteorology and Atmospheric Physics, Dresden, East Germany, August 9-17, 1976. Lawrence Livermore Laboratory, UCRL-78037 Preprint (July 1976).

Duewer, W. H., D. J. Wuebbles, H. W. Ellsaesser, and J. S. Chang (1976), "NO_x Catalytic Ozone Destruction: Sensitivity to Rate Coefficients," abstract presented at American Chemical Society National Meeting, San Francisco, Calif., August 29-September 3, 1976. Lawrence Livermore Laboratory, UCRL-77917 Preprint (March 1976); submitted to *J. Geophys. Res.*

Ellsaesser, H. W. (1975), "The Role of Deserts on Global Climates," paper presented at American Geophysical Union Fall Meeting, San Francisco, Calif., Dec. 8-12, 1975. Lawrence Livermore Laboratory, UCRL-77309 Abstract (Sept. 1975).

Ellsaesser, H. W. (1976), *Ozone Drop and Depletion Theories*, Lawrence Livermore Laboratory, UCRL-77833 Preprint (Feb. 1976). Submitted to *Science News*.

Ellsaesser, H. W. (1976), *Has the Solar Constant Kept Pace with Solar Luminosity?*, Lawrence Livermore Laboratory, UCRL-77854 Preprint (Feb. 20, 1976). Submitted to *Nature*.

Ellsaesser, H. W. (1976), "A Reassessment of Stratospheric Ozone: Credibility of the Threat," paper submitted to Symposium on Stratospheric Pollution and Skin Cancer, 50th Anniversary Congress Pan-American Medical Association, Hollywood, Fla., Oct. 24-29, 1976. Lawrence Livermore Laboratory, UCRL-78285 Abstract Rev. 1 (June 1976).

Ellsaesser, H. W., M. C. MacCracken, G. L. Potter, and F. M. Luther (1976), "An Additional Model Test of Positive Feedback from High Desert Albedo," *Quart. J. Roy. Meteorol. Soc.* **102**, 543-554. Lawrence Livermore Laboratory, UCRL-77121 Preprint (Aug. 1, 1975).

Luther, F. (1976), "One-Wavelength Solar Radiation Calculations: Rayleigh Scattering and Gaseous Absorption," paper presented at 2nd Conference on Atmospheric Radiation, Arlington, Va., Oct. 29-31, 1975. Lawrence Livermore Laboratory, UCRL-76680 Preprint (Feb. 1976).

Luther, F. M. (1976), "Aerosols and the Radiation Budget: One-Wavelength Versus Full-Flux Calculations," paper presented at Symposium on Radiation in the Atmosphere, Radiation Commission and Commission on Atmospheric Chemistry and Global Pollution, Garmisch-Partenkirchen, Germany, Aug. 19-28, 1976. Lawrence Livermore Laboratory, UCRL-77870 Abstract Rev. 1 (Aug. 6, 1976).

Luther, Frederick M. (1976), "Solar Absorption in a Stratosphere Perturbed by NO_x Injection," *Science* **192**, 49-51.

Luther, Frederick M. (1976), "A Parameterization of Solar Absorption by Nitrogen Dioxide," *J. Appl. Meteorol.* **15**, 479-481.

Luther, F. M., J. Chang, and D. Wuebbles (1975), "Radiation Feedback Effects in a One-Dimensional Stratospheric Model," paper presented at American Geophysical Union Fall Meeting, San Francisco, Calif., Dec. 8-12, 1975. Revised version (Lawrence Livermore Laboratory, UCRL-77298 Preprint, March 1976) submitted to *J. Geophys. Res.*

Luther, Frederick M., and Robert J. Gelinas (1976), "Effect of Molecular Multiple Scattering and Surface Albedo on Atmospheric Photodissociation Rates," *J. Geophys. Res.* **81**, 1125-1132.

Potter, J., and H. W. Ellsaesser (1975), "Climatic Consequences of the Removal of the Tropical Rain Forest," paper presented at American Geophysical Union Fall Meeting, San Francisco, Calif., Dec. 8-12, 1975. Lawrence Livermore Laboratory, UCRL-77286 Abstract (Sept. 1975).

Potter, G. L., M. C. MacCracken, H. W. Ellsaesser, and F. M. Luther (1975), "Possible Climatic Impact of Tropical Deforestation," *Nature* **258**(5537), 697-698 (Dec. 25, 1975).

WEC/hr/wl/lmc